Experimental Investigations of Residual and Fatigue Capacities of Timber Connections with Glued-in FRP Rods

by

Hong Zhu

A THESIS SUMITTED IN PARTIAL FULFILLMENT OF

THE REQUIREMENTS FOR THE DEGREE OF

MASTER OF APPLIED SCIENCE

in

The Faculty of Graduate and Postdoctoral Studies

(Forestry)

THE UNIVERSITY OF BRITISH COLUMBIA

(Vancouver)

August, 2014

ABSTRACT

Well-designed and executed glued-in rod connections can provide excellent structural performance in terms of strength, stiffness, and efficiency in load transfer. The pull-out residual and fatigue capacity of timber connections with glued-in Glass Fibre Reinforced Polymer (GFRP) rods bonded by Polyurethane adhesive (PUR) have been studied extensively. Previous research conducted at the University of British Columbia in Vancouver (UBC) investigated the impact of anchorage length and rod diameter on the performance of glued-in GFRP rods glulam joints. Each of the test specimens consisted of two glued-in rod connections, with one rod inserted in each end-grain face. One side joint failed brittle but the other side joint survived under quasi static tensile test. The first rod connection to fail could be called the broken side or first side and the unbroken rod could be called the surviving side or second side. However, universal agreement on the design of glued-in rod connections has not yet been reached.

The experimental work for this thesis was performed in the Timber and Material Laboratories at UBC. In the pull-out tension test, which is a follow-up test to previous study regarding the geometric characters of the glued-in GFRP rods joints, the short term tensile capacities of the surviving sides of symmetrical glued-in rod test specimens were determined. A total of 25 test series were tested with 5 replicates each where the anchorage length and the rod diameter were the same. The surviving side capacities were not always higher than the first sides, possibly explained by damage caused through the previous quasi static tensile tests. Subsequently, the average capacities from each series based two sides data were compared to the calculated predictions from different design approaches and it was shown that the German Design Code could best predict the capacity of symmetrical glued-in-rod connections.

The fatigue tests were conducted based on the novel “PYHBAL” loading protocol which involves two single step tests and one load increase test. Compared to conventional fatigue tests, the “PHYBAL” method can provide fast and economic fatigue estimation. The fatigue capacity of the glued-in GFRP rod joints was approximately 65% of short-term capacity.

PREFACE

The research presented in this thesis has not been published. Results from Chapter 3 are included in an accepted conference contribution: “Tannert T, Faghani P, Zhu H, Garekani A, Vallee T (2014) Timber joints with glued-in FRP rods. In Proceedings of World Conference on Timber Engineering, Quebec City, Canada.”

TABLE OF CONTENTS

LIST OF TABLES

LIST OF FIGURES

ACKNOWLEDGEMENTS

First and foremost I would like to thank my research supervisor, Dr. Thomas Tannert, for his inspiration, vision, help, patience and support which made it possible for me to accomplish this research and produce the original contributions that comprise this dissertation.

I also I would like to express my gratitude to my research supervisory committee, Dr. Frank Lam and Dr. Gregory Smith, for the help and advice that I received from them during these two years of my research program at UBC.

I would like to thank my colleagues in the Timber Engineering research group at UBC. Particularly, I would like to thank Pedram Faghani for his time and guidance for this research I also owe many thanks to George Lee, John Wong, Harald Schrempp and Jane Wu, and Manuel Fekter for their help in my experiment. I thank all my dear friends who made my student life at UBC colourful and meaningful.

I would like to express my sincere gratitude toward my mother who has been giving me support during all the years of studying at UBC, her endless love and belief in me and my future success; and to my father who always showed me the way when I was lost. I also thank all my family members who were always in my heart and provided a strong support for me.

1. INTRODUCTION

1.1 BACKGROUND AND PROBLEM STATEMENT

Timber is the preferred building material for housing in North America and is becoming increasingly popular in commercial and industrial construction. As with all other structural materials, a critical aspect of timber structures is the method by which members are connected. Timber products can be easily drilled or shaped to facilitate the connection of members and a number of methods are available to facilitate a connection such as by adhesively bonding. Wood adhesion has been studied and applied to timber structures for decades, most prominently in the production of solid glued-laminated timber, but also as component or enhancement for more contemporary hybrid connections which can support higher loads and longer spans [1].

Glued-in rod connections are a promising joint technique comprised of one or more rods bonded into timber using adhesive (see Figure 1-1). Such connections are successfully used for both constructing new and strengthening existing timber structures. An example from Solothurn, Switzerland is shown in Figure 1-2.

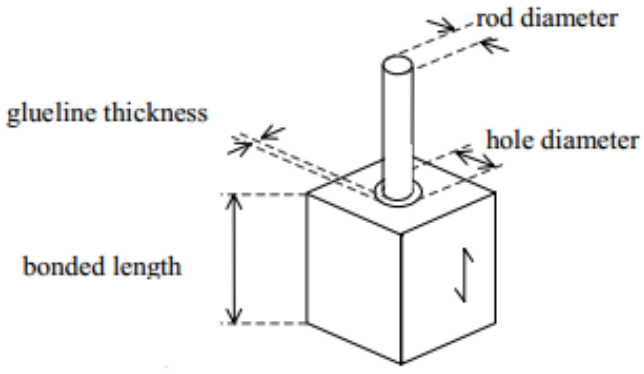

Figure 1-1: Configurations of Glued-in Rods

Figure 1-2: Timber Structure With Glued-in Rods Connections

Well-designed and executed glued-in rod connections provide excellent strength, stiffness properties, and efficient load transfer [2]. These connections also possess desirable attributes in terms of manufacture, performance, weight, aesthetics and cost. For instance, when used as reinforcement, glued-in rods perform well at preventing cracks in areas of high stresses perpendicular to the grain, such as tapered or curved glulam beams and end-notched beams [3]. Substantial research regarding timber joints with glued-in rods has been conducted during the past decades [4-14]. However, universal agreement on design criteria for these connections has not been reached and more research is needed to offer a general method for evaluating the capacity of glued-in rod connections of any given geometric parameter or loading condition.

Steel is presently the most widely used rod material, but since steel is susceptible to corrosion, consequently surface protection is required. Rods produced from Fiber-Reinforced-Polymers (FRP) are not only impervious to Chloride and low pH chemical environments; they are also lighter, electrically non-conductive, and thermally low-conductive.

Threaded FRP rods bounded into timber with polyurethane adhesive are shown in Figure 1-3. Few past studies have investigated timber joints using glued-in FRP rods joints under quasi static loading [8, 15]; the results from those which did revealed that the pull-out tensile capacity of glued-in FRP is related to the adhesive type, bonded length and timber species.

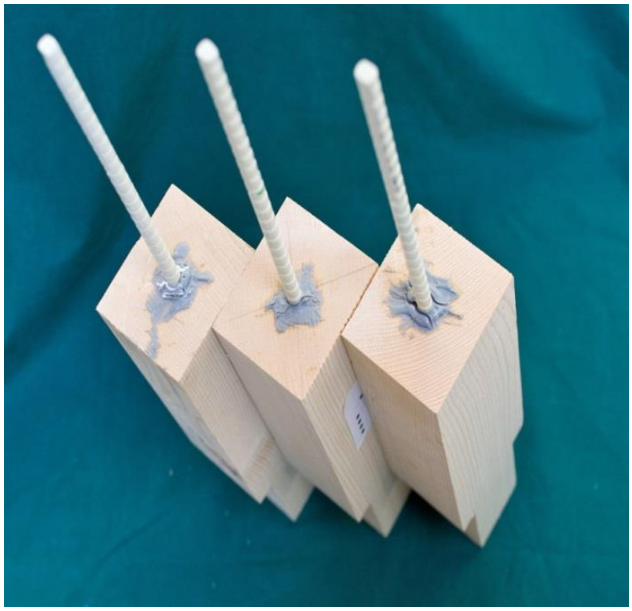

Figure 1-3: Timber Joints with Glued-in Profiled FRP Rods

1.2 RESEARCH NEED

The majority of previous research on glued-in rods focused on testing single rods, usually steel, and relatively little attention has been paid to materials other than steel. Additionally, most of these studies focused on the pull-out capacity of single rod and so little guidance exists for multiple rod configurations. A universal agreement regarding design criteria for these connections has not been reached.

Research on the influence of geometric characteristics on the structural performance of timber joints with glued-in glass FRP (GFRP) rods – conducted by Faghani [15] at the

University of British Columbia (UBC) – showed that the anchorage length and the diameter of the rod affect the pull-out capacity of timber joints with glued-in rods together. These test specimen joints were symmetrically designed, fabricated, and tested with a glued-in rod at both ends of the test specimens. Only the weaker side failed and the effect of the tests on the residual capacity of the surviving sides was unknown. Whether the chosen set-up using two-sided symmetrical test specimens increased the statistical power of the test results had also not been determined by testing the unbroken part of the joints.

Furthermore, most previous research focused on the static capacity of glued-in FRP rods joints which is not enough for possible practical applications such as structures under wind loads for which research regarding fatigue loading is relevant. With these considerations research regarding cyclic loading and the residual capacity of timber joints with glued-in FRP rods was deemed valuable.

1.3 OBJECTIVES

The objectives of the present research are:

i) To determine the residual capacity of the surviving second sides of previously tested glued-in rod connections subjected to quasi-static monotonic tension loads and compare the capacity of the two sides; and

ii) To determine the fatigue capacity of glued-in GFRP rods using a novel loading protocol named as PYHBAL.

2. STATE OF THE ART

2.1 HYBRID SYSTEMS OF GLUED-IN ROD JOINTS

Timber joints with glued-in rods represent a category of hybrid systems involving three materials (timber, rod, and adhesive) in which these materials work together to resist externally applied loads.

2.1.1 TIMBER

A good quality of the timber should be guaranteed to get a reliable connection. Timber as structural material has many advantages such as a high strength to weight ratio, it is a lightweight material, and high aesthetic value. The most common applications for glued-in rods connections are for large joints with high load demands. When designing the connection, whether the rods are set either parallel or perpendicular to the grain direction of the timber should be taken into account. Usually the connecting members are glulam made of softwood. Laminated-Veneer-Lumber (LVL) members have also been used for investigating the tension and moment-resisting performance of glued-in rod connections [5]. In these investigations, it was found that high moisture content (MC) may severely decrease the connection capacity.

2.1.2 ADHESIVE

The purpose of the adhesive or resin is to provide a continuous bond between the timber and the rod to transfer and sustain loads. Over the years a wide range of different types of adhesives have been tested in glued-in rod connections. In general, in earlier years, wood adhesives were based on phenol-resorcinol (PRF) or epoxy adhesives (EPX), while later work has included the use of polyurethanes (PUR). The pull-out capacities of three types of adhesives, namely i)

phenol-resorcinol, ii) epoxy and iii) polyurethane, were tested and compared as part of the large-scale European research project GIROD (Glued-in Rods for Timber Structures) [8]. It was concluded from the GIROD project that the pull-out capacities work strongest for EPX, followed by PUR and PRF [8].

The degree to which the adhesive bonds with the rod and the timber controls the capacity of the connection. An effective design will ensure that the adhesive bond will not be the weakest link in the connection [6], thus avoiding a brittle failure mode. However, the choice of adhesive depends not only on its adhesion to the adherends but also the connection geometry, the material type and strength of the rod and the wood species, since different adherents may form different bonding strength with different adhesives [9]. However, in most studies where the influence of geometrical parameters has been of interest, the adhesive was not a variable in the tests.

2.1.3 ROD MATERIAL

Steel is the most commonly used rod material for connections, since it permits the design of joints with a ductile failure mode. In most cases, steel with threads is used because the increased area for adhesion and mechanical interlocking provides a better connection performance. A large number of studies investigated the pull-out capacity of single threaded glued-in steel rods. [16-21]. Results revealed that threads provide mechanical interlock and convenience for assembling steel members. Connections using reinforcement bars glued-in at angles have shown to be an efficient selection regarding both production method and performance [11].

Compared to steel, FRP is less commonly used for rods. Nevertheless, rods made from GFRP and carbon-FRP (CFRP) revealed that these materials perform well in terms of light weight, high resistance to corrosion and ease of manufacturing (as long as surface preparation by

sandpapering the rod provided good adhesion [12, 13]. Another material for glued-in joints are hardwood dowels [14], which provide the advantage of smaller differences between the moduli of elasticity of the connected materials and are commonly applied in Japan.

2.2 MECHANICS OF GLUED-IN RODS

For the structural analysis of glued-in rod connections, it is important to understand the mechanisms that govern their behavior. The connection represents a hybrid joint made up of three different materials (wood, adhesive, and rod), each with different stiffness and strength properties which have to resist external loading simultaneously. This complexity is one of the reasons for the current lack of full understanding of the behavior of this joint type, as well as a contributing factor obstructing agreement on a unified design approach [15].

The behavior of joints with glued-in rods depends on geometric parameters such as the spacing between rods (e_1), edge distance (e_2) and diameter of rod (d), see Figure 2-1 and Table 2-1. The influence of these factors as well as the loading and boundary conditions has been the subject of past research to develop design formulas for connections with glued-in rods [16, 17]. Most previous studies focused on pull-out tests of the glued-in rods and showed that a rod diameter close to the diameter of hole is beneficial [16]. During axial tensile loading, the load transfer between timber and the rod is governed by the shear stiffness and strength of the adhesive.

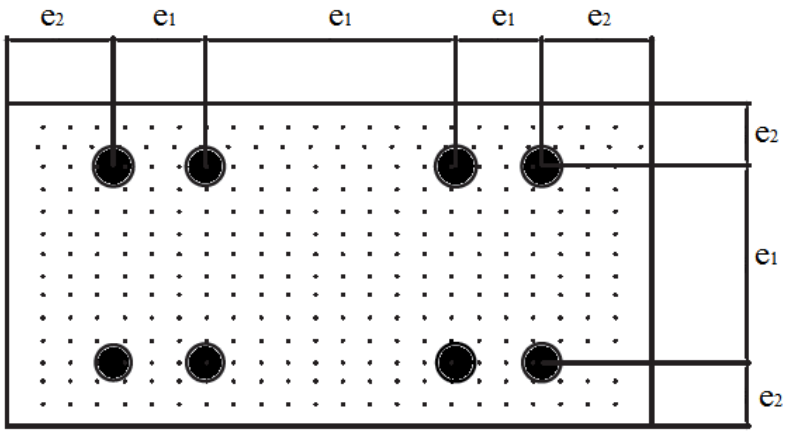

Figure 2-1: Edge Distance for Glued-in Parallel to Grain

Table 2-1: Recommendations Regarding Edge Distance for Glued-in Rods Parallel to Grain

Rods glued-in parallel to grain	prEN1995:2001 [18]	STEP1 [19]	French Professional Guide [20]	DIN 1052:2004-08 [21]
e_1-distance between the rods	4d	2d	3d	5d
e_2-edge distance	2.5d	1.5d	2.5d	2.5d

The number of rods can be treated as another parameter. Testing of multiple rod connections, however, is not frequently done and is difficult to assess, since the number of variables influencing the behavior of these connections compounds with each additional rod and the failure mechanisms; thus, the load transfer behaviors are more complex. In addition, only a few studies have focused on combined loading modes (e.g. combined shear and bending), which are relevant for applications like moment-resisting connections in which not only axial loading of the rods is involved [22].

2.3 GEOMETRIC CHARACTERICS OF JOINTS

2.3.1 ANCHORAGE LENGTH

Previous experimental studies on the pull-out capacity of glued-in rods showed that the capacity is proportional to the anchorage length and suggested using average shear stress as indicator of connection strength. A previous numerical study [15], however, investigated the distribution of shear stresses parallel to the grain around the bounded area for joints with a 150mm anchorage length and identified the contact area at both ends of the rod as the locations of highest stresses (as shown in Figure 2-2). The different lines in Figure 2-2 represent stresses at different distances from the bond line showing that the stress concentrations are most severe close to the bond line.

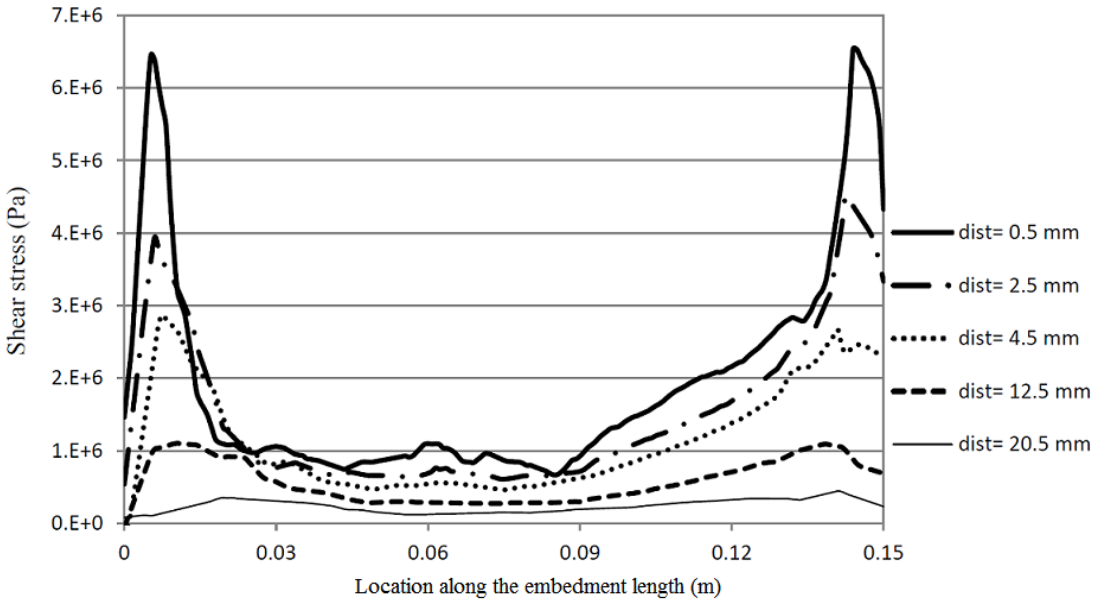

Figure 2-2: Shear Stress along the Embedment at Different Distances from the Bond-line [15]

Broughton and Hutchinson [3] found no significant effect of diameter of the rod on pull-out capacity. They concluded that a larger diameter of the rod could decrease the shear stress at the

interface of rod and adhesive due to larger bonding area. Turkovsky [23] suggested that the parameters of glued-in length l and rod diameter d_h should be combined into a slenderness parameter ($\lambda=l/d_h$). The influence of both anchorage length and diameter of the rod based on a constant was recommended to be taken into account with different exponents.

2.3.2 LOADING CONFIGURATION

The GIROD project concluded that the connection capacity is highest when the load acts along the grain direction and lowest perpendicular to grain [9]. Tests performed on GFRP rods bonded into LVL members, however, did not reveal any significant difference between these two directions [7]. In addition, the failure load will be affected by the loading mode. Several studies regarding assessing the influence of other factors and conditions on the pull-out capacity, such as loading mode were conducted. Rods inserted parallel to the grain (pull-pull loading, Figure 2-3) was the usual case when performing the tests.

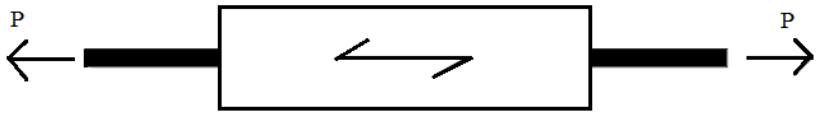

Figure 2-3: Pull-pull Loading Mode [9]

Other types of loading configurations to carry out pull-out strength tests perpendicular to the grain were investigated, e.g. pull-compression, pull-beam and pull-pile foundation, see Figure 2-4 [9]. Due to the large required test specimens size, the pull-beam situation (Figure 2-4, a) is inefficient for testing but closet to practice, since the pull-out strength could be influenced by bending stresses in the beam. The pull-compression setup (Figure 2-4, b) does not correspond to practical construction and additionally, the pull-out capacity is influenced by local excessive compression stresses perpendicular to the grain in the area of the load transfer. Compared to

these two modes, the pull-pile foundation (Figure 2-4, c) where piles are set around the rod with a length equal to that of rod is the most efficient, since, in this mode, the tensile force in the steel rod is balanced by shear force in the timber [9]. The screws act like pile foundations and avoid excessive compression perpendicular to grain due to crushing of timber.

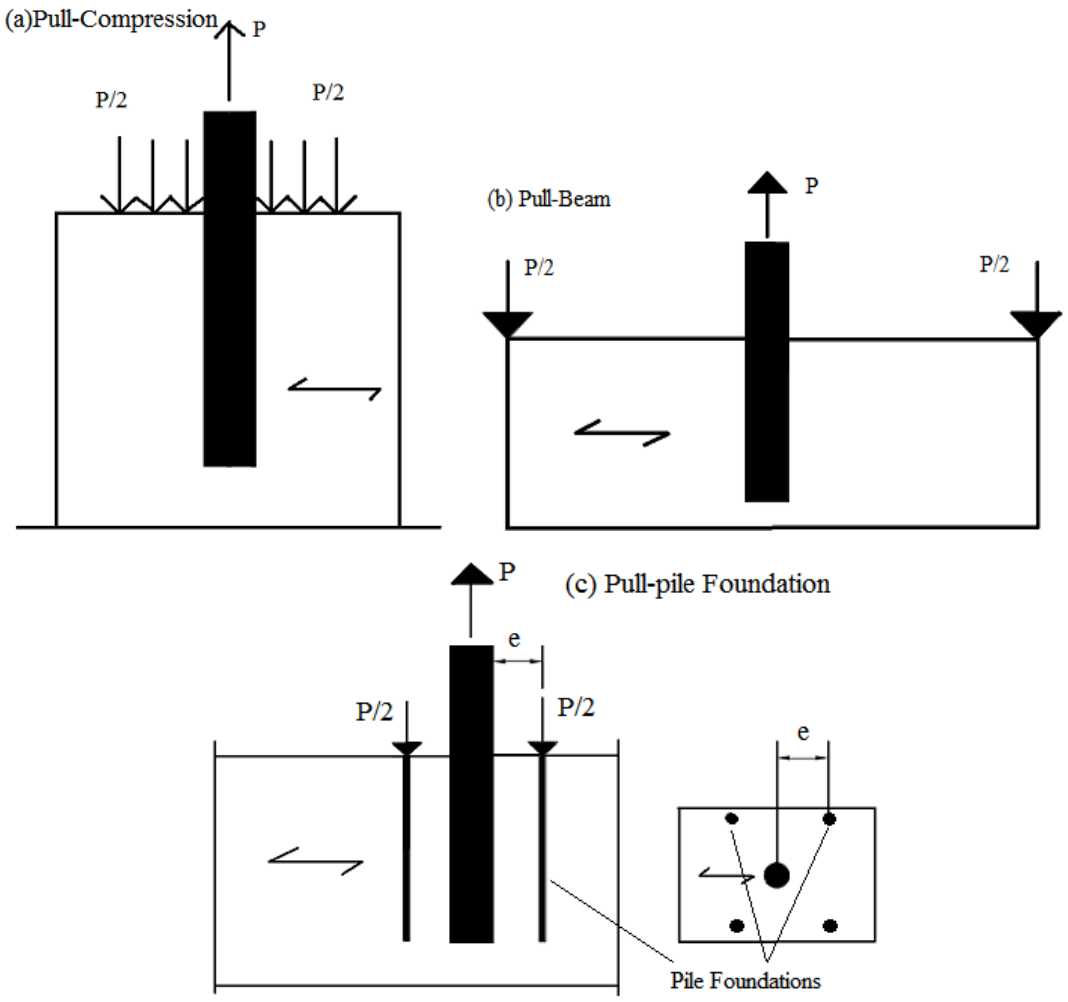

Figure 2-4: Possible Loading Modes: a) Pull-Compression, b) Pull-Beam, c) Pull-pile Foundation [9]

2.3.3 GLUE-LINE THICKNESS

In general, the thickness of bond line used varied between 0.5 and 3mm in prior studies [9]. Three types of adhesives, epoxy (EPX), PRF and PUR were studied by Bengtsson and Johansson

[18]. The differences in capacities between the adhesives when increasing the thickness of the adhesive layers were substantial. While EPX and PUR adhesives exhibited a small increase in pull-out strength with increasing glue line thickness, the PRF adhesive showed a significant decrease of strength which was partially caused by the larger effect of chemical shrinkage during curing [8]. Harvey and Ansell [5] recommended that a minimum glue-line thickness should be 2mm for reaching optimum strength of GFRP rods; beyond that thickness the pull-out capacity does not change very much.

2.3.4 TIMBER DENSITY, CLIMATE AND DURATION OF LOAD EFFECTS

Various opinions exist on the effect of wood density on the pull-out strength of glued-in rods. Theoretically, higher wood density can affect the load bearing capacity by increasing the shear strength of the wood, reducing adherence to the wood, increasing strength of the wood and other effects [22]. The shrinkage and swelling of wood with changing MC can cause considerable stresses and cracking together with a possible loss of adhesion in glued-in joints. Therefore it is recommended to use these connections in service class 1 (temperature and relative humidity conditions resulting in a MC not exceeding 12% corresponding to a typical indoor condition) and service class 2 (temperature and relative humidity conditions resulting in a MC not exceeding 20%, corresponding to unheated but covered conditions, but only with caution in class 3 (temperature and relative humidity conditions resulting in a MC higher than in class 2) [7].

Testing of full-size single rod joints bonded by EPX adhesive [8] revealed that the bonded-in rods perform satisfactory until temperature reached 50 °C. Significant strength loss with EPX and PRF bonded rods were found at temperatures above about 50°C, especially when the test specimens were under load. PUR bonded rods showed a considerable reduction in short term strength slightly above 40°C [8]. Thus, the use of PUR only in non-load bearing applications

when high temperatures may be reached is recommended. Duration of load effect has a similar impact on rods bonded by EPX to the long-term strength loss of timber. However, the load duration effect for PUR bonded rods increased at elevated temperatures and humid ambient conditions [8].

2.4 MANUFACTURING PRINCIPLES

Manufacturing a high quality glued-in rod joint is a challenging process. Different methods for gluing-in rods have been described in the literature. One of the chief concerns is the proper application of adhesive during rod installation. Johansson [18] tested the uniformity of adhesive distribution in a connection; in many cases the adhesive was distributed non-uniformly and the pull-out strength substantially as a result of poor adhesive distribution.

If the joint is to be manufactured with an oversized hole, one quick method is to apply a well-defined amount of adhesive into the bottom of the hole and then insert the rod while rotating it to guarantee a uniform adhesive spread around the sides. Rotating also helps remove entrapped air bubbles in the adhesive layer. Another possible alternative method (shown in Figure 2-5) is to introduce the adhesive through a small perpendicular hole drilled close to the end of the embedment hole until the residual adhesive emerges from the gap near the entrance.

In Sweden, glued-in rod connections are manufactured with undersized holes, where the diameter of the hole normally equals the nominal diameter of the threaded rod minus the depth of the thread [24]. The glued-in connection is formed by applying adhesive to the hole and screwing adhesive-applied rods into the hole. The advantage of this method is that the adhesive is better kept in the hole before curing. The shortcoming is that it is very difficult to guarantee that the adhesive has reached all parts of the rod [24]. Grooving was suggested to assure the spread of

adhesive within the hole uniformly, but as with all adhesive bonded connections, a clean surface is one of the conditions to guarantee proper adhesion [25]. Navigating this dichotomy in a satisfactory manner remains a question for present and future research.

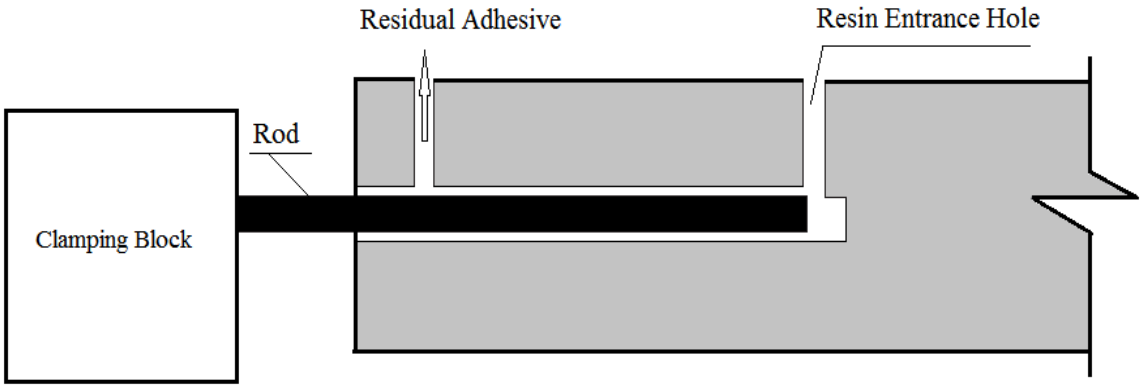

Figure 2-5: One of Glued-in Rods from Sweden [10]

2.5 FAILURE MODES

The location and failure mode, brittle, ductile or a combination of both, are considered the two defining characteristics of a glued-in rod connection failure [25]. The failure location expresses where the failure occurred in the connection. This depends on the materials and their mechanical properties. There exist only five possible failure modes for timber connections with glued-in rods which are I) shear failure along the rod, II) tensile failure of the timber, III) splitting failure of timber, IV) yielding (or breaking) of the rod, and V) shear block failure (shown Figure 2-6).

Shear failure modes I and VII are symptomatic for single or multiple glued-in rods when timber volume around the rods is not sufficient or single rod in axial tension or compression load. Shear failure mode II occurs at the interface between rod and adhesive and is indicative of weak bound strength between rod and adhesive [24].

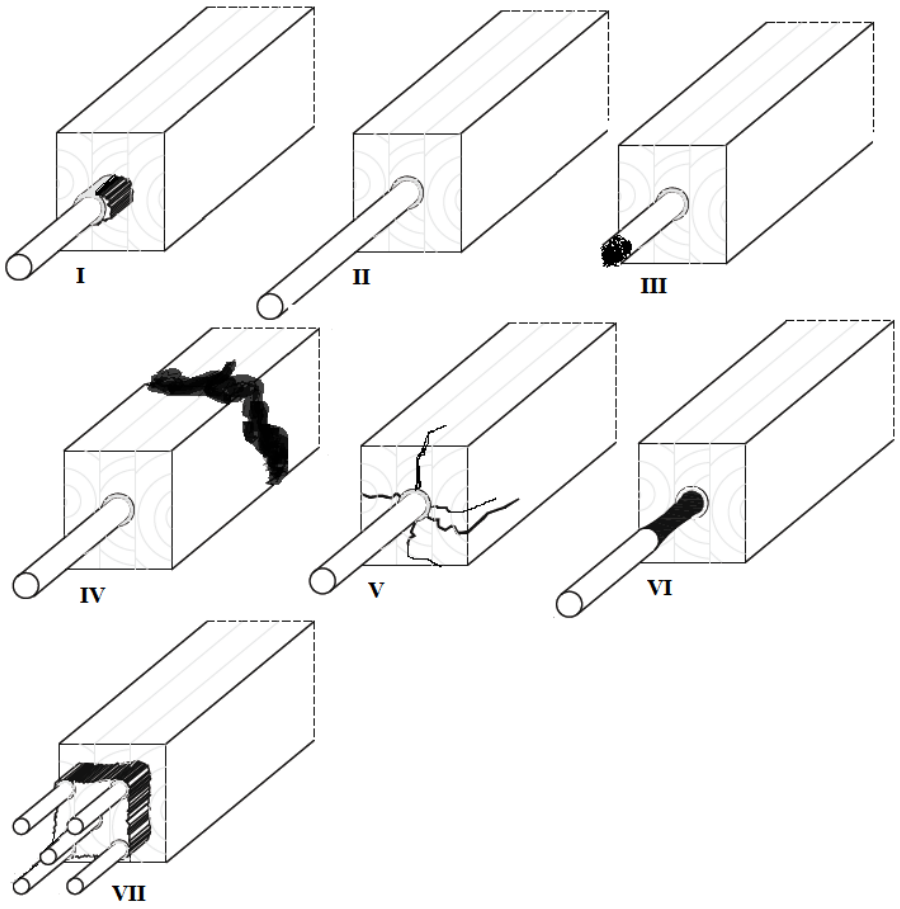

Figure 2-6: Possible Failure Modes: I) Shear Failure at Timber-Adhesive Interface, II) Shear Failure at Adhesive-Rod Interface III) Tensile Failure in Rod, IV) Tensile Failure in Timber, V) Timber Splitting, VI) Yielding of the Rod, VII) Shear Block Failure [28]

Failure modes resulting from tensile loading can happen in the rod or in the timber (III and IV). Failure mode V: Timber Splitting was shown as dominating failure mode for samples with insufficient edge distances, ranging from 1.5-2.25 times the diameter of the rod, and subjected to tensile loading perpendicular to grain. Ductile yielding of the rod is the preferred failure mode for design, since it not only provides a gradual, visible indication of connection failure but also offers the possibility of dissipating and absorbing energy under earthquakes or wind loads [25].

2.6 USE OF FRP AS ROD MATERIAL

2.6.1 Overview

FRP was recommended as an alternative to steel glued-in rods by Harvey and Ansell at the University of Bath in 2000 [5]. GFRP is a cheaper option than CFRP and testing of GFRP rods has revealed that these have advantages compared with steel rods including better compatibility with resin and timber, higher resistance to humid or acid environments and improved performance due to better bonding and reduced weight [12, 13, 23]. Furthermore, other tests of glued-in GFRP rods applied in L-shaped moment resisting LVL structure and U-shaped LVL frame subjected to cyclic loading revealed that connections showed good ductility and capability for the dissipation of energy under dynamic loading [6]. Additional tests of moment-resisting and shear joints using GFRP rods [7] determined that the most suitable resin condition for the bonding of rods into LVL was epoxy applied with a glue-line thickness of at least 2 mm. It was recommended that the surfaces of GFRP pultruded rods should be treated by sandpapering to eliminate splinters and dust resultant from cutting process.

2.6.2 PARAMETRIC STUDY OF GLUED-IN FRP RODS

In 2013 at UBC, Faghani designed, manufactured and tested timber joints with glued-in GFRP rods [15]. Douglas-fir (*Pseudotsuga menziesii*) Glulam with 89 by 89mm cross-section was used. The MC was measured before every test by a moisture meter at three points along each specimen. On average, the MC was 10.8%. Also, the density of randomly selected samples was determined. The average wood density was 562 kg/m^3. The specimen configuration is shown in Figure 2-7. Here, L_3 was an intermediate separation equal to the anchorage length (L_2). The length L_1 was is equal to 120mm to provide gripping length for the testing machine.

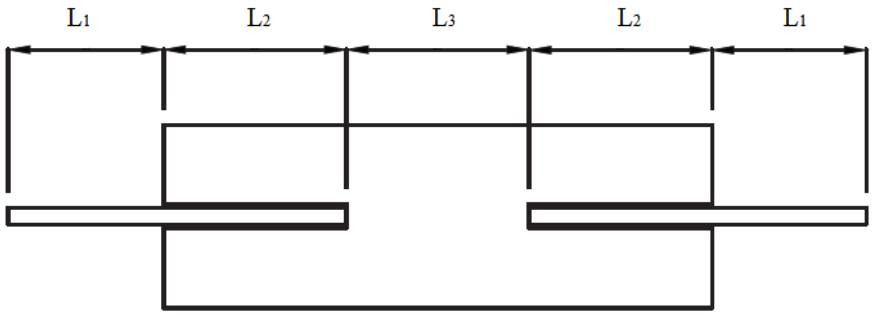

Figure 2-7: Specimen Configuration

Five different anchorage lengths (*L*: 50, 100, 150, 200 and 250mm) were tested for five different rod diameters (*d*: 2/8, 3/8, 4/8, 5/8 and 6/8 in). The two factors: diameter of the rod (Factor A) and anchorage length (Factor B) were completely crossed in the experimental design leading to a total of 25 treatments. Five replicates per series led to a total number of specimens of 125 [15]. The series of specimens were named according to different anchorage length and diameters of rod (shown in Table 2-2). Load-displacement curves were recorded for each specimen; the average capacities per test series are illustrated in Figure 2-8.

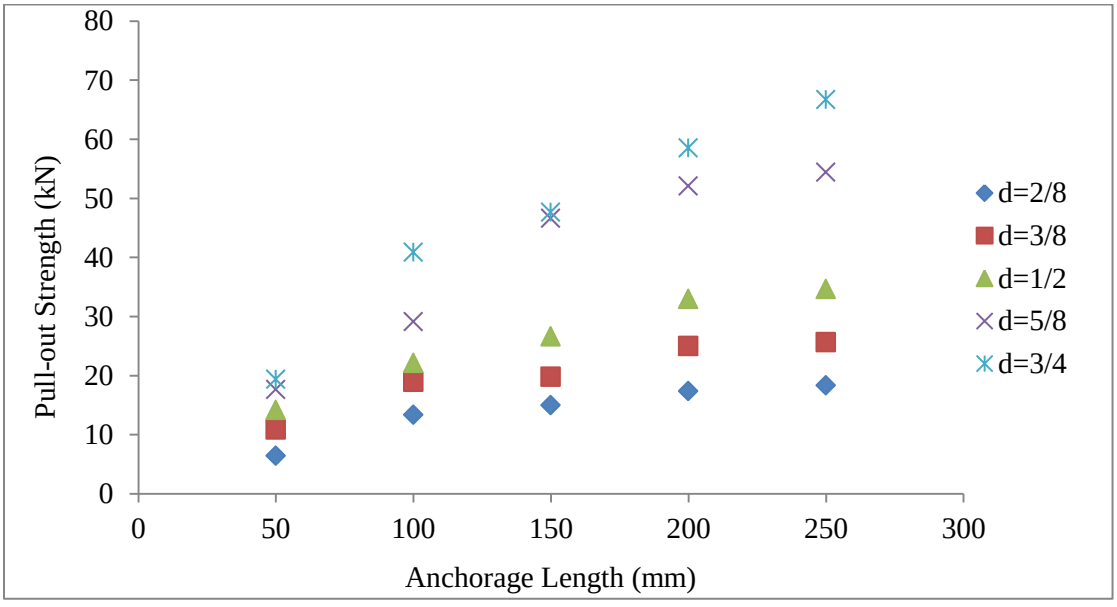

Figure 2-8: Average Capacity of Test Series from Faghani [15]

Table 2-2: Series Names

Series Name	Diameter of Rod (inch)	Anchorage Length (mm)
A1	2⁄8	50
A2	2⁄8	100
A3	2⁄8	150
A4	2⁄8	200
A5	2⁄8	250
B1	3⁄8	50
B2	3⁄8	100
B3	3⁄8	150
B4	3⁄8	200
B5	3⁄8	250
C1	1⁄2	50
C2	1⁄2	100
C3	1⁄2	150
C4	1⁄2	200
C5	1⁄2	250
D1	5⁄8	50
D2	5⁄8	100
D3	5⁄8	150
D4	5⁄8	200
D5	5⁄8	250
E1	3⁄4	50
E2	3⁄4	100
E3	3⁄4	150
E4	3⁄4	200
E5	3⁄4	250

Using these, data provided by Faghani [15], Zhu[1] analyzed the data using the PROC GLM procedure in the software package SAS 9.3 [26]. The assumptions of normal distributions, equal variances and independent observations were tested and confirmed. The level of significance α was set as 0.05. The results of the analysis of variance using the rod diameter (Factor A), the anchorage length (Factor B) and the interaction (A*B) are shown in Table 2-2.

[1] Zhu, H. (2013). Experimental Investigations of the Pull-out Strength of the Timber Joints with Glued-in Rods. Report for FRST 533C. The University of British Columbia, Vancouver, Canada.

Table 2-3: Analysis of Variance for Tests with Glued-in FRP Rods

Source	Degrees of Freedom	Type III SS	Mean Square	F-Value	P-Value
A	4	17,668	4,417	570.9	<0.0001
B	4	10,773	10,773	348.1	<0.0001
A*B	16	3,073	3,073	24.8	<0.0001
Error	97	751	7.7		

The F-value for the interaction ($p< 0.05$) was 24.8 and the null hypothesis of there was no interaction was rejected. Given the apparent interaction between diameter of rod and anchorage length, pairs of mean tests were conducted. The results of pairs of *t* tests and are shown in Figure 2-2. The treatments are sorted in ascending order in respect to the least squares mean of pull-out strength. The black lines indicate the treatments with the mean strength. For example, the average capacity of treatment D2 is statistically not different from those of treatments B4, B5, C3, C4 and C5. As it is shown in Figure 2-9, when diameter of rod and anchorage length are both relatively large, the treatment mean strengths exhibit larger differences. For example, treatment E4 with relatively big diameter of rod (3/4 in) and anchorage length (200 mm) has similar mean strength only to treatments D4 and D5. Treatment A5 with relatively small diameter of rod (2/8 in), however, has similar mean strength to treatments A2, C1, A3, A4, D1, B2 , E2, B3 , C2 and B4. By increasing the anchorage length, the mean strength of glued-in rods becomes more sensitive to the change of the diameter, and vice versa, by increasing the diameter of rods, the mean strength sensitivity to the anchorage length is increasing. This study indicated that by increasing the anchorage length or diameter of rod, the mean strength of glued-in rods is becoming more sensitive to the change of the diameter of rod or anchorage length.

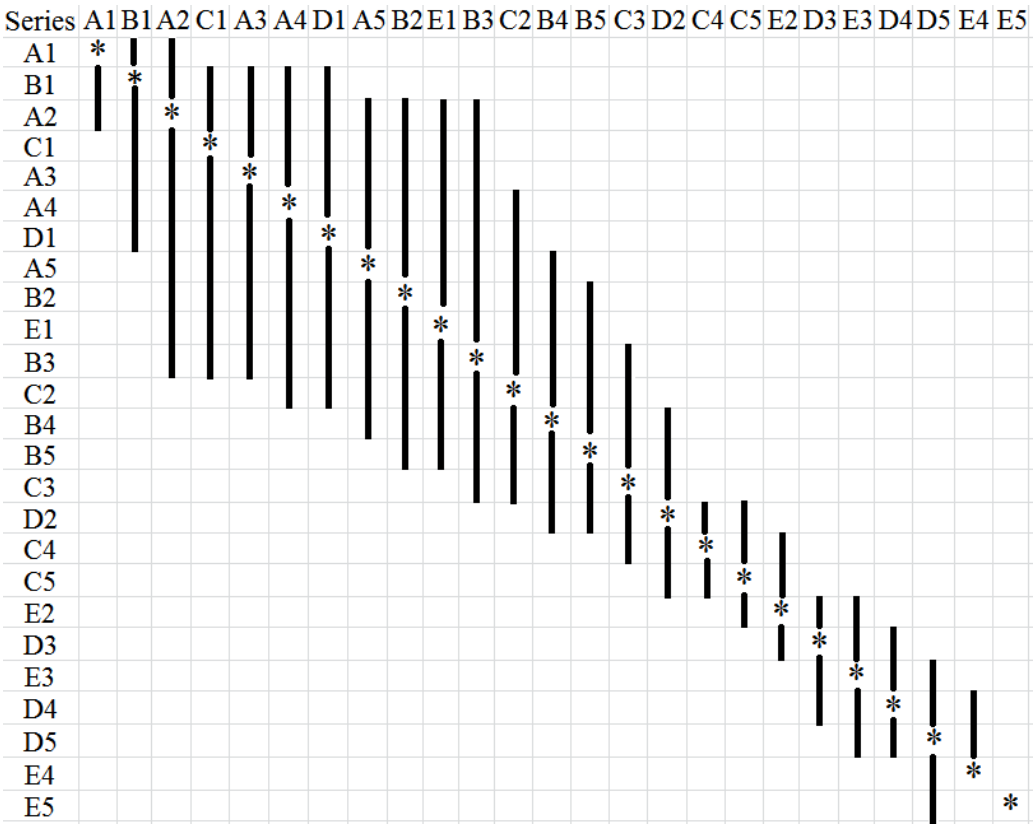

Figure 2-9: The Results of Pairs of T-Tests for Treatments

2.7 EXISTING DESIGN RECOMMENDATIONS

2.7.1 RIBERHOLT

Several sets of formulas have been proposed regarding designing timber connections with axially loaded glued-in rods. The formulas proposed by the pioneer in the field, Riberholt [2], for the axial pull-out capacity, *F*, for a single-rod are as follows:

$$F=f_{ws}\rho d\sqrt{l_g} \quad \text{for } l_g \geq 200\text{mm} \tag{2-1}$$

$$F= f_{wl}\rho d l_g \quad \text{for } l_g < 200\text{mm} \tag{2-2}$$

Here the material withdrawal parameters f_{ws} and f_{wl} are given as f_{ws} = 650N/mm$^{1.5}$ and f_{wl}= 46N/mm^2 for non-brittle glues, such as two-component PURs. For brittle glues, such as resorcinol and EPX, f_{ws} = 520N/mm$^{1.5}$ and f_{wl}= 37N/mm^2. Variable d is the larger value of either the diameter of the drill hole or the outer diameter of the rod; ρ is density of the wood; and l_g is the anchorage length of the rod inside the wood.

2.7.2 GIROD

For the GIROD project [27], the following equations were proposed to calculate the mean shear strength ($f_{v,mean}$) for glued-in rods joints and the capacity of the joint can be calculated by the mean shear strength and the contact area.

For rods bonded with EPX and brittle PUR:

$$f_{v,mean} = \min\begin{cases} 8.0\ \mathrm{N/mm^2} \\ 129 d^{-0.52} \lambda^{-0.62} (\rho/480)^{0.45} \end{cases} \quad (2\text{-}3)$$

and for soft PRF adhesive:

$$f_{v,mean} = \min\begin{cases} 6.3\ \mathrm{N/mm^2} \\ 10.3 d^{-0.17} \lambda^{-0.08} (\rho/480)^{0.45} \end{cases} \quad (2\text{-}4)$$

where d is the larger value of either the diameter of the drill hole or the outer diameter of the rod and $\lambda = l_a/d_h$ ($d_h$diameter of drilled hole in mm, l_a rod anchorage length in mm); and $\rho=\rho_{12}$ (characteristic density of timber at a MC of 12% in kg/m^3).

2.7.3 DIN 1052

According to the German timber design code DIN 1052:2008-12 [28], the design capacity, F, for axially loaded rods glued-in parallel or perpendicular to the grain can be calculated as:

$$F = \pi d l_a f_{v,mean} \quad (2\text{-}5)$$

where d is diameter of the rod (mm), l_a is anchorage length (mm) and $f_{v,mean}$is design value of bond line strength (N/mm^2). The design value of the bond line strength $f_{v,mean}$ (N/mm^2) is derived from the characteristic value $f_{v,k}$ (N/mm^2) which depends on the glued-in length l_a:

$f_{v,mean} = f_{v,k}$= *4.0*, if $l_a \leq$ 250mm

$f_{v,mean} = f_{v,k}$ =*5.25-0.005*l_a, if 250< $l_a \leq$500mm

$f_{v,mean} = f_{v,k}$ =*3.5-0.0015*l_a, if 500< $l_a \leq$1000mm

2.7.4 STEIGER AND WIDMANN

Widmann and Steiger [29] proposed another set of equations for the axial pull-out capacity of glued-in rods parallel to the grain, specifically:

$$F = f_{v,mean}\pi d_h l_a \quad (2\text{-}6)$$

where the nominal shear strength ($f_{v,mean}$) of a single rod bonded parallel to grain is:

$$f_{v,mean} = 7.8N/mm^2 * (\frac{\lambda}{10})^{-1/3} * (\rho/480)^{0.6} \quad (2\text{-}7)$$

The pull-out capacity of glued-in rods oriented perpendicular to the grain can be determined with:

$$F = k_1 A_g^{k_2} \quad (2\text{-}8)$$

where $A_g = l_a * \pi * d_h$, $l_a$is the anchorage length, $d_h$is the drilled hole diameter, factor k_1= *0.045* and factor k_2= *0.8*; $\lambda = l_a/d_h$ and $\rho=\rho_{12}$ (characteristic density of timber at MC 12%).

2.7.5 EUROCODE 5

The formula to calculate the pull-out capacity, *F*, of a single glued-in rod from Eurocode 5, Part 2: Design of Bridges [30] is as follows:

$$F = \pi \, d_{equ} \, l_a \, f_{v,k} \tag{2-9}$$

$$f_{v,k} = 1.2 \, 10^{-3} \, d_{equ}^{-0.2} \, p_k^{1.5} \tag{2-10}$$

where ρ_k=380kg/m^3; $d_h$is the drilled hole diameter; d_{equ} is the minimum of the drilled hole diameter and the 1.25 time diameter of the rod $d_{equ}=min\ (d_h,\ 1.25d)$; $l_a$is the anchorage length; and $f_{v,k}$ the shear strength of the timber.

2.8 ESTIMATION OF SECOND SIDE CAPACITY

In many studies, the capacity of connections with glued-in rods is determined through pull-pull tests that use test specimens with a rod glued-in at each side of the specimen. In most studies, the stronger side is not subsequently tested and its strength is unknown. For the second side capacities, a Weibull distribution could be used. Alternatively, a censored Weibull distribution using the capacities of the first sides may better repeat the distribution of the second sides. In timber engineering, the Weibull distribution has been successfully applied [32].

The Weibull distribution, based on the "Weakest link theory" which assumes that the weakest component in the assembly will control its behaviour, uses a continuous probability distribution and is commonly used in reliability and lifetime data analysis [32]. The Weibull distribution can be applied to relate the stress of *m* sequentially arranged identical brittle structural components, as represented in Figure 2-10. The probability distribution of the stress of a sequential arrangement of *m* elements, namely, the strength of the weakest element can be simulated with

the Weibull distribution with the parameters n and k, where $n = \frac{w}{\sqrt[k]{m}}$ and w and k are the Weibull distribution parameters.

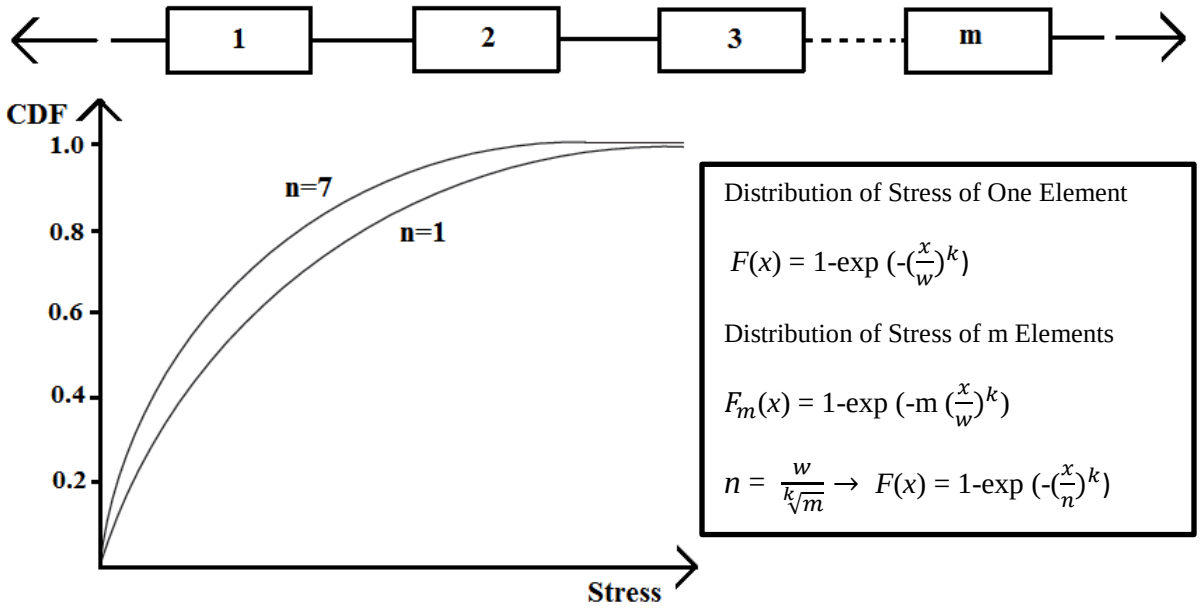

Figure 2-10: Weibull's Weakest Link Theory to Model the Stress Probability Distribution [32]

2.9 FATIGUE TESTS

2.9.1 FATIGUE

Apart from static loading, timber structures may be subjected to fatigue loading. Wind is the most likely source, but fatigue loading can also be caused by any other repetitive force, such as mechanical systems, moving traffic, or testing equipment. Fatigue is the condition in which a material is weakened by applied cyclic deformations. These deformations cause stresses below the ultimate strength of the material, but the repeating action causes microstructural changes associated with cyclic softening or hardening phenomena, leading to micro-cracks which propagate and grow into macro-cracks, eventually leading to material failure [33]. An S-N, or

Woehler, curve for a particular structural component relates a prescribed number of cycles (N) within a nominal, usually constant magnitude, applied stress range (S), that the component can safely withstand. This curve is used as part of overall structural design process [34]. Conventional methods to get design S-N curves are based on observations from experimental fatigue tests that are conducted over the span of many years.

2.9.2 CONVENTIONAL FATIGUE TESTS

The objective of fatigue tests is to determine the fatigue life and the failure location of the specimen under a prescribed sequence of stress amplitudes. Different methods of fatigue tests are classified based upon the sequence of stress amplitudes. Applying reversed constant amplitude stresses to the test specimens until failure occurs is the simplest sequence. Depending upon the applied stress level, constant amplitude tests may be classified into three groups [33] : i) the routine test, where applied loads are selected with the intention that all specimens are expected to fail after a moderate number of cycles (between 104 and 107); ii) the short-life test, where stress levels are selected above the yield stress so that some of the specimens are expected to fail statically; and iii) the long-life test, where stress levels are chosen below or just above the endurance limit and the specimens so that a portion of the specimens do not fail after a pre-assigned number of cycles (between 106 and 107). In some tests, complicated sequences with varying peak stress amplitudes will be required, e.g. the amplitude increasing test exposes each test specimen to reversals of monotonic stresses with increasing amplitudes.

2.9.3 THE PYHBAL FATIGUE LIFE CALCULATION

The PHYBAL fatigue life calculation method was proposed by Starke [36] for the short-time calculation of S-N curves of metals. This method has been successfully applied to steel in heat

treatment conditions and the resulting calculated lifetime predictions has been verified at great length by conventional constant amplitude tests [35]. The PHYBAL method requires only $\varepsilon_{a,p}$ (the plastic strain amplitude), ΔT (the change in temperature), or ΔR (the change in electrical resistance) metallic-material data, which can be determined from just one load increase test and two constant load tests [35]. This is a substantial reduction in required experimental time and costs compared to the conventional determination of S-N curves.

The power law according to Morrow (2-11) and Basquin equations (2-12) can be used to describe cyclic stress-strain curves of load increase tests and constant loading tests.

$$\sigma_a = K \cdot (\varepsilon_{a,p})^n \tag{2-11}$$

$$\sigma_a = \frac{\Delta\sigma}{2} = \sigma_f \, (2N)^b \tag{2-12}$$

Where σ_a is the stress level, K is the cyclic hardening coefficient, n is cyclic hardening exponent, $\Delta\sigma$ is the stress range which is the difference between maximum and minimum stress in a cycle, σ_f is the fatigue strength coefficient, $2N$ is the number of reversals to failure or N (full cycles) and b is the fatigue strength exponent.

To include additional quantities such as the change in temperature ΔT, the change in electrical resistance ΔR and the plastic strain amplitude, $\varepsilon_{a,p}$, the power law can be written in a generalized formula with the cyclic hardening coefficient K_M instead of K, the cyclic hardening exponent n_M instead of n and the measured values M=$\varepsilon_{a,p}$, ΔT or ΔR instead of $\varepsilon_{a,p}$ to obtain:

$$\sigma_a = K \cdot (\varepsilon_{a,p})^n \rightarrow \sigma_a = K_M \cdot (M)^{n_M}$$

The Basquin equation can be expressed similar to (2-12) with the fatigue strength coefficient σ_{fM} instead of σ_f and the fatigue strength exponent b_M instead of b to obtain:

$$\sigma_a = \sigma_f \cdot (2N)^b \rightarrow \sigma_a = \sigma_{fM} \cdot (2N)^{b_M} \quad (2\text{-}14)$$

The fatigue strength exponent b_M can be calculated using the cyclic hardening exponent n_M resulting in:

$$b = \frac{-n}{5n+1} \rightarrow b_M = \frac{-n_M}{5\,n_M+1} \quad (2\text{-}15)$$

Now the fatigue strength coefficient σ_{fM} can be determined and S-N curved can be calculated using the σ_a-N relation from one constant loading test to obtain:

$$N = \frac{1}{2} \cdot \left(\frac{\sigma_a}{\sigma_{fM}}\right)^{\frac{1}{b_M}} \quad (2\text{-}16)$$

The PHYBAL method has been used successfully to calculate the fatigue life of high-strength steel [30]. Moreover, Myslicki [36] conducted a short-term procedure evaluating the fatigue behaviour of adhesively bonded beech-joints using the PHYBAL method in conjunction with a ramp test and constant amplitude test. Results from that analysis showed that fatigue failure of timber joints occurred when the dynamic peak load reached 50% of their tensile strength. The S-N curves from different specimens were drawn based on data collected from tensile and single step tests. In addition, load increase tests yields reliable information about fatigue performance and plastic strain and temperature measurements are qualified for fatigue assessment.

2.9.4 FATIGUE BEHAVIOUR OF JOINTS WITH GLUED-IN RODS

There is little published work on the fatigue behavior of glued-in rod joints, and even less on the fatigue performance of these joints bounded with GFRP rods. As part of the GIROD project, Bainbridge and Harvey [33] investigated the use of commercial adhesives to bond threaded steel rods into oversized holes. Three types of adhesives were compared under cyclic tension loading. It was demonstrated that different adhesives behaved in fundamentally different ways with

respect to the fatigue performance and the eventual mode of failure at the fatigue ultimate limit state. In addition, the fatigue failure modes were similar to those observed in static tests.

Mehrab and Martin [37] conducted research regarding the fatigue behavior of pairs of GFRP rods bonded by epoxy resin in LVL beams. The results of compression-compression fatigue loading tests showed that different joint geometries did not affect the capacity significantly. Solid LVL beams had substantially higher fatigue strength than beams connected by GFRP glued-in rods but the capacity of LVL beams connected by GFRP rods was much higher. However, glued-in rods for beam to beam joints provided significant ductility and energy absorbing capacities.

Rosowsky and Reinhold [27] determined the rate of loading on timber joints is more critical than duration the load. Furthermore, the study regarding the glue line thickness of glued-in GFRP rods and load rate from another study by Mehrab and Martin [37] showed that in fatigue resin is a critical feature of this type of joint and epoxy is sensitive to rate of loading. Moreover, the fatigue strength decreased as glue line thickness increased. Finally, the fatigue failure mode in timber connections with GFRP bounded-in rods was shear failure at the resin and rod interface.

3. PERFORMANCE OF THE SECOND SIDE OF PRE-TESTED JOINTS

The first objective of this research was to compare the capacities of two identical sides of glued-in rod connections. The work done by Faghani [15] showed that a test series provides the strength values of the "weaker" side of each of the *n* specimens. Implicitly, *n* sides survived the tests. The pull-out tension tests of the second unbroken connections were conducted as a follow-up to Faghani's research to test the surviving sides of those specimens and investigate their residual capacity.

3.1 MATERIALS

Pull-out test of these specimens involve three components: timber, rod and adhesive. Industrial stress grade 24f-E Glulam members were boned with GFRP (PLIOGRIP 7779) rods by Polyurethane adhesive, a polymer composed of a chain of organic units joined by urethane links. Relevant mechanical properties were tested under the ASTM standards D638. The Glulam was manufactured by Structurlam Ltd. using Douglas-fir (*Pseudotsuga menziesii*) and resorcinol-formaldehyde Relevant mechanical properties were tested under the ASTM standards and are illustrated in Table 3-1.

Table 3-1: Mechanical Properties of Glulam, PUR and GFRP [MPa]

Material	Glulam	GFRP	Polyurethane
Tension Strength	20.4	469	29
Modulus of Elasticity	13,100	35	1,184

3.2 SPECIMEN DESCRIPTION

The specimen assembly is illustrated in Figures 3-1 and 3-2. An image of a generic specimen before being cut is presented in Figure 3-3. Here, the five different anchorage lengths (L_2: 50, 100, 150, 200 and 250mm) were tested for each of five different rod diameters (d: 2/8, 3/8, 4/8, 5/8 and 6/8 in). Timber sectional dimensions (L4 and L5) are 89 by 89 mm for all specimens.

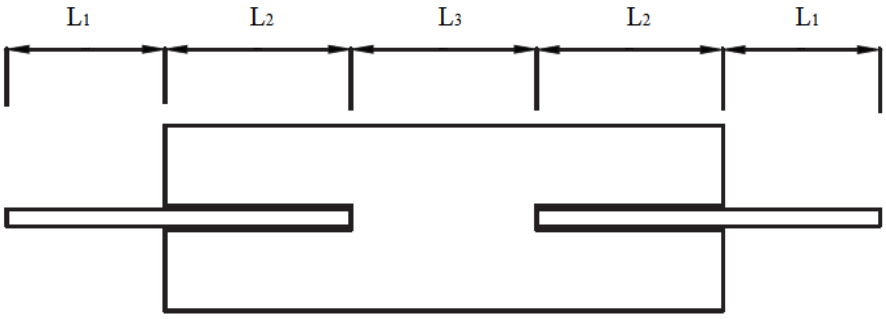

Figure 3-1: Specimen Configuration (Front View)

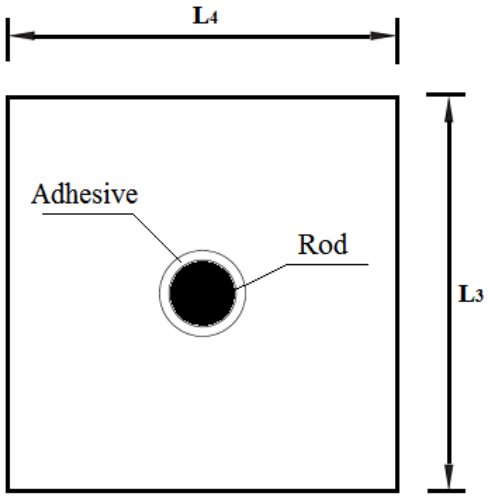

Figure 3-2: Specimen Configuration (Side View)

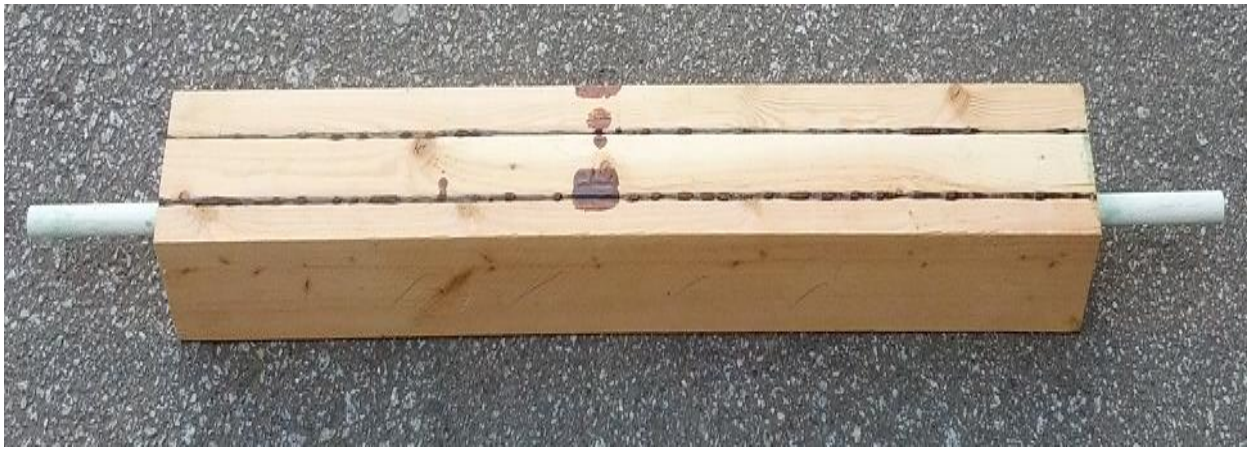

Figure 3-3: Specimen before Being Cut

The surviving rods also had some surface damage caused by the test machine grip during the original testing (shown in Figure 3-4), meaning that the broken rods would not be able to provide proper fixed anchorage for testing. To test the unbroken sides of these specimens necessitated removing the failed side by cutting it away and attaching a bolted connection (see Figure 3-5) to the cut end to provide a fixed end for the specimen to rest in while in the test machine. The cuts also exposed the interior cross-sections of the specimens, showing the variability of the timber and the glue-lines between layers (Figure 3-6).

Figure 3-4: Surface Damage of FRP Rods on Surviving Side of Joints

Figure 3-5: 1/2 in Steel Bolts

Figure 3-6: Variation of Timber Part in Connections with Glue-in FRP Rods

The number of bolts in the new connection was based on the dividing the previous static tension strength of each specimen by the capacity of a single 1/2 in steel bolt (16 kN). Bolt holes were drilled into the timber according to the number of bolts required (Figure 3-7). The centre-to-centre distance between holes was 50 mm within each row; rows were spaced 55 mm centre-to-centre.

Figure 3-7: Specimens after Being Cut and Drilled

For example, a connection specimen with a 50 mm anchorage length had maximum tensile load of 21 kN from previous testing. Its bolted connection therefore consisted of two bolts, providing 32kN of tensile capacity. When anchorage lengths were 100 and 150 mm and the maximum load from previous data was 52 kN, four bolts were selected to provide a design capacity of 63 kN under tension. Also, when the anchorage lengths were 200 and 250 mm and the maximum load from previous data was 69 kN, six bolts with a design capacity of 89 kN were used (see in Table 3-2).

Table 3-2: Capacities of Specimens and Bolts Connections

Anchorage Length [mm]	Static Capacity [kN]	No. of Bolts	Connection Design Capacity [kN]
50	21	2	32
100 and 150	52	4	63
200 and 250	69	6	89

The test specimens were attached to 6 mm thick 125mm by 222 mm steel plates (Figure 3-8) with bolts. The bolts were 1/2 inch diameter and those two steel plates were connected by each other with a 900*900 mm bottom plate with additional 1/2 inch steel bolts.

Figure 3-8: 6mm Thick Steel Plates for Fixing Specimens

3.3 METHODS

Specimens were tested until failure under quasi-static monotonic tension in a universal test machine (UTM). The UTM in this research was a Material Test System 810 Machine, with a capacity of 250 kN located at the Wood Mechanics Lab at UBC under laboratory conditions (23°C and 50% RH). The test was displacement-controlled with a speed of 2.5 mm/min until failure, or when the applied load fell below 80% of the maximum load. Load and relative displacements between the rod and the timber member for all specimens were recorded using a Linear Variable Differential Transducer. The test set up is shown in Figure 3-9.

Figure 3-9: Pull-out Tensile Test Setup of Glued-in Rod Connection

3.4 RESULTS AND ANALYSES

3.4.1 FAILURE MODES

Shear failure occurring between adhesive and timber was the dominant failure mode (Figure 3-10) occurring on 61 specimens involving *A, B, C , D , E* series (series names refer to the Table 2-2). Of the remaining 64 specimens, 4 failed at the interface between adhesive and timber with timber splitting (Figure 3-11), and 23 (all from series D and E) failed in pulling-out a small timber block (Figure 3-12); 26 specimens with small diameter rods (series A3-A5 and B3-B5) failed in the rods themselves (Figure 3-13); only 1 specimen in series D failed in the rod but this

was due to substantial damage on the remaining rod from the previous test.1 specimen from series E5 with the deepest anchorage length and biggest diameter, failed in timber splitting (Figure 3-14), followed by shear failure along the embedment length which occurred in the whole contact area (shown in Figure 3-15).

Figure 3-10: Shear Failure between Glue and Timber Surface

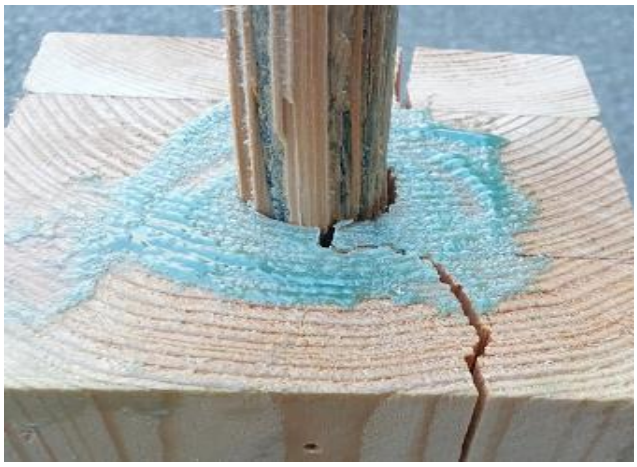

Figure 3-11: Shear Failure with Splitting in Timber Part

Figure 3-12: Rod Pulled Out with Small Timber Block

Figure 3-13: Tension Failure in Rods

Figure 3-14: Timber Splitting

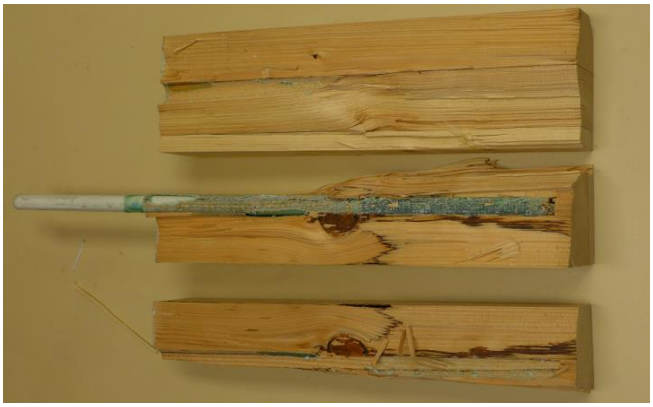

Figure 3-15: Shear Failure along the Whole Embedment Length

3.4.2 JOINT CAPACITY

Table 3-3 summarizes the average capacities and average relative displacements at failure of the two sides from all test series. The individual test results and failure modes of each specimen are given in Appendix-A; the individual relative displacements are shown in Appendix-B. The average capacities for the first side ranged from 6.4 to 70.2 kN versus 10.5 to 70.2 kN for the second side. The average displacements at failure for the first side ranged from 0.5 to 1.7 mm and from 0.4 to 2.6mm for the second side.

For engineering design purposes, the 5th percentile strength values of connection capacities are of interest. For each series by side, the Weibull and the normal distributions were estimated by using MLM. For the second side, a censored Weibull distribution was also filled for the A1 series. Since the normal distribution was similar to the Weibull distribution, the normal distribution was used to calculate capacity percentiles.

The 5th percentile strength values from the cumulative distribution functions are presented in Table 3-3 and were based on sampled standard deviations and means, using the assumption that the capacities of glued-in rod joints follow a normal distribution.

Table 3-3: Comparison of Capacity and Displacement between First and Second Side

	Average Strength [kN]			5th % Capacity [kN]		Average Relative Displacement [mm]		
Series	1st side	2nd side	p-value	1st side	2nd side	1st side	2nd side	p-value
A1	6.4	10.5	0.01	5.8	8.4	0.7	1.7	0.03
A2	13.4	17.2	0.01	10.7	14.8	1.0	1.4	0.01
A3	15.0	15.9	0.10	13.5	14.9	1.0	2.1	0.11
A4	17.0	16.9	0.59	16.1	14.5	1.0	1.6	0.06
A5	18.3	16.3	0.08	17.4	13.4	1.0	2.0	0.28
B1	10.9	12.1	0.48	8.7	6.5	0.6	1.6	0.13
B2	19.0	22.6	0.03	15.6	18.7	1.1	1.0	0.02
B3	19.8	25.2	0.01	15.6	24.0	1.3	2.0	0.03
B4	25.0	24.6	0.76	21.4	20.8	1.1	1.7	0.57
B5	26.0	21.6	0.01	22.0	20.0	1.0	2.0	0.01
C1	14.2	13.0	0.29	11.1	10.8	0.5	1.4	0.13
C2	22.1	26.4	0.10	16.3	21.3	1.0	2.6	0.16
C3	26.6	34.9	0.02	22.2	26.4	1.3	1.7	0.01
C4	32.9	41.5	0.02	30.3	32.8	1.4	1.1	0.01
C5	34.7	38.2	0.11	31.6	32.0	1.3	2.0	0.22
D1	17.6	18.3	0.63	14.6	14.6	0.5	1.3	0.89
D2	29.1	36.5	0.01	23.3	34.2	1.1	1.2	0.02
D3	46.6	49.0	0.24	41.8	44.1	1.5	1.4	0.55
D4	52.1	52.9	0.89	41.3	35.8	1.5	1.4	0.78
D5	54.4	62.3	0.09	44.0	54.6	1.8	1.8	0.32
E1	19.3	20.4	0.33	16.3	18.2	0.5	0.4	0.56
E2	40.8	42.1	0.60	37.8	34.4	1.0	0.6	0.67
E3	47.6	50.8	0.24	43.1	41.9	1.3	1.3	0.45
E4	58.5	61.3	0.35	52.1	53.3	1.5	1.3	0.35
E5	66.7	70.2	0.37	62.0	61.6	1.7	1.9	0.34

Table 3-3 also lists the p-value results from t-tests applied to assess whether there is a difference in mean capacities and displacements between the two sides. The t-tests were conducted under the condition that the two sides have different variances, the populations are normally distributed, and each value is sampled independently. The resulting p-values were compared to the level of significance, α, which was set as 0.05. The p-value is smaller than α

which means that the null hypothesis of no difference between those two means is very unlikely. However, if the p-value is bigger than α, then it fails to reject the null hypothesis of no difference. In series of A1, A2, B2, B3, B5, C3, C4 and D2, the t test results demonstrated that there was difference of the mean capacities in both sides. In contrast, there was no difference of the mean capacities at both sides in the rest series.

3.4.3 CONTACT AREA SHEAR STRENGTH

From the experimental results, it can be concluded that both anchorage length and rod diameter affect the pull-out capacities of glued-in rods joints. The relationship between the contact area (the interface between adhesive and timber as function of length and diameter) and the pull-out capacity is of interest. A linear regression model was fitted to evaluate the relationship between the contact area and the pull-out capacities of glued-in GFRP joints. The data of pull-out capacities are from the two sides, in total 250 operations. The coefficient of multiple determination, R^2, ranging from 0 (poor relationship) to 1 (strong relationship) was used to evaluate the goodness of fit. The model results (R^2 = 0.83) showed that the relationship between contact area and pull-out strength can be considered high, see Figure 3-15.

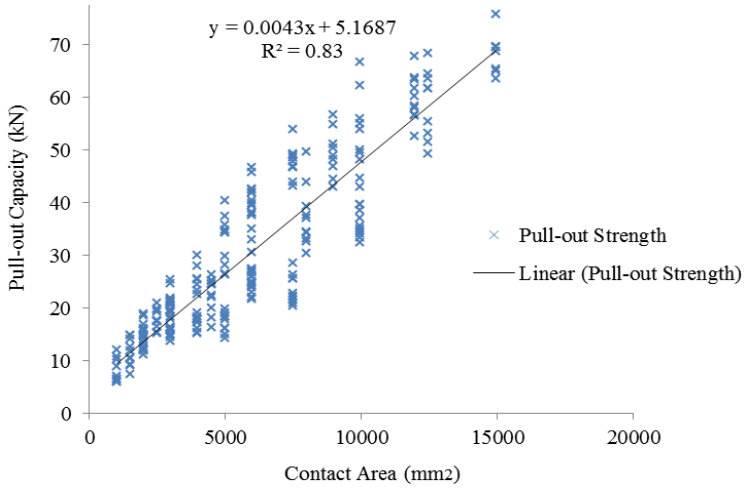

Figure 3-16: The Relationship between Contact Area and Pull-out Strength

3.4.4 COMPARISON WITH DESIGN METHOD ESTIMATES

Working with the preliminary test results, Maximum Likelihood Method was used to estimate the 5th % tensile capacity of glued -in GFRP rod joints. Subsequently, these values were compared to the design values calculated with the equations provided by RIBERHOLT [27], GIROD [28], DIN 1052 [29], Steiger and Widmann [30] and EuroCode 5 [31].

Results from these comparisons (see Figures 3-17 to 3-21) reveal that the design values based on the design equations are higher than the 5th % experimental values. Linear regression modelling used to evaluate how design values from each design procedure method fit the 5th percentile values from the tests. The design equations provide by DIN1052 were closest to the 5th percentile capacities with the highest R^2 value (see in Figure 3-17).

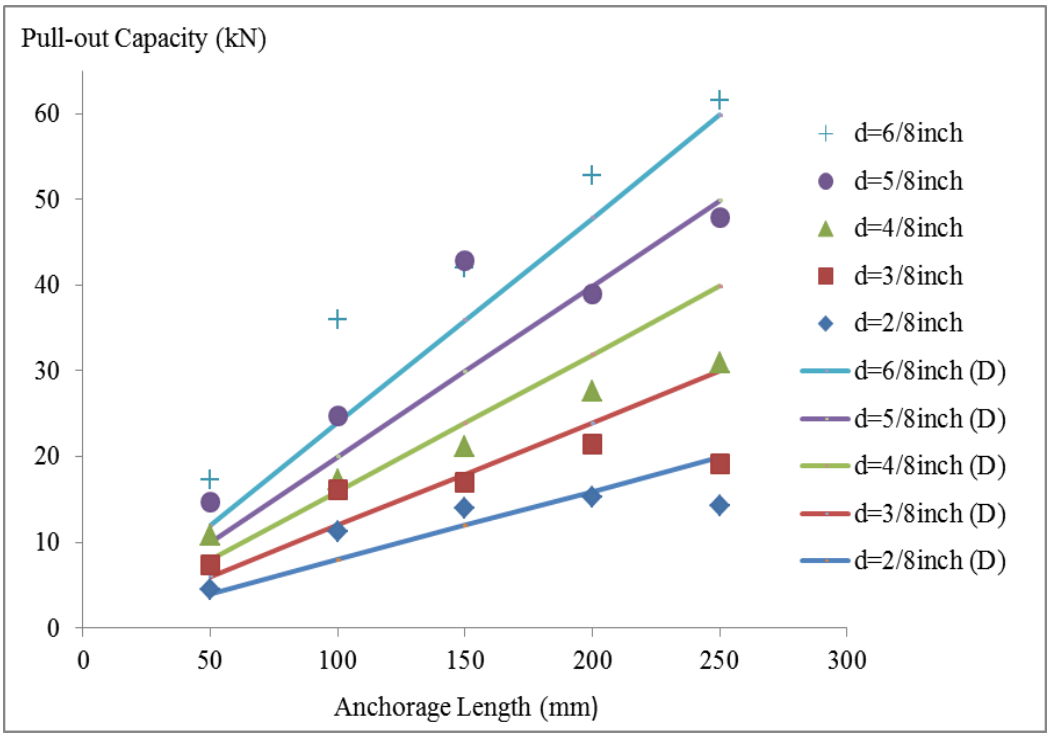

Figure 3-17: 5th % of Test Values vs Design Values (D) according to DIN 1052

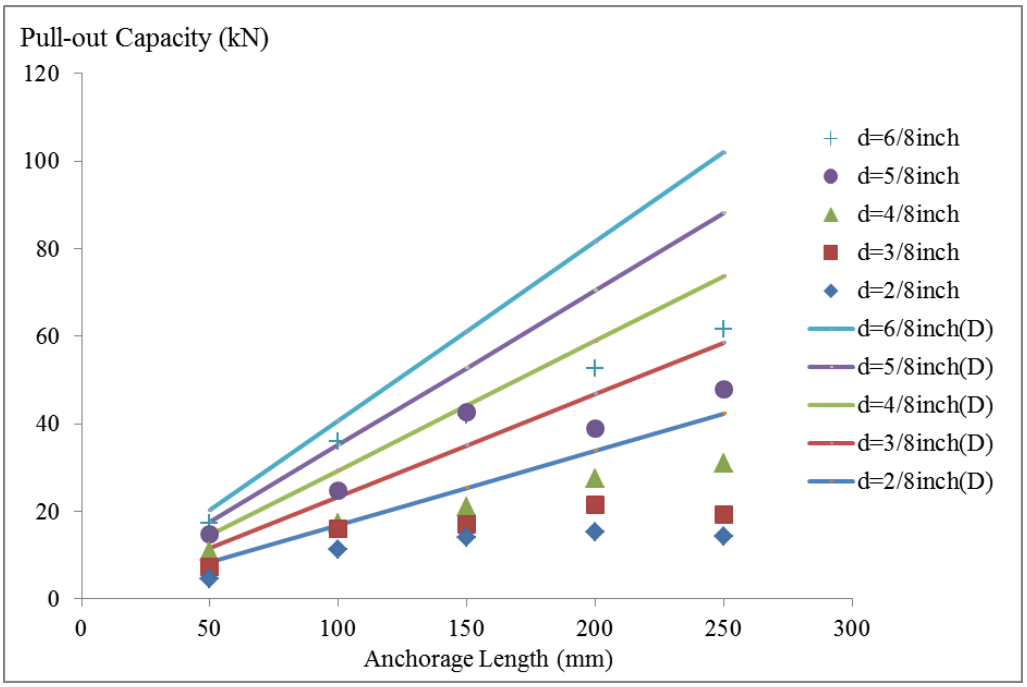

Figure 3-18: 5th % of Test Values vs Design Values (D) according to EuroCode 5

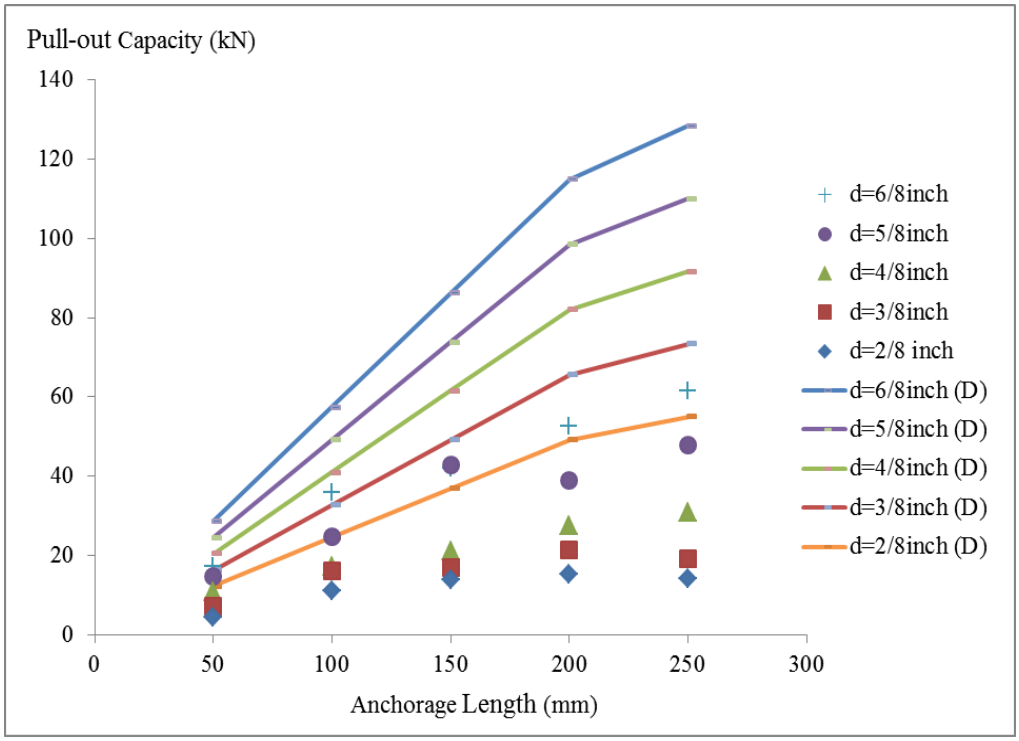

Figure 3-19: 5th % of Test Values vs Design Values (D) according to RIBERHOLT

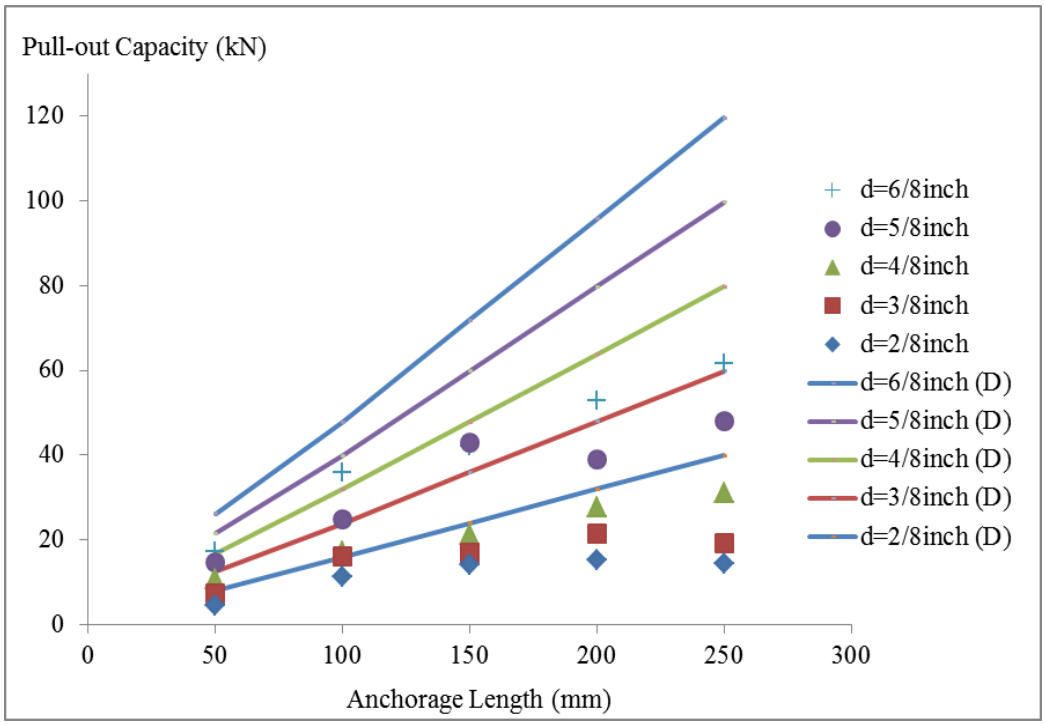

Figure 3-20: 5th % of Test Values vs Design Values (D) according to GIROD

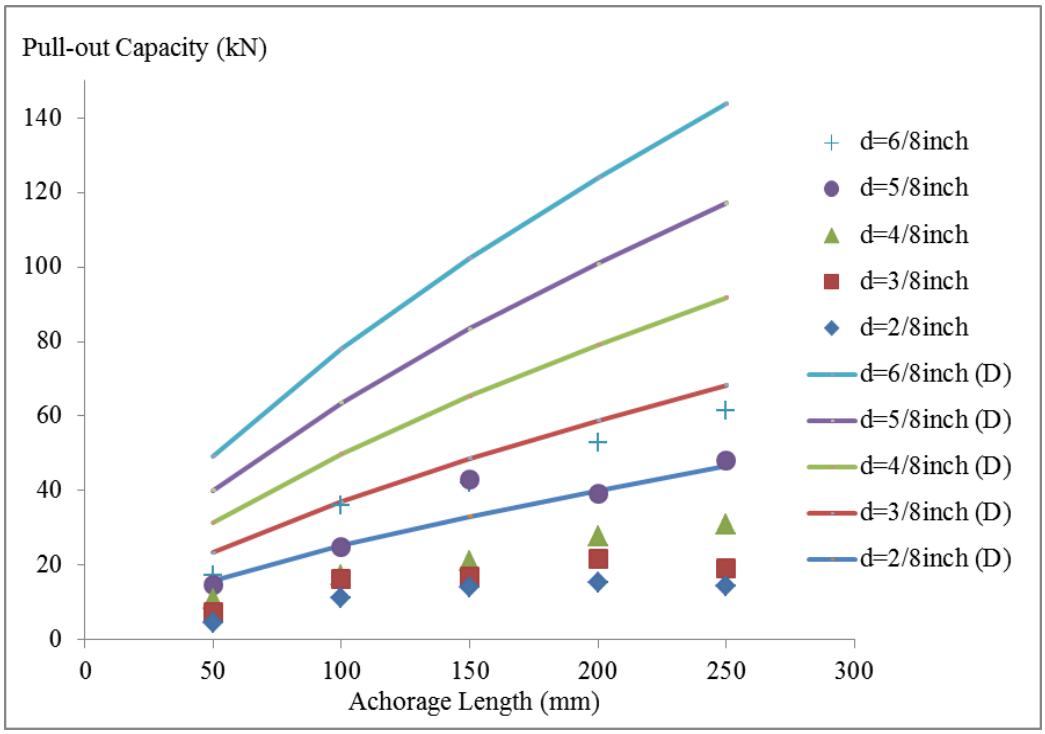

Figure 3-21: 5th 5th % of Test Values vs Design Values (D) according to Steiger and Widmann

3.5 DISCUSSION

In the quasi-static monotonic tension tests, five different failure modes were observed and attributed to various geometric characters, mainly the diameter of the rod and the anchorage length. The anchorage length and the diameter of the rod were confirmed as proportional to the pull-out capacity of glued-in rods joints. Moreover, the linear regression model showing the relationship between pull-out capacity and contact area demonstrated that pull-out capacity is proportional to the pull-out capacity of glued-in rods joints.

The capacities and mean displacements for both ends were compared by means of t tests to determine whether there were statistically significant differences between the mean capacities and mean displacements of the first and second sides. There were differences in mean capacities of first sides that broken in initial tests, versus second sides that survived in initial tests for Series A1, A2, B2, B3, B5, C3, C4, D2. The surviving sides in the second tests from several series were weaker than the sides that failed in the first tests; this finding can possibly be explained by an accumulation of damage accrued from the two tests. The *t* tests were conducted to compare the mean capacities from both sides. In most series, there was no difference of mean capacities at both sides. Only in series of A1, A2, B2, B3, B5, C3, C4 and D2, the *t* test results demonstrated that there was difference of the mean capacities in both sides.

The 5^{th} % capacities of glued-in rods joints from two sides were determined. The design values from design codes were higher than 5^{th} percentile values estimated from experimental data. Those design values may be applied to estimate the steel rods, thus, higher than those experimental valued for GFRP rods.

4. FATIGUE TESTS

The second objective of the research was to investigate the fatigue capacities of timber connections with glued-in GFRP rods. For this purpose, the PHYBAL fatigue estimation method was applied which requires a lower number of tests and allows for a faster estimation of fatigue performance than conventional fatigue tests. Using this method the *S-N* curves for different specimen configurations can be calculated with results from Load Increase Tests (LIT) and subsequent Single Step Tests (SST).

4.1 MATERIALS

A total 35 specimens of glued-in GFRP rods with two identical ends were designed, fabricated and tested, which are similar to a subset of materials tested previously in static tensile experiment for series C1, C2, C3, C4 and C5. The Glulam members were manufactured with Douglas-fir (*Pseudotsuga menziesii*), resorcinol-formaldehyde glue. GFRP rods were fixed into the Glulam members with PUR adhesive. The mechanical properties of the three materials applied are illustrated in Table 3-1.

4.2 SPECIMEN DESCRIPTION

Five different anchorage lengths (L: 50, 100, 150, 200 and 250 mm) were tested for a constant rod diameter of d = 1/2 in. Connection specimens were divided into two groups. The first, named F series, consisted of five replicates for each anchorage length, 25 specimens in total, and was produced in 2012. The second group, named G series, was produced in 2013 with two replicates for each anchorage length, or 10 specimens in total. Figure 4-1 illustrates samples from group F and G specimens.

Figure 4-1: F Specimen and G Specimen

4.3 METHODS

4.3.1 LOAD INCREASE TENSILE TESTS

Fifteen specimens from series F representing five different anchorage lengths were used in the LIT. Thus, there were three replicates for each anchorage length. The fatigue capacity was estimated as 50% of static capacity before experimental test; the loading protocol for each anchorage length was estimated separately. It should be noted that the initial loads and the subsequent load steps varied among the test series. Figure 4-2 shows exemplarily the loading steps of specimens with 150 mm anchorage lengths.

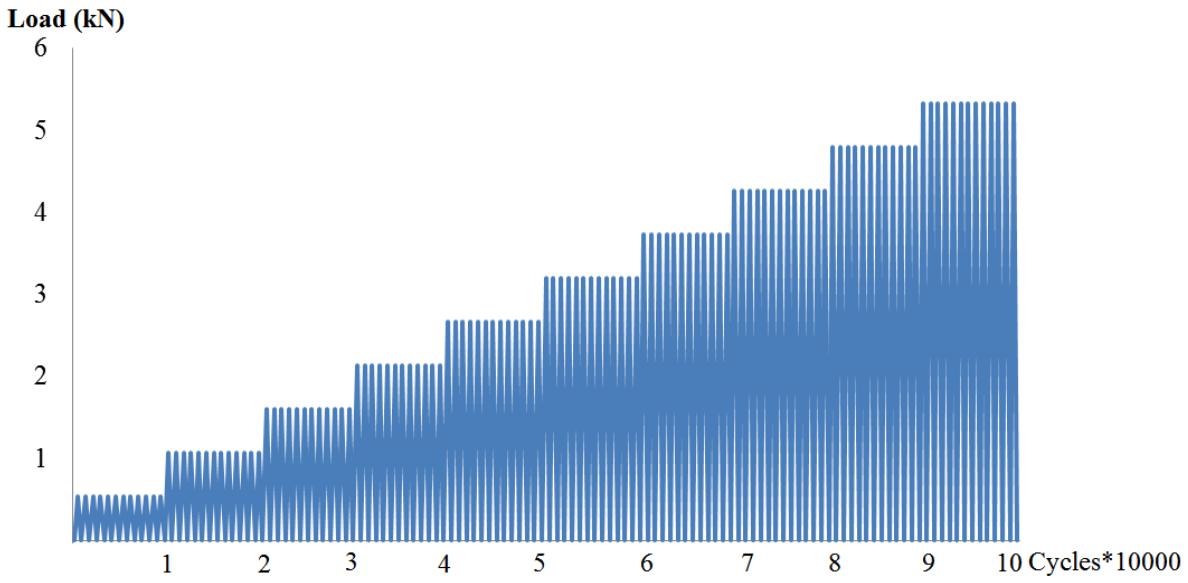

Figure 4-2: Loading Protocol (Load Increase Test)

The initial tensile load was 7.5% of the estimated fatigue capacity. Each subsequent load step increased the load by an additional 7.5% of the estimated fatigue capacity. Table 4-1 shows the initial loads and load increments for each series. There were 10,000 repeated cycles per step under load control with a 1 Hz frequency. The waveform is triangular and load ratio is zero (meaning that the load was varied between maximum tension and Zero). Specimens were tested in an INSTRON Machine 8802 with load capacity of 250 kN under laboratory conditions (23°C and 50% RH). Loading was stopped when the specimen failed. Two Linear Variable Differential Transformers (LVDTs) installed at two end ends to record the relative displacement of each specimen. The applied load, the obtained relative displacements between rod and timber on both sides of the connection, and the number of cycles until failure for all specimens were recorded. The test set up of the LIT is presented in Figure 4-3.

Figure 4-3: Test Setup of Load Increase Tensile Test

Table 4-1: Initial Loads and Load Increments for Each Series

Series	Anchorage Length [mm]	Initial Load and Step Load [kN]
F1	50	0.5
F2	100	0.8
F3	150	1.0
F4	200	1.2
F5	250	1.3

4.3.2 CONSTANT AMPLITUDE TENSILE TESTS

The second step of the PHYBAL method is composed of constant amplitude tests (SST). A total of 20 specimens were tested, ten F specimens and ten G specimens, which were selected to provide two replicates for each anchorage length. The SST involves lower bound and upper bound tests. Since SST were performed to estimate the endurance limit and to select appropriate stress amplitudes for constant amplitude tests. The loading amplitudes for these tests were chosen according to the LIT results. The LIT results revealed that failure occurred at approximately 65% of static joint capacity. Thus, 60% and 70% of static capacity was chosen as lower and upper bound loading amplitudes for the SST under cyclic loads. The SST were performed at a load ratio of R=0 with frequency of f = 1 Hz using triangular load-time functions. Figure 4-4 illustrates a loading pattern. The set-up for the SST was identical to the LIT set-up. Specimens were tested under load control by INSTRON Machine 8802 which has a load capacity of 250 kN under laboratory conditions. Two LVDTs were installed at each end of every specimen. All tests were performed under laboratory conditions (23°C and 50% RH). The applied loads and resulting relative displacements between rods and timber were recorded as well as the number of cycles until specimen failure.

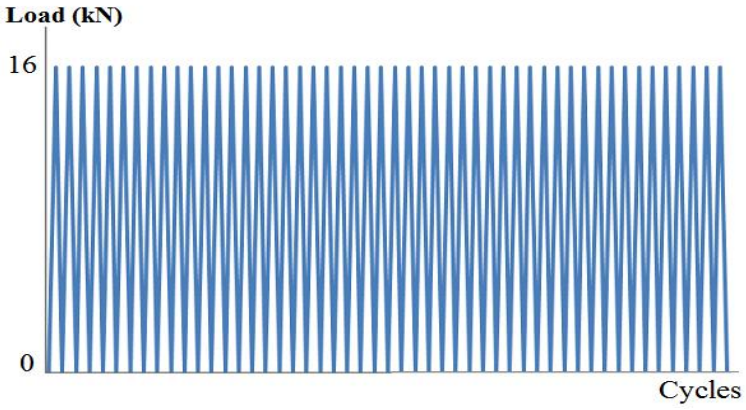

Figure 4-4: Lower Bound Test for Specimens with Anchorage 150mm

4.4 RESULTS AND ANALYSES

4.4.1 LOAD INCREASE TESTS

Fatigue LIT results showed that shear failure was the main failure mode. Most of specimens failed at the interface between the adhesive layer and timber surface as shown in Figures 4-5 and 4-6. Figure 4-5 illustrates the withdrawal failure of an entire rod with small pieces of still attached to the surface of the bonded area with some small unbounded area along the rod. Few specimens failed with some partial blocks of timber still attached to the rods (see Figure 4-7) since specimens with longer anchorage length tended to exhibit purer interface failure.

Figure 4-5: Shear Failure in Specimen with 250mm Anchorage Length

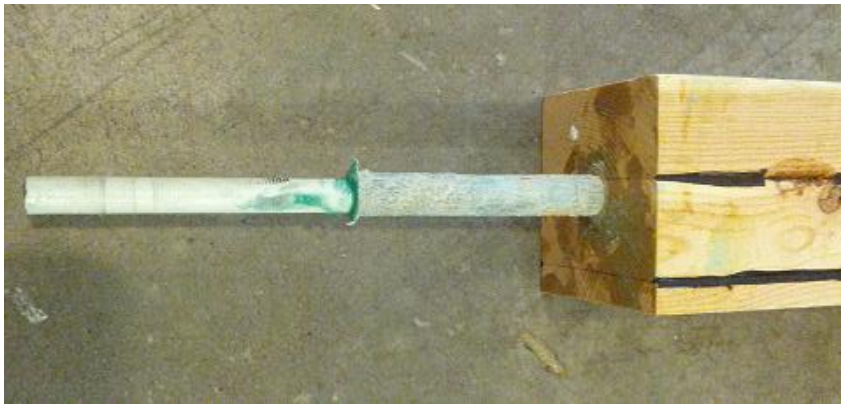

Figure 4-6: Shear Failure in Specimen with 250mm Anchorage Length

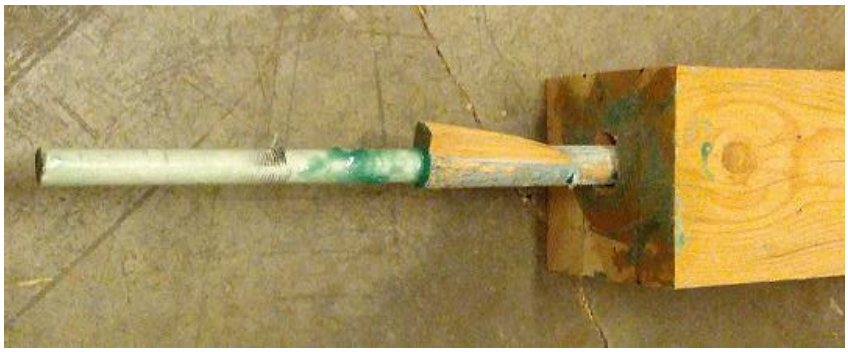

Figure 4-7: Pulled-out Rod with Timber Block

The LIT results are presented in Table 4-2. The fatigue limit can be estimated based on the first change in the slopes of displacement and the number of cycles until failure. The average failure load in the fatigue tests was around 65% of static capacity. The average failure capacities increased as the anchorage length increased. However, the ratio of fatigue and static capacity was the highest in the F-3 collection of specimens (150mm anchorage length).

Table 4-2: Load Increase Test Results

Samples	Length [mm]	Capacity [kN]	Average Capacity [kN]	Average Static Capacity [kN]	Ratio (Fatigue/ Static) [%]
F-1-1	50	7.5	8.9	14.2	63
F-1-3	50	12.2			
F-1-5	50	6.9			
F-2-1	100	13.3	13.8	22.1	63
F-2-3	100	10.8			
F-2-6	100	17.4			
F-3-1	150	13.0	19.0	26.6	69
F-3-2	150	21.0			
F-3-3	150	23.0			
F-4-2	200	19.8	21.0	32.9	64
F-4-3	200	23.5			
F-4-5	200	19.8			
F-5-2	250	23.4	21.3	34.7	62
F-5-4	250	23.4			
F-5-6	250	16.9			

4.4.2 CONSTANT AMPLITUDE TESTS

The results from the upper bound tests (70% of static capacity) and lower bound tests (60% of static capacity) are shown in Table 4-3. Most specimens exhibited longer fatigue life when subjected to 60% of their static short term capacity. Only F-4 Series showed the opposite trend. The possible reason is that some of the F-4 specimens were not well bonded, as shown in Figure 4-8, with the adhesive not being evenly distributed along the rod.

Table 4-3: Constant Amplitude Test Results

Specimen	Anchorage Length [mm]	Capacity [kN]	Ratio (Fatigue/Static) [%]	Failure Cycles [n]
F-1-2	50	8.5	60	32,566
G-1-5	50	8.5	60	2,799
F-1-4	50	9.9	70	2,132
G-1-2	50	9.9	70	1,783
F-2-3	100	13.3	60	11,670
G-2-3	100	13.3	60	3,920
F-2-4	100	15.5	70	4,332
G-2-2	100	15.5	70	293
F-3-4	150	16.0	60	7,756
G-3-2	150	16.0	60	4,034
F-3-5	150	18.6	70	2,212
G-3-2	150	18.6	70	1,971
F-4-6	200	19.8	60	2,502
G-4-4	200	19.8	60	1,382
F-4-1	200	23.1	70	5,910
G-4-3	200	23.1	70	312
F-5-1	250	20.8	60	11,309
G-5-5	250	20.8	60	1,740
F-5-5	250	24.3	70	873
G-5-2	250	24.3	70	449

Figure 4-8: Poorly Bounded F-4-6 Specimen

In most cases, the fatigue life of specimens from series G was much shorter than that of the specimens from series F. The possible reason for this is old adhesive: prior to application PUR has a service life is one year and the G specimens were produced with PUR close to its expiry date. This hypothesis is supported by the color of the adhesive in G specimens which was lighter than it was in F specimens, see Figure 4-9. In addition, the curing environment and gluing skills could also be considered as possible influences on the joint performance.

Figure 4-9: F Specimens (Left) vs G Specimens (Right)

4.5 DISCUSSION

In the numerical analysis of glued-in rods joints [15], the distribution of stresses in this joint was analyzed. Results proved/identified that the interface at the end and top of the embedded rod was the highest stressed location. Moreover, during the load increase test small cracks (shown in Figure 4-10) began to form at both sides of joints when the applied load reached less than half of its final failure load.

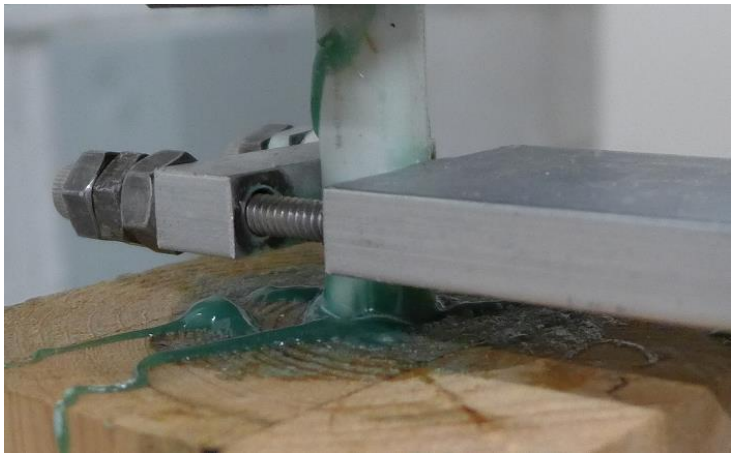

Figure 4-10: Crack at the Top of the Embedded Rod

The relative displacement of both sides from specimens F-1-1 and F-1-5 recorded by LVDTs during the LIT are presented in Figures 4-11 and 4-12. The displacements from the rest of other specimens are presented in the Appendix C. During the LIT the displacements of failed sides of specimens were constant (no displacement) until a certain load step was reached. Then, the displacements increased linearly or abruptly until the specimen failed (shown in the zoomed-in zones in Figures 4-11 and 4-12). After the initial small deformation the displacements increased substantially, up to 2 mm, until failure load level. The displacements of the surviving sides were close to zero, but cracks around the bond lines were visible (shown in Figure 4-13).

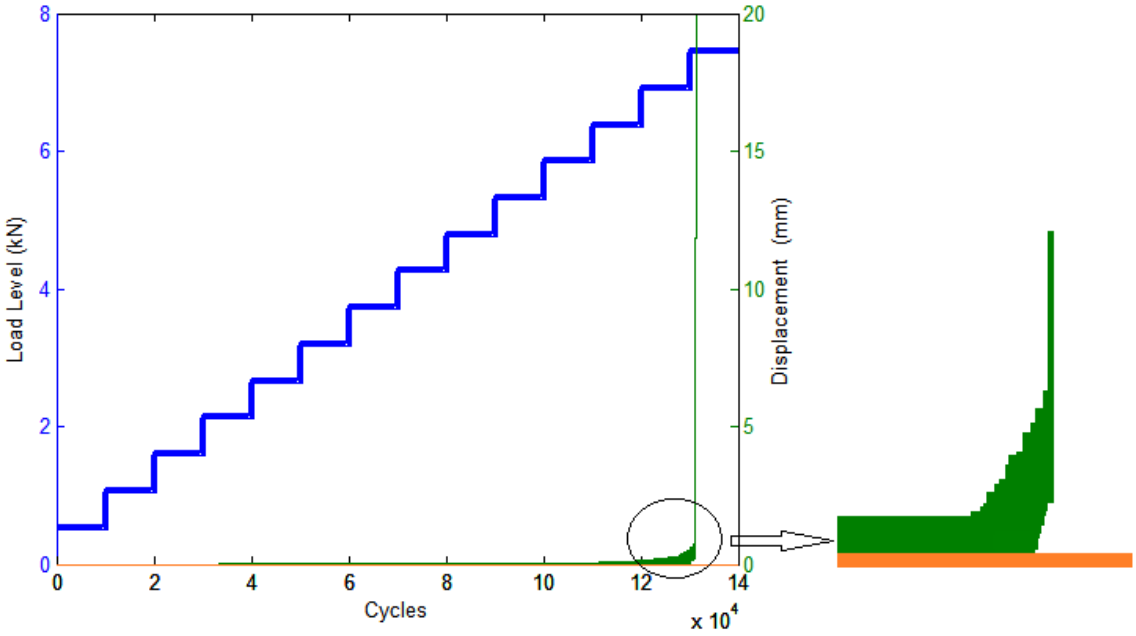

Figure 4-11: Load Displacement of F-1-1 Specimen (Green: Failure Side, Yellow: Surviving Side)

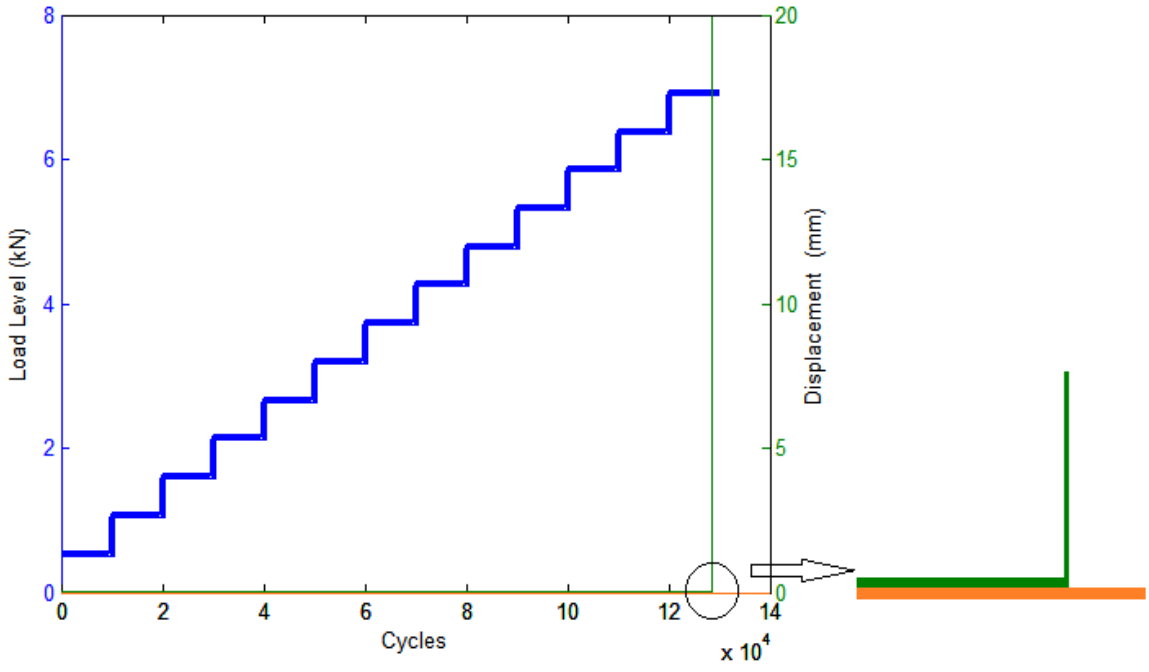

Figure 4-12: Load Displacement of F-1-5 Specimen (Green: Failure Side, Yellow: Surviving Side)

Figure 4-13: Surviving Sides with Small Cracks around the Rod

Constant amplitude test results show that the number of cycles that this joint can survive will reduce substantially after applied loading exceeds 65% of its static strength. The S-N curves based on tensile and single step tests are shown in Figure 4-14. The results show that the fatigue strength increases with anchorage length: for example, specimens from series F exhibited much better fatigue strength than series G specimens with the same anchorage length. F3 series have the highest slope value among F series and G3 series have the highest slope value among G series. The variation in fatigue life decreases as the anchorage length increases in both series.

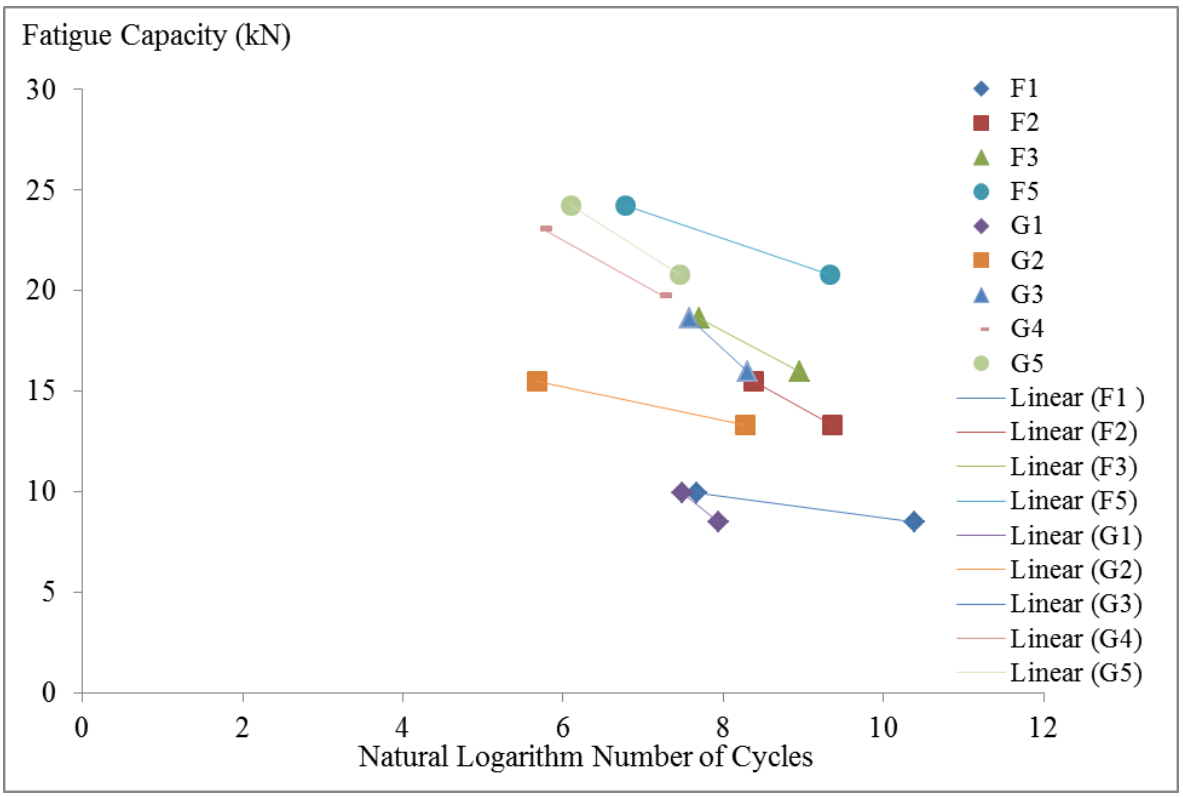

Figure 4-14: Woehler Curves (F1, 2, 3, 5 and G1, 2, 3, 4, 5 Lines) of F (F1, 2, 3, 5 Points) and G (G1, 2, 3, 4 and 5 Points) Specimens Based on Tensile and Single Step Tests

5. CONCLUSIONS

5.1 SECOND SIDE TESTS

This experimental study focused on unbroken surviving sides of connections made with GFRP rods glued into Douglas-fir Glulam specimens with PUR adhesive on both ends. These previously tested symmetrical specimens were re-tested to determine the residual capacity of the surviving rods. To do so, the broken ends of 125 specimens with different anchorage lengths and rod diameters were removed and new bolted connection was installed at the cut end to attach the specimens to a test machine. Those specimens were subsequently tested under uniaxial monotonic quasi-static tension load until failure. The pull-out tensile tests showed that capacities of re-tested surviving sides were usually higher, but sometimes slightly lower than the capacities of the rods that failed during the first tests. The 5th % capacities of glued-in rods joints were estimated based on the testing data and were compared to the predicted capacities based on different design proposals. It was shown that the best fit between test result and design values were obtained using equations based on the German Design Code DIN 1052.

5.2 FATIGUE TESTS

The “PHYBAL” method, which involves load increase and constant load tests, was applied to estimate the fatigue strength of glued-in rod joints. The results of LIT showed that specimens failed when fatigue loads reached approximately 65% of static capacities. Thus, 70% and 60% of static capacities of glued-in rod joints were selected as the upper and low bound loadings of constant amplitude tests. The SST results demonstrated that the fatigue life increases as the peak dynamic load is reduced. When the loading passes 65% of static capacities, the fatigue lives of

glued-in rods joints is reduced substantially. These results indicate that fatigue capacities of glued-in rods joints have a direct relationship with anchorage length. Observations and fatigue lives presented herein, however, are based upon a limited data set, lacking confirmatory data at high numbers of load cycle.

5.3 RECOMMENDATIONS FOR FUTURE WORK

While the existing knowledge gap regarding the structural performance of glued-in FRP rods joints has been decreased, there is still much work to be done to develop universally acceptable design codes. Different wood-based materials and adhesives should be studied and the range of loading and boundary conditions needs to be extended. The most common failure mode in the two experiments was shear failure between adhesive and glulam. Thus, comparisons of different adhesives are recommended. Aging problems should be avoided during the storing of the adhesives. The effect of glulam grain orientations (perpendicular or parallel) on pull-out strength of glued-in FRP rods should be investigated, because although this study focused only on rods parallel to the grain, manufacturing inaccuracies caused some rods to be installed imperfectly and not parallel to the drilled holes. This also affected measurements of rods displacements as well. More work regarding whether an inclination of rods affect the capacities of the joints are recommended. Regarding the fatigue tests, more tests are recommended to investigate a wider range of geometric parameters and the influence of loading rate and peak load on fatigue life.

REFERENCES

[1] Moehler, K., Hemmer, K. (1981). Eingeleimte Gewindestangen. Bauen mit Holz, 83(5), 296–298.

[2] Riberholt, H. (1978). Eingeleimte Gewindestangen. Danmarks Tekniske Hojskole, Lyngby, Denmark, 99(4)-12-23.

[3] Broughton, G., Hutchinson, R. (2001). Adhesive Systems for Structural Connections in Timber, International Journal of Adhesion and Adhesives 21(3), 177–186.

[4] Steiger, R., Gehri, E., Widmann, R. (2007). Pull-out Strength of Axially Loaded Steel Rods Bonded in Glulam Parallel to the Grain. Materials and Structures Journal, 40(10), 827–838.

[5] Harvey, K., Ansell, P. (2000). Bonded-in Pultrusions for Moment Resisting Timber Connections. Proceedings of 33rd Conference of CIB-W18, Delft, Netherlands, 33(12)-7-11.

[6] Kangas, J., Kevarinmaki, A. (2001).Quality Control of Connections Based on V-Shaped Glued-in Steel Rods. Proceedings of 34th Conference of CIB-W18, Venice, Italy, 34(7)-7-4.

[7] Madhoushi, M., Ansell, P. (2008). Behavior of Timber Connections Using Glued-in GFRP Rods under Fatigue Loading. Composite Engineering Journal, 39(2), 249–257.

[8] Kemmsies, M. (1999). Comparison of Pull-out Strength of 12 Adhesives for Glued-in Rods for Timber Structures. SP REPORT 1999:20.SP Swedish National Testing and Research Institute, Building Technology, Boras.

[9] Steiger, R., Gheri, E., Widmann, R. (2004). A Design Approach for Axially Loaded Single Rods Set Parallel to the Grain. Proceedings of 37th Conference of CIB-W18, Edinburgh, Scotland, 37(9)-7-8.

[10] Kangas, J. (2000). Capacity of Fire Resistance and Gluing Pattern of the Rods in V-Connections. Proceedings of 33rd conference of CIB-W18, Delft, Netherlands, 33(12)-7-10.

[11] Gustafsson, J., Serrano, E. (2001). Glued-in Rods for Timber Structures—Development of a Calculation Model. Research Report. Lund University, Division of Structural Mechanics, Lund, Sweden.

[12] Madhoushi, M., Ansell, P. (2004). Flexural Fatigue of Beam to Beam Connections Using Glued-in GFRP Rods. Composites Engineering, 39(2)-243-248.

[13] Moss, J., Buchanan, H., Wong, L. (2000). Moment-resisting Connections in Glulam Beams. Proceedings of 6th World Conference on Timber Engineering, Vancouver, Canada.

[14] Koizumi, A. (2001). Structural Joints with Glued-in Hardwood Dowels. Joints in Timber Structures Journal. 2(9)-28-4.

[15] Faghani, P. (2013). Experimental and Numerical Investigations of Pull-out Strength of Timber Joints with Glued-in Rods. Master Thesis. The University of British Columbia. Vancouver, Canada.

[16] Meierhofer, U. (1988). Schraubenauszugsfestigkeit und Tragfahigkeit von Fichtenund Tannenholz. Holz als Roh und Werkstoff, 46(1), 15–17.

[17] Timber Structure (2003). Design Code SIA 265, Swiss Society of Engineers and Architects. SIA, Zurich, Switzerland.

[18] Johansson, C. J. (1995). Glued-in Bolts. In: Timber Engineering, STEP 1 Basis of Design. Material Properties, Structural Components and Joints. Centrum Hot, Almere, Netherlands.

[19] Faye, C., Magorou, L., Morlier, P. (August 2004). French Data Concerning Glued-in Rods. Proceedings of 37th Conference of CIB-W18, Edinburgh, Scotland, 37(9)-7-10.

[20] Del, M., Piazza, M., Tomasi, R. (2004). Axial Glued-in Steel Timber Joints Experimental and Numerical Analysis. Holz als Roh und Werkstoff, 62(2), 137–146.

[21] DIN 1052:2004-08 (2004). Entwurf, Berechnung und Bemessung von Holzbauwerken. Deutsches Institut fuer Normung E.V. DIN, Berlin, Germany.

[22] Pedersen, U., Clorius, O., Damkilde, L. (1999). Strength of Glued-in Bolts after Full Scale Loading. Journal of Performance of Constructed Facilities, 13(3), 107–113.

[23] Turkovsky, B. (1989). Designing of Glued Wood Structures Joints on Glued-in Bars. Proceedings of the 22nd Conference of CIB-W18, Berlin, German, 22-7-13.

[24] Buchanan, H., Moss, J., Wong, N. (2001). Ductile Moment Resisting Connections in Glulam Beams. Proceedings of NZSEE Conference, Taupo, New Zealand.

[25] Tlustochowicz, G., Serrano, E., Steiger, R. (2011). State-of-the-art Review on Timber Connections with Glued-in Steel Rods. Journal of Material and Structures, 44 (5), 997-1020.

[26] Clark. V. (2004). SAS/STAT 9.1 User's Guide. Cary, North Carolina, USA.

[27] Rosowsky, D. and Reinhold, T. (1999). Rate-of-Load and Duration-of-Load Effects for Wood Fasteners. Journal of Structural Engineering, 125(7), 719–724.

[28] Destuches Institut fuer Normung DIN. (2008). Bericht von Norm 1052:2008-12 Entwurf, Berechnung und Bemessung von Holzbauwerken. DIN, Berlin, Germany.

[29] Widmann, R., Steiger R. (2007). Pull-out Strength of Axially Loaded Steel Rods Bonded in Glulam Perpendicular to the Grain. Journal of Materials Engineering, 40(8): 827-838.

[30] European Committee for Standardization CEN. (1997). Eurocode 5- design of timber structures-Part 2: Bridges ENV 1995-2:1997. Brussels, Belgium.

[31] Steiger, R. and Koehler, J. (August 2005). Analysis of Censored Data-Examples in Timber Engineering Research. Timber Structures CIB-W18 Conference. Karlsruhe, Germany 38-17-1.

[32] Weibull, W. (1961). Fatigue Testing and Analysis of Results. Pergamon, Oxford, London.

[33] Bainbridge, R. and Harvey, K. (August 2011). Fatigue Performance of Bonded-in Rods in Glulam, Using Three Adhesive Types. Timber Structures CIB-W18, Alghero, Italy, 33-7-11.

[34] Nebel, T. and Eifler, D. (2003). Cyclic Deformation Behaviour of Austenitic Steels at Ambient and Elevated Temperatures. Journal of Sadhana, 28(1), 187-208.

[35] Starke, P., Walther, F. (2009). PHYBAL a Short-time Procedure for a reliable Fatigue Life Calculation. Journal of Advanced Engineering Materials, 4(30), 276-282.

[36] Myslicki, S. (2013). Fatigue Behaviour of Adhesively Bounded Beech-joints: Preliminary Experimental Evidence Using a Short-term Procedure. Research Report, Department of Materials Test Engineering, Dortmund University, Dortmund, Germany.

[37] Mehrab, M. and Martin, P. (2004). Experimental Study of Static and Fatigue Strengths of Pultruded GFRP Rods Bonded into LVL and Glulam. Journal of Adhesion and Adhesives, 7 (5) 535-545.

APPENDIX A: TEST RESULTS

Table A-1: Failure Modes of Each Specimen

Specimen	Diameter of Rod (inch)	Anchorage Length (mm)	Failure Modes
A-1-1	2⁄8	50	Shear failure (glue and timber)
A-1-2	2⁄8	50	Shear failure (glue and timber)
A-1-3	2⁄8	50	Shear failure (glue and timber)
A-1-6	2⁄8	50	Shear failure (glue and timber)
A-2-1	2⁄8	100	Tensile failure in rod
A-2-2	2⁄8	100	Shear failure (glue and timber)
A-2-3	2⁄8	100	Shear failure (glue and timber)
A-2-4	2⁄8	100	Shear failure (glue and timber)
A-2-6	2⁄8	100	Shear failure (glue and timber)
A-3-1	2⁄8	150	Tensile failure in rod
A-3-2	2⁄8	150	Tensile failure in rod
A-3-3	2⁄8	150	Tensile failure in rod
A-3-4	2⁄8	150	Tensile failure in rod
A-3-5	2⁄8	150	Shear failure (glue and timber)
A-4-3	2⁄8	200	Shear failure (glue and timber)
A-4-6	2⁄8	200	Shear failure (glue and timber)
A-5-1	2⁄8	250	Tensile failure in rod
A-5-2	2⁄8	250	Tensile failure in rod
A-5-3	2⁄8	250	Tensile failure in rod
A-5-4	2⁄8	250	Tensile failure in rod
A-5-5	2⁄8	250	Tensile failure in rod
B-1-1	3⁄8	50	Shear failure (glue and timber)
B-1-2	3⁄8	50	Shear failure (glue and timber)
B-1-3	3⁄8	50	Shear failure (glue and timber)
B-1-5	3⁄8	50	Shear failure (glue and timber)
B-1-6	3⁄8	50	Shear failure (glue and timber)
B-2-1	3⁄8	100	Shear failure (glue and timber)
B-2-2	3⁄8	100	Shear failure (glue and timber)
B-2-3	3⁄8	100	Shear failure (glue and timber)
B-2-5	3⁄8	100	Shear failure (glue and timber)
B-2-6	3⁄8	100	Shear failure (glue and timber)
B-3-1	3⁄8	150	Tensile failure in rod
B-3-2	3⁄8	150	Tensile failure in rod
B-3-4	3⁄8	150	Tensile failure in rod
B-3-5	3⁄8	150	Tensile failure in rod
B-3-6	3⁄8	150	Tensile failure in rod
B-4-1	3⁄8	200	Tensile failure in rod
B-4-2	3⁄8	200	Tensile failure in rod

Table A-1: Failure Modes of Each Specimen

Specimen	Diameter of Rod (inch)	Anchorage Length (mm)	Failure Modes
B-4-4	3⁄8	200	Tensile failure in rod
B-4-5	3⁄8	200	Tensile failure in rod
B-4-6	3⁄8	200	Tensile failure in rod
B-5-2	3⁄8	250	Tensile failure in rod
B-5-3	3⁄8	250	Tensile failure in rod
B-5-4	3⁄8	250	Tensile failure in rod
B-5-5	3⁄8	250	Tensile failure in rod
B-5-6	3⁄8	250	Tensile failure in rod
C-1-1	1⁄2	50	Shear failure (glue and timber)
C-1-2	1⁄2	50	Shear failure (glue and timber)
C-1-3	1⁄2	50	Shear failure (glue and timber)
C-1-5	1⁄2	50	Shear failure (glue and timber)
C-1-6	1⁄2	50	Shear failure (glue and timber)
C-2-1	1⁄2	100	Shear failure (glue and timber)
C-2-2	1⁄2	100	Shear failure (glue and timber)
C-2-4	1⁄2	100	Shear failure (glue and timber)
C-2-6	1⁄2	100	Shear failure (glue and timber)
C-3-1	1⁄2	150	Shear failure (glue and timber)
C-3-2	1⁄2	150	Shear failure (glue and timber)
C-3-3	1⁄2	150	Shear failure (glue and timber)
C-3-4	1⁄2	150	Shear failure (glue and timber)
C-4-1	1⁄2	200	Shear failure (glue and timber)
C-4-3	1⁄2	200	Shear failure (glue and timber)
C-4-4	1⁄2	200	Shear failure (glue and timber)
C-4-5	1⁄2	200	Shear failure (glue and timber)
C-4-6	1⁄2	200	Shear failure (glue and timber)
C-5-1	1⁄2	250	Shear failure (glue and timber)
C-5-2	1⁄2	250	Shear failure (glue and timber)
C-5-3	1⁄2	250	Shear failure (glue and timber)
C-5-5	1⁄2	250	Shear failure (glue and timber)
C-5-6	1⁄2	250	Shear failure (glue and timber)
D-1-1	5⁄8	50	Shear failure (glue and timber)
D-1-3	5⁄8	50	Shear failure (glue and timber)
D-1-4	5⁄8	50	Shear failure (glue and timber)
D-1-5	5⁄8	50	Shear failure (glue and timber)
D-1-6	5⁄8	50	Shear failure (glue and timber)
D-2-1	5⁄8	100	Shear failure (glue and timber)
D-2-2	5⁄8	100	Shear failure (glue and timber)
D-2-3	5⁄8	100	Shear failure (timber splitting)
D-2-4	5⁄8	100	Shear failure (glue and timber)

Table A-1: Failure Modes of Each Specimen

Specimen	Diameter of Rod (inch)	Anchorage Length (mm)	Failure Modes
D-2-5	5⁄8	100	Shear failure (timber block)
D-3-1	5⁄8	150	Shear failure (timber block)
D-3-2	5⁄8	150	Shear failure (timber block)
D-3-4	5⁄8	150	Shear failure (timber block)
D-3-5	5⁄8	150	Shear failure (timber block)
D-3-6	5⁄8	150	Shear failure (timber block)
D-4-1	5⁄8	200	Shear failure (timber block)
D-4-2	5⁄8	200	Shear failure (timber block)
D-4-3	5⁄8	200	Shear failure (timber splitting)
D-4-5	5⁄8	200	Shear failure (timber splitting)
D-4-6	5⁄8	200	Shear failure (timber block)
D-5-1	5⁄8	250	Shear failure (timber splitting)
D-5-2	5⁄8	250	Shear failure (timber block)
D-5-3	5⁄8	250	Shear failure (timber block)
D-5-4	5⁄8	250	Tensile failure in rod
E-1-1	3⁄4	50	Shear failure (glue and timber)
E-1-2	3⁄4	50	Shear failure (glue and timber)
E-1-3	3⁄4	50	Shear failure (glue and timber)
E-1-5	3⁄4	50	Shear failure (glue and timber)
E-1-6	3⁄4	50	Shear failure (glue and timber)
E-2-1	3⁄4	100	Shear failure (timber block)
E-2-2	3⁄4	100	Shear failure (timber block)
E-2-3	3⁄4	100	Shear failure (timber block)
E-2-4	3⁄4	100	Shear failure (timber block)
E-2-5	3⁄4	100	Shear failure (timber block)
E-3-1	3⁄4	150	Shear failure (timber block)
E-3-2	3⁄4	150	Shear failure (timber block)
E-3-3	3⁄4	150	Shear failure (timber block)
E-3-5	3⁄4	150	Shear failure (timber block)
E-4-1	3⁄4	200	Shear failure (timber block)
E-4-2	3⁄4	200	Shear failure (timber block)
E-4-4	3⁄4	200	Shear failure (timber block)
E-4-5	3⁄4	200	Shear failure (timber block)
E-4-6	3⁄4	200	Shear failure (timber block)
E-5-1	3⁄4	250	Shear failure (timber block)
E-5-4	3⁄4	250	Timber splitting
E-5-5	3⁄4	250	Shear failure (glue and timber)

APPENDIX B: LOAD-DISPLACEMENTS IN STATIC TESTS

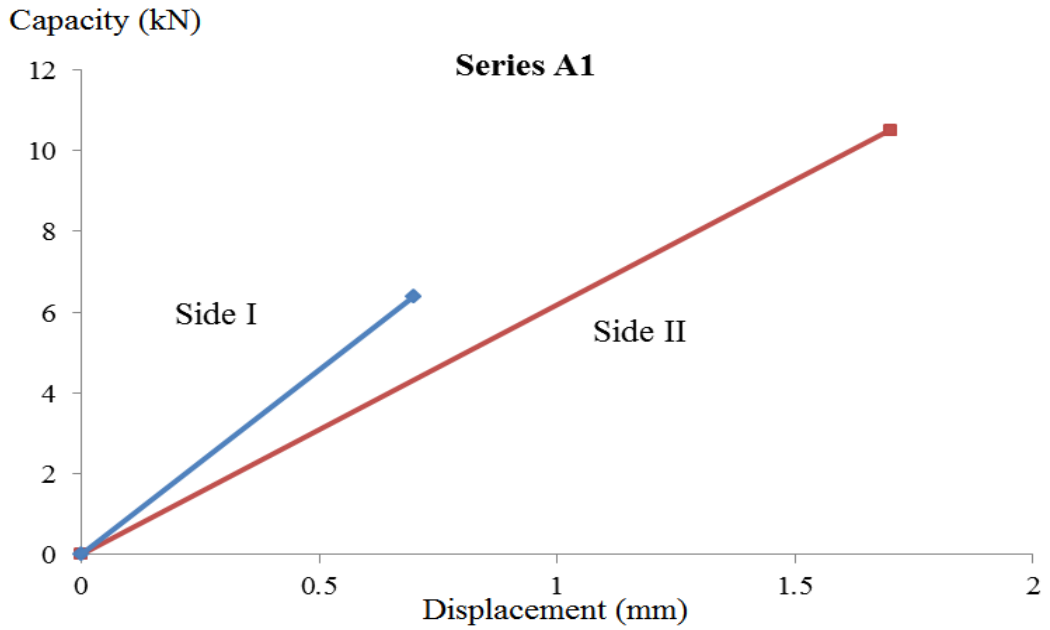

Figure B-1: Displacement vs Capacity of Two Sides (Series A1)

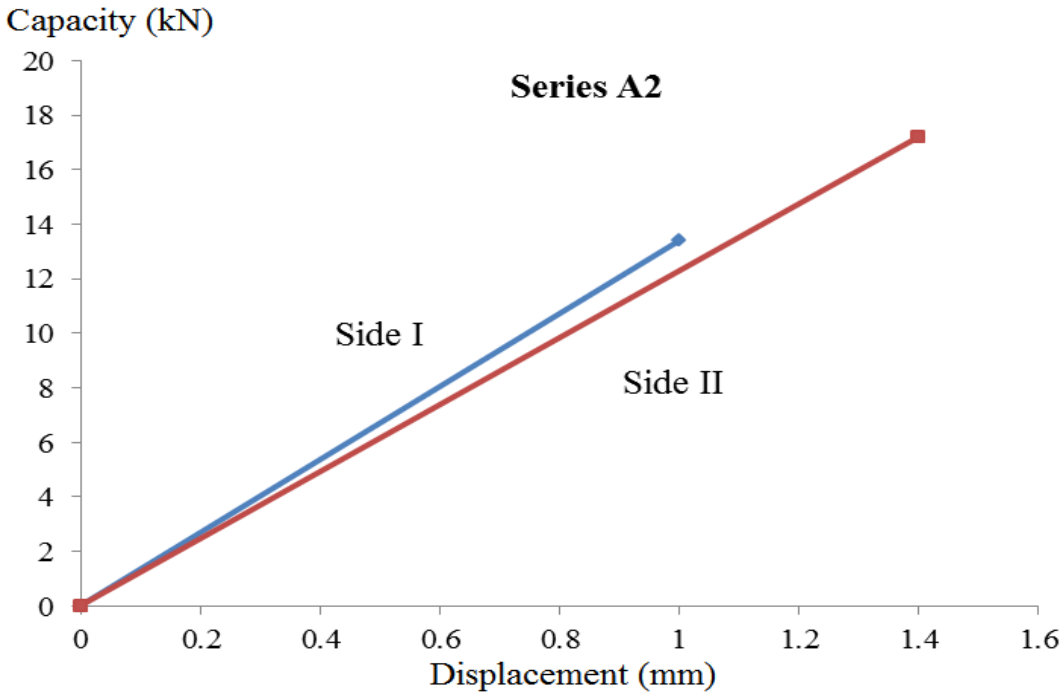

Figure B-2: Displacement vs Capacity of Two Sides (Series A2)

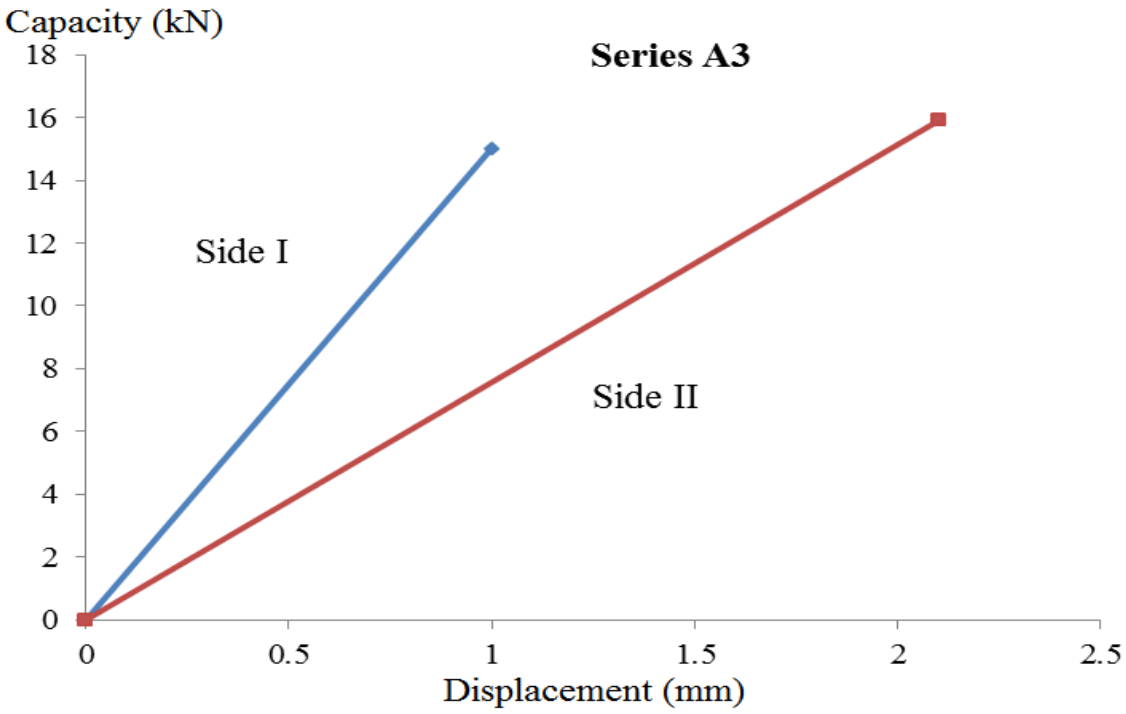

Figure B-3: Displacement vs Capacity of Two Sides (Series A3)

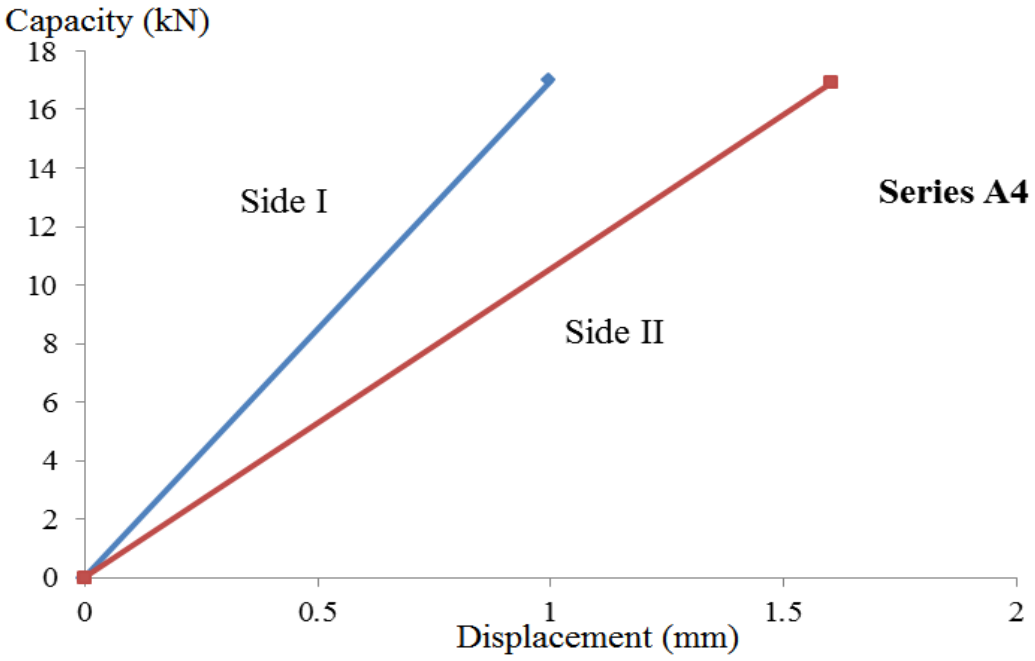

Figure B-4: Displacement vs Capacity of Two Sides (Series A4)

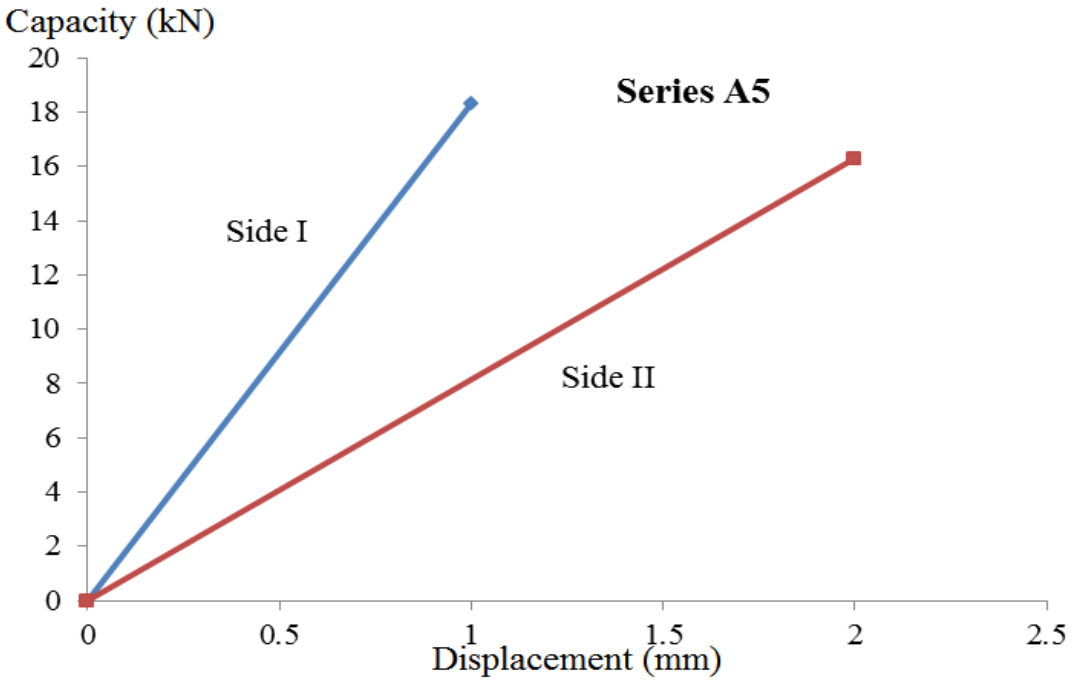

Figure B-5: Displacement vs Capacity of Two Sides (Series A5)

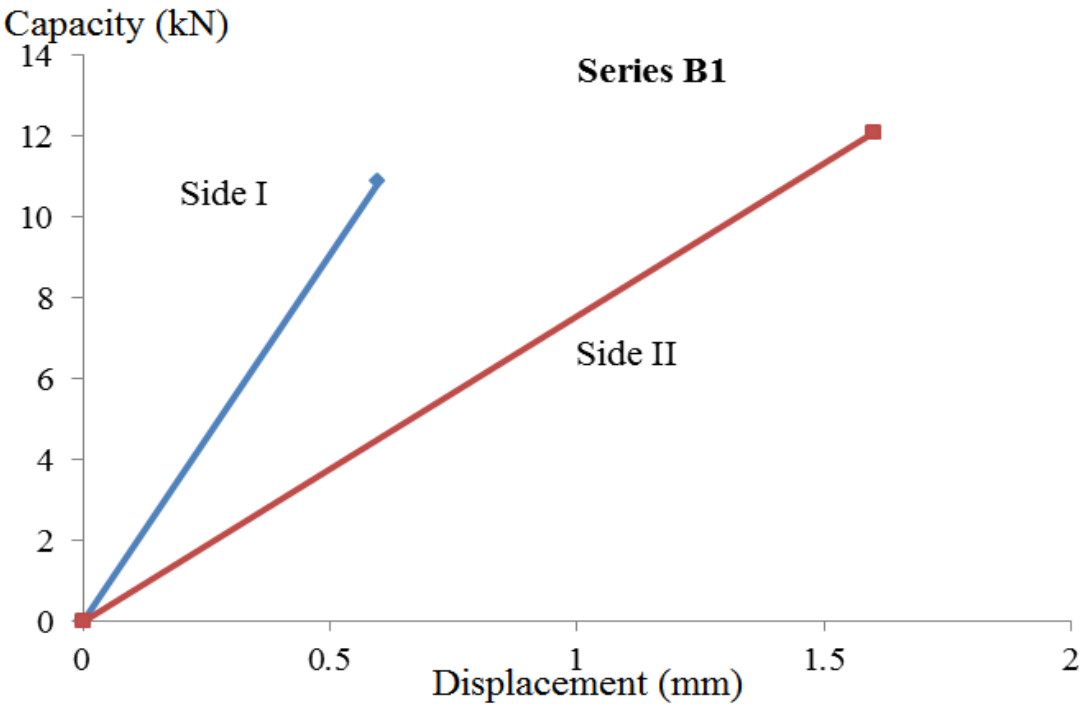

Figure B-6: Displacement vs Capacity of Two Sides (Series B1)

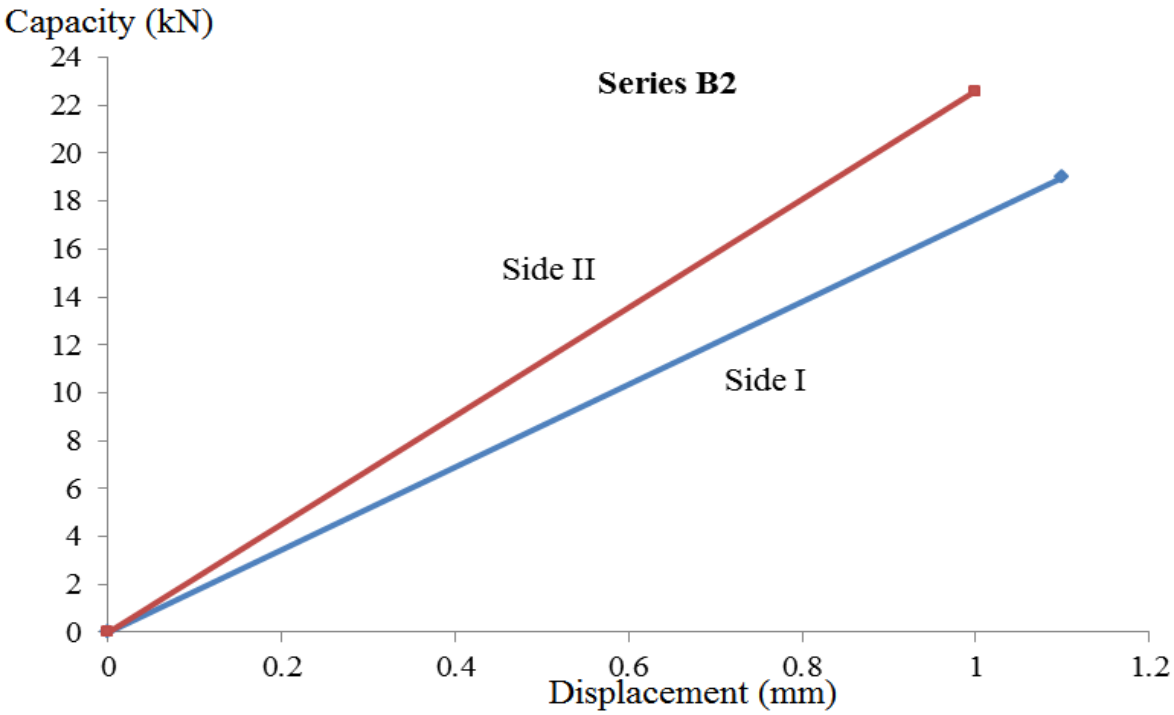

Figure B-7: Displacement vs Capacity of Two Sides (Series B2)

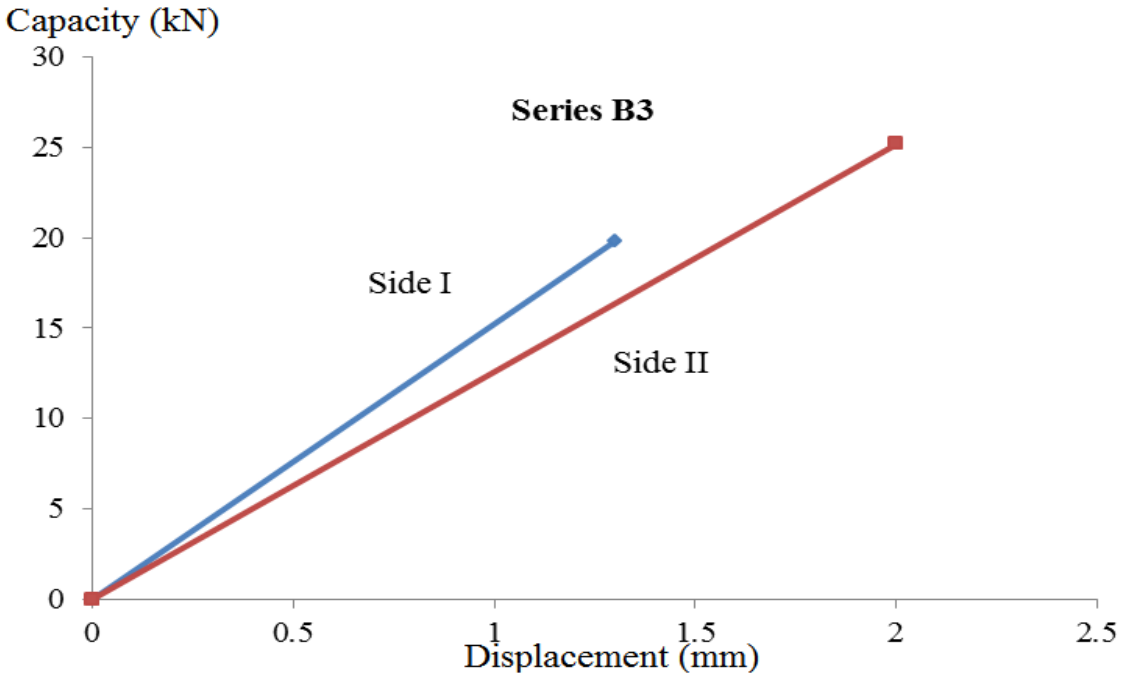

Figure B-8: Displacement vs Capacity of Two Sides (Series B3)

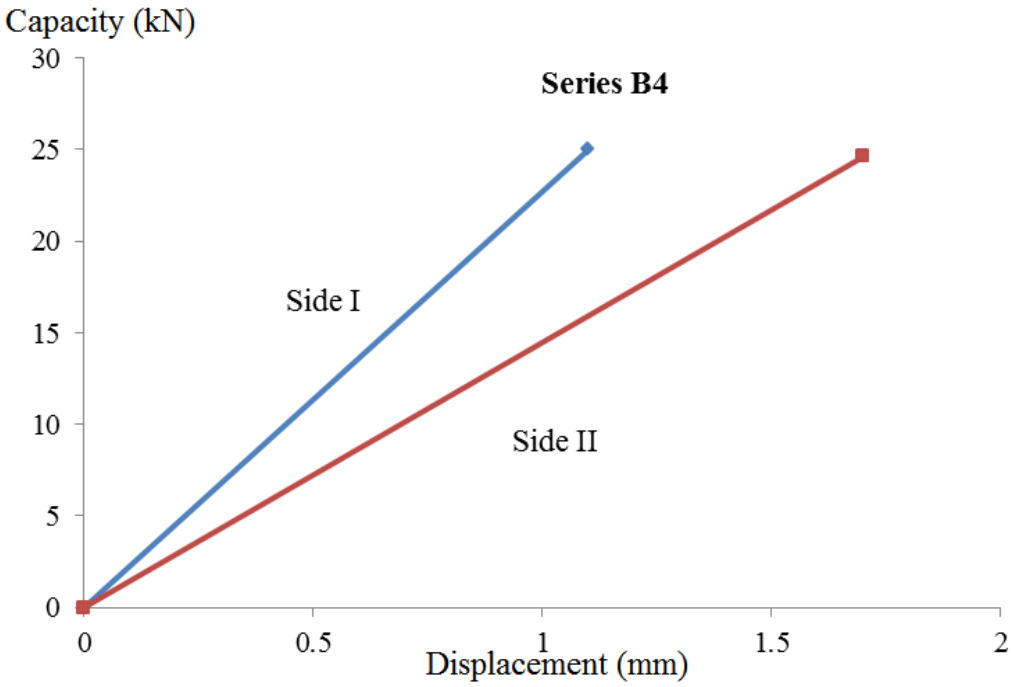

Figure B-9: Displacement vs Capacity of Two Sides (Series B4)

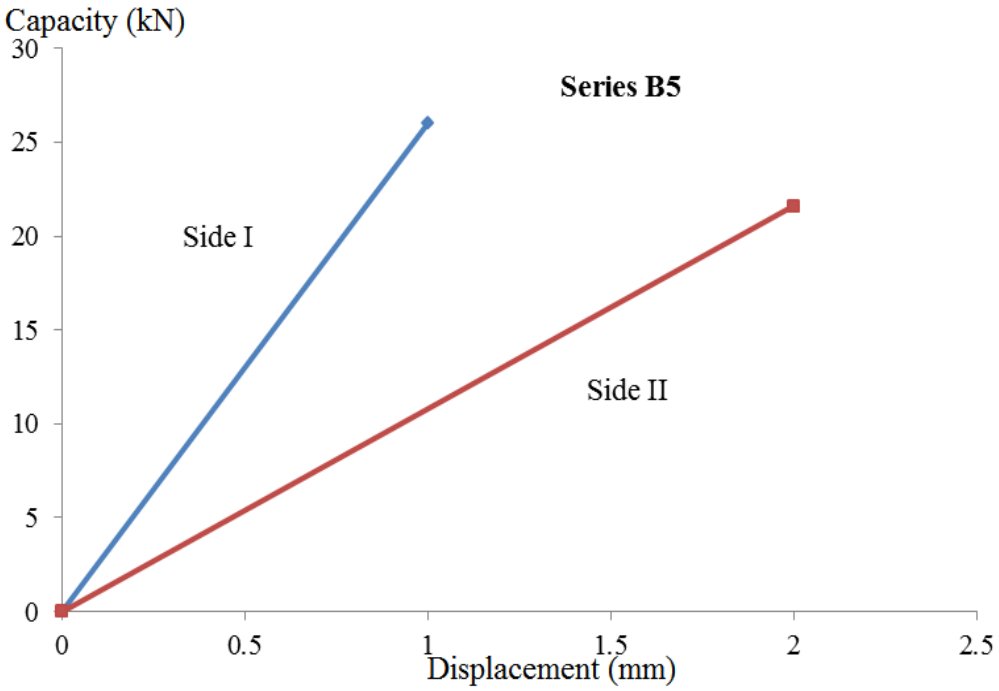

Figure B-10: Displacement vs Capacity of Two Sides (Series B5)

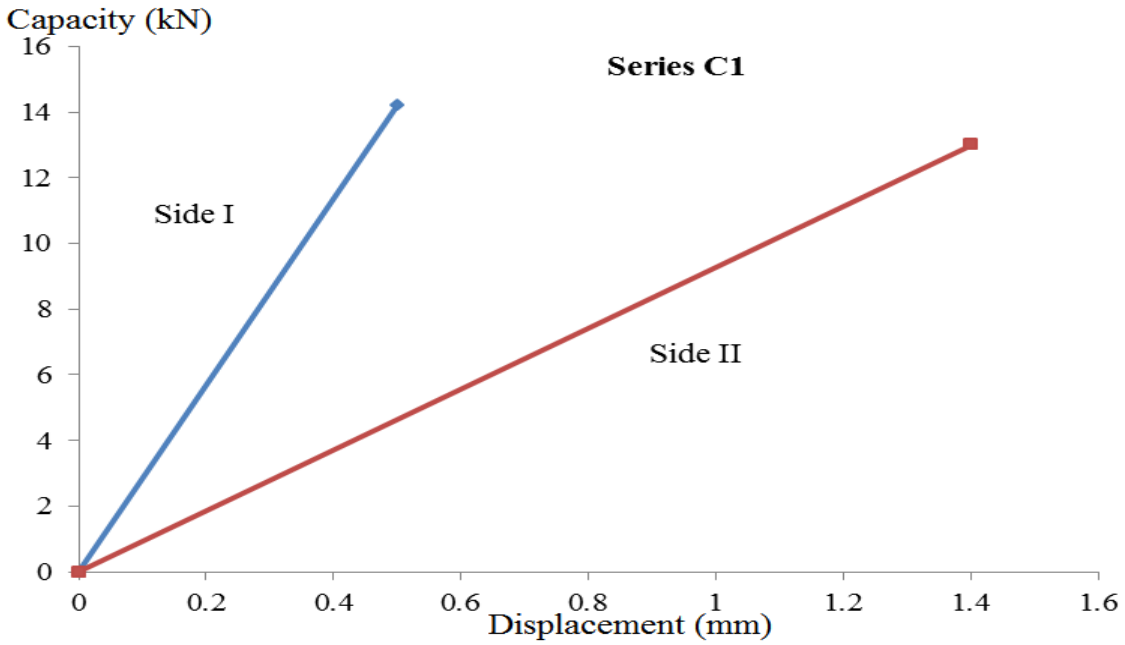

Figure B-11: Displacement vs Capacity of Two Sides (Series C1)

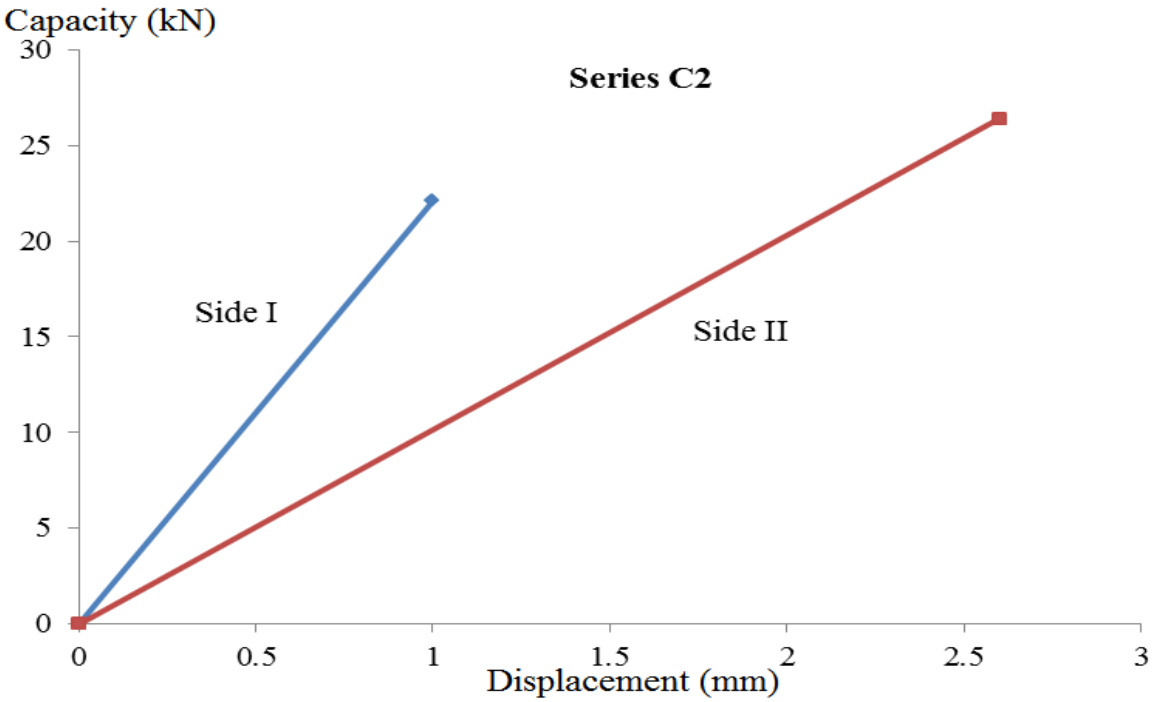

Figure B-12: Displacement vs Capacity of Two Sides (Series C2)

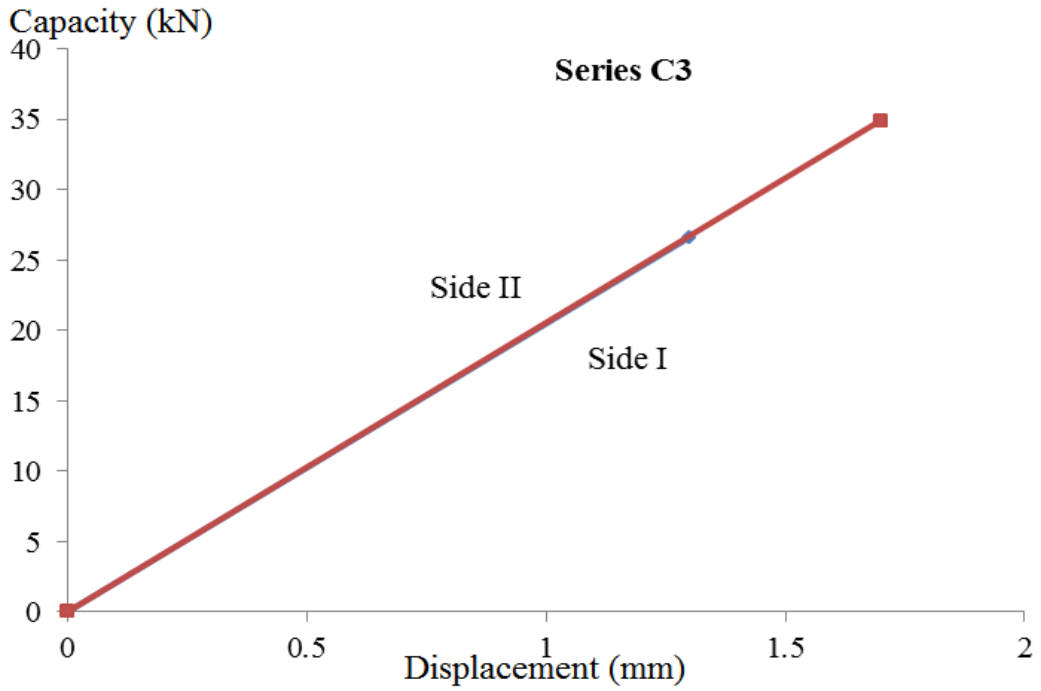

Figure B-13: Displacement vs Capacity of Two Sides (Series C3)

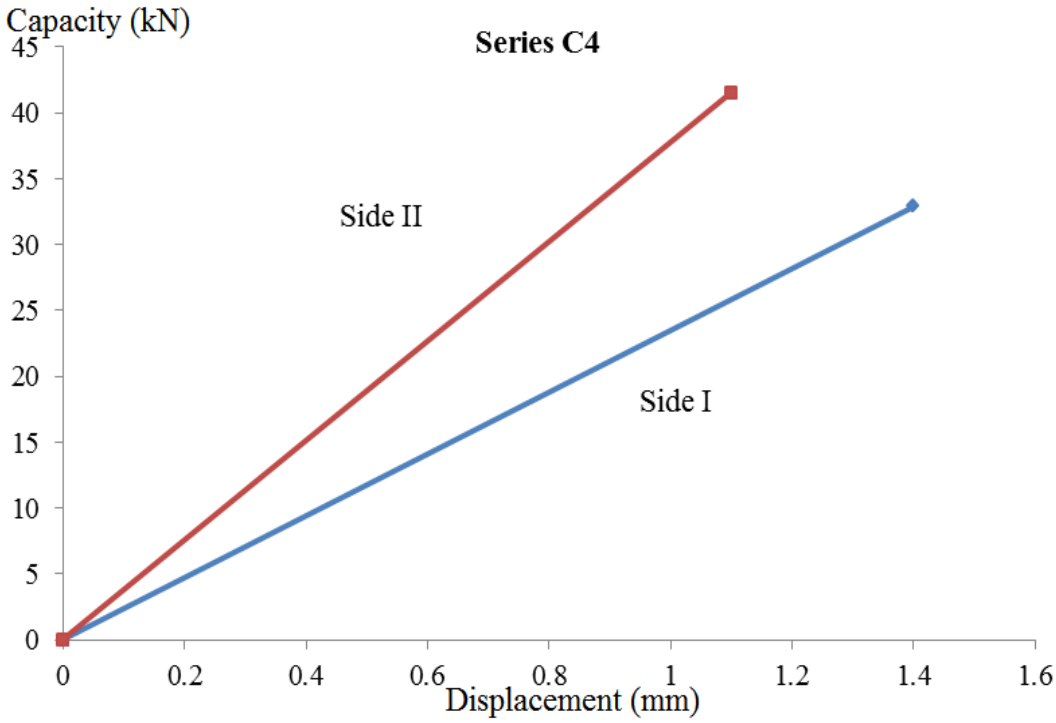

Figure B-14: Displacement vs Capacity of Two Sides (Series C4)

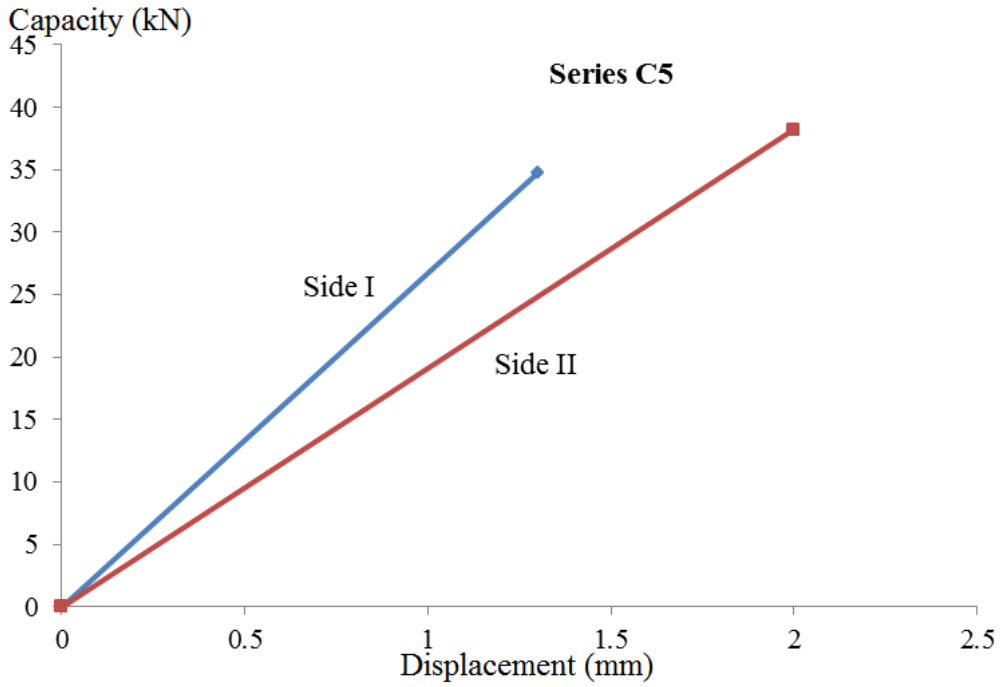

Figure B-15: Displacement vs Capacity of Two Sides (Series C5)

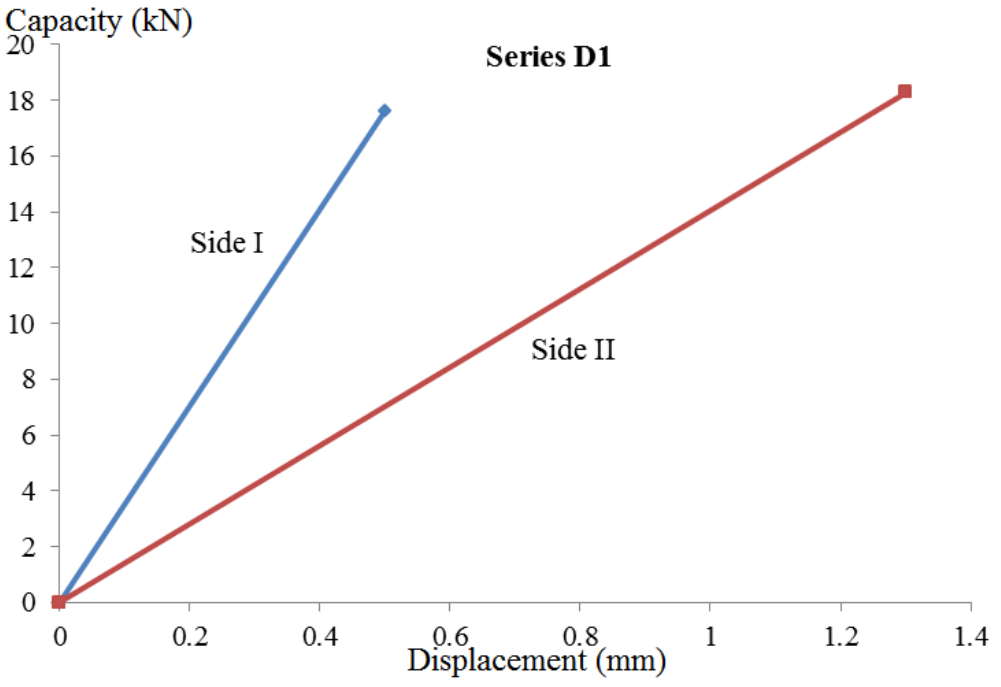

Figure B-16: Displacement vs Capacity of Two Sides (Series D1)

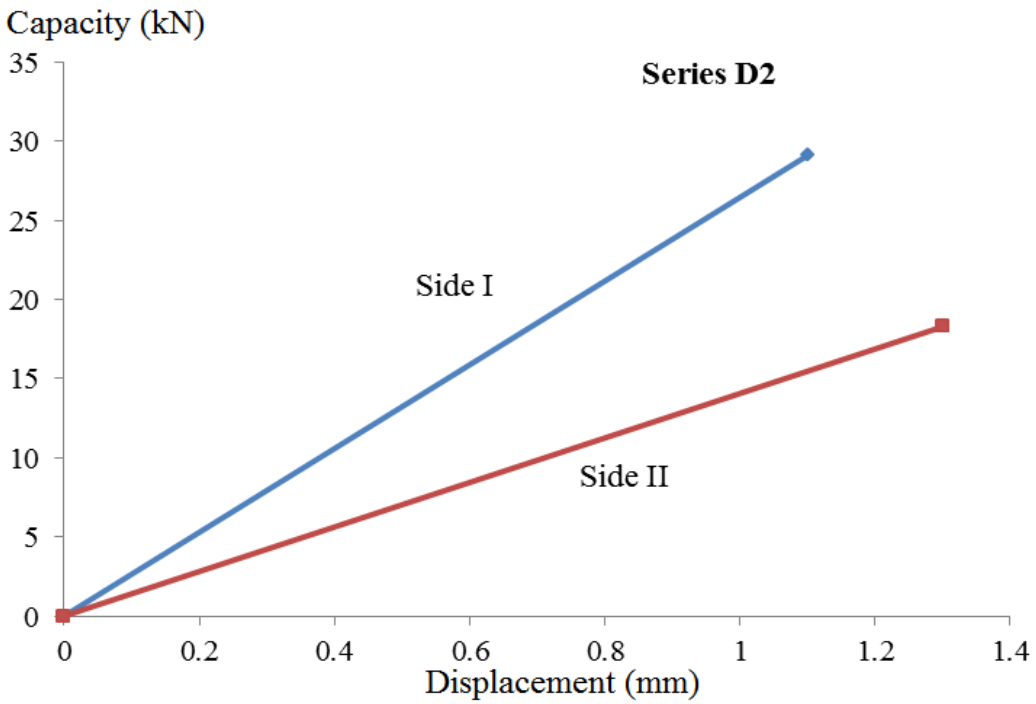

Figure B-17: Displacement vs Capacity of Two Sides (Series D2)

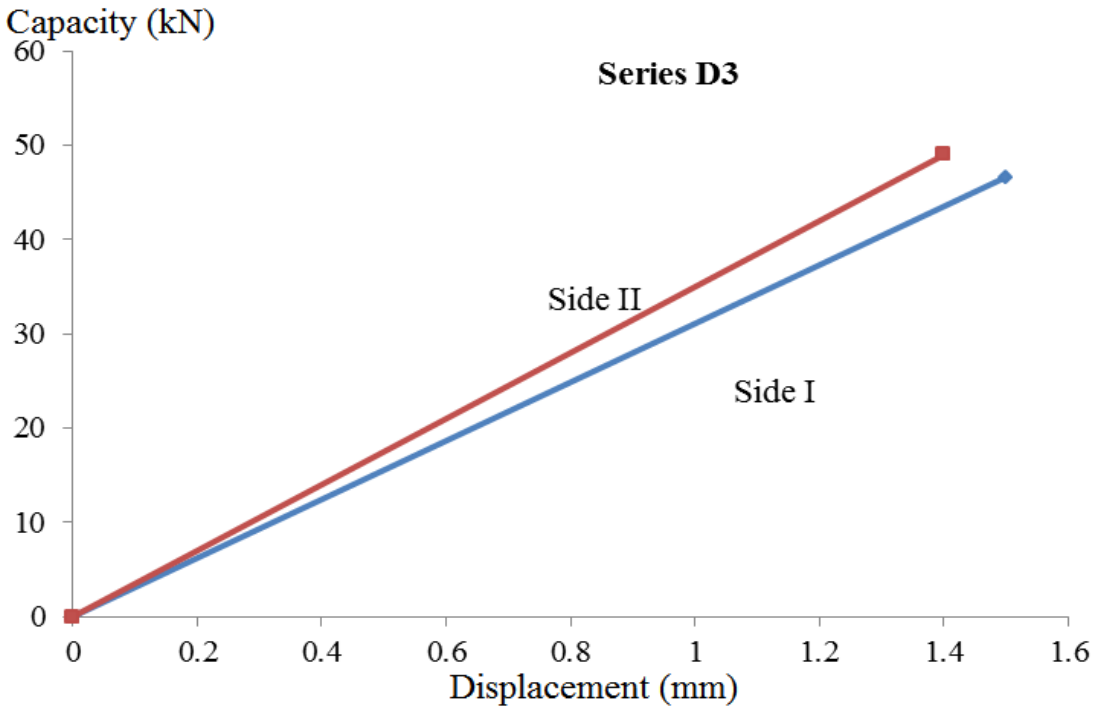

Figure B-18: Displacement vs Capacity of Two Sides (Series D3)

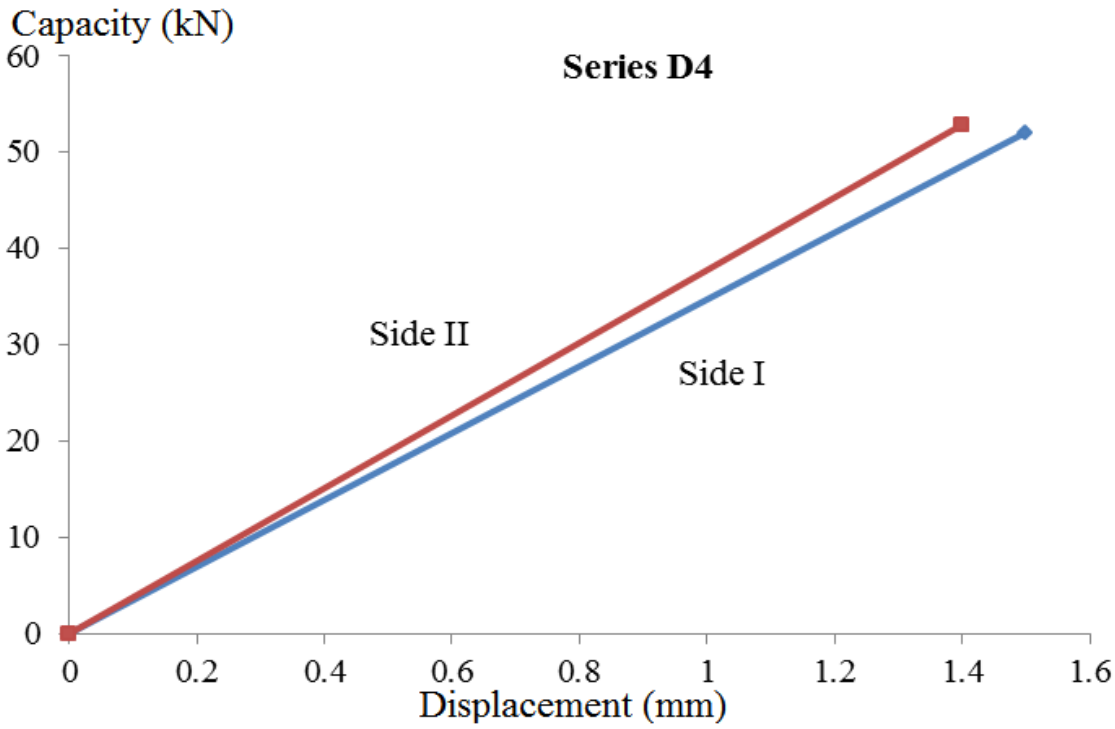

Figure B-19: Displacement vs Capacity of Two Sides (Series D4)

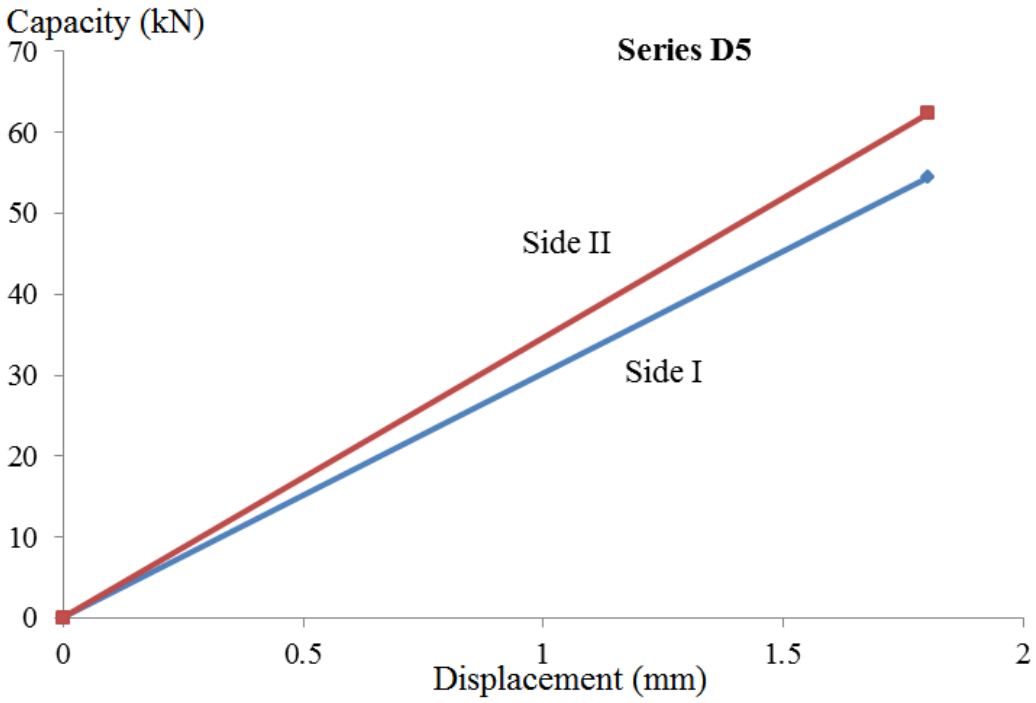

Figure B-20: Displacement vs Capacity of Two Sides (Series D5)

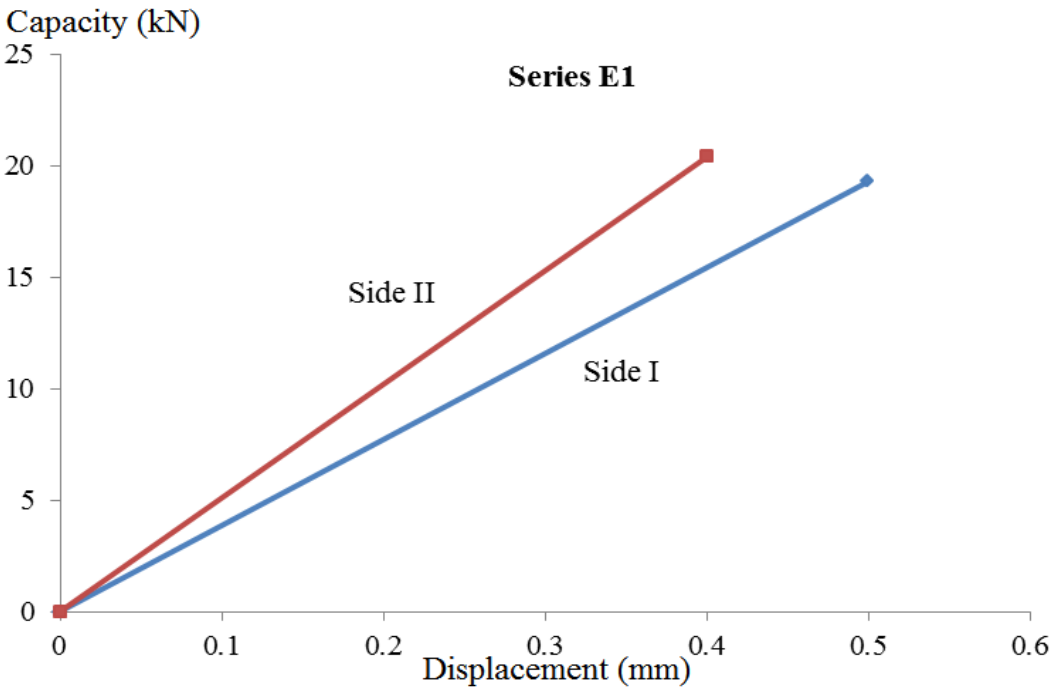

Figure B-21: Displacement vs Capacity of Two Sides (Series E1)

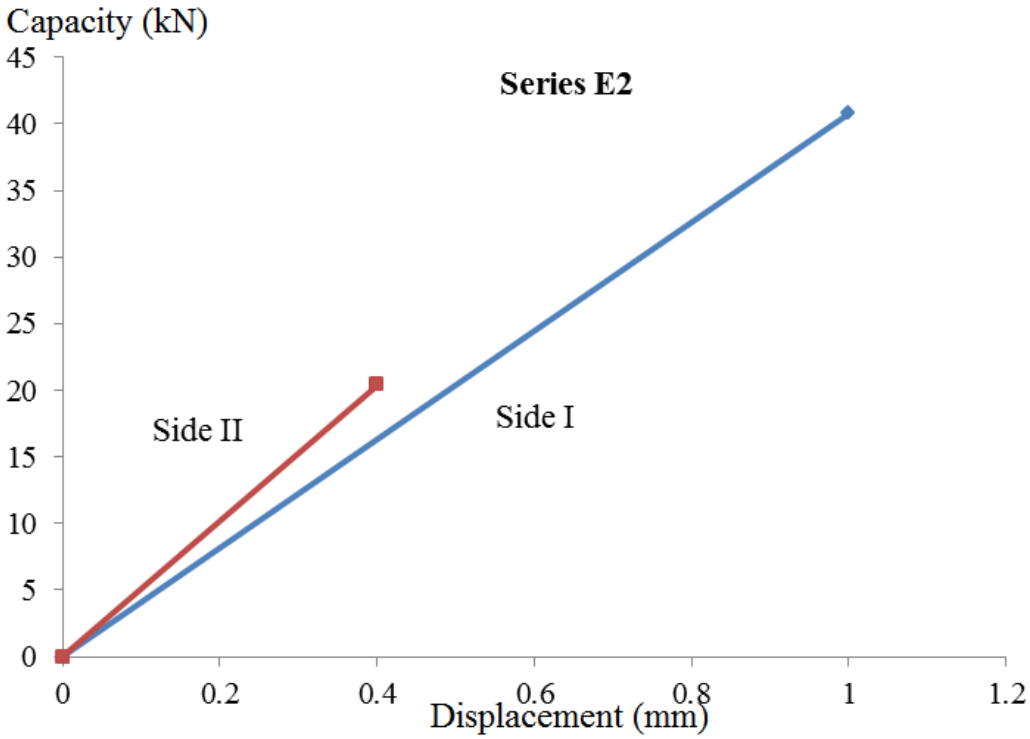

Figure B-22: Displacement vs Capacity of Two Sides (Series E2)

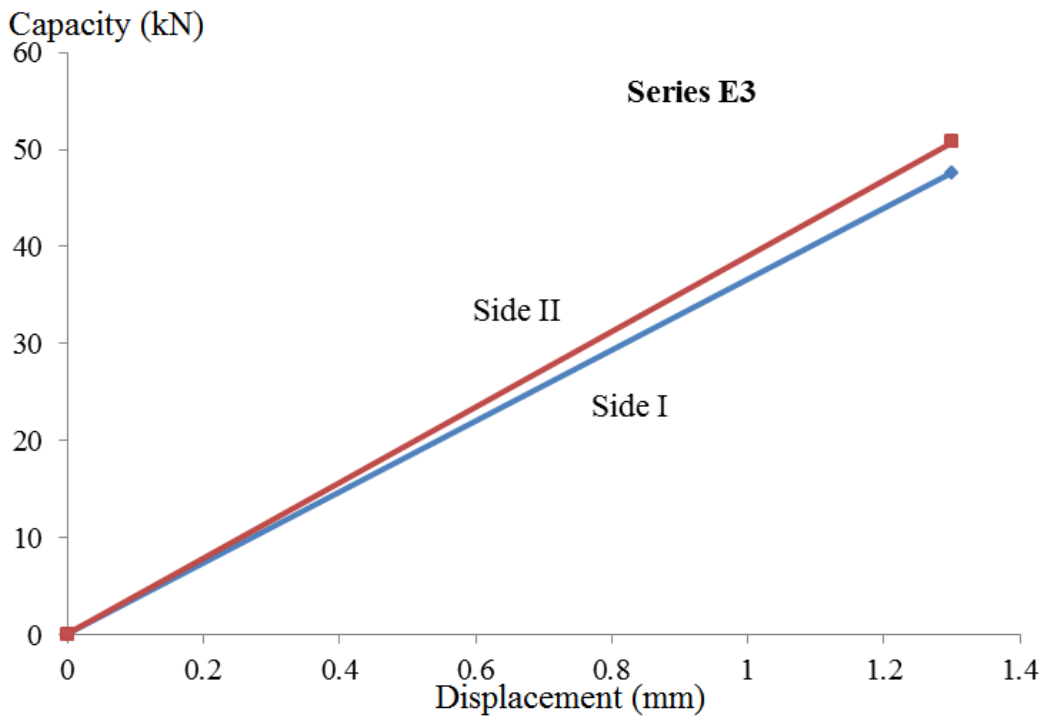

Figure B-23: Displacement vs Capacity of Two Sides (Series E3)

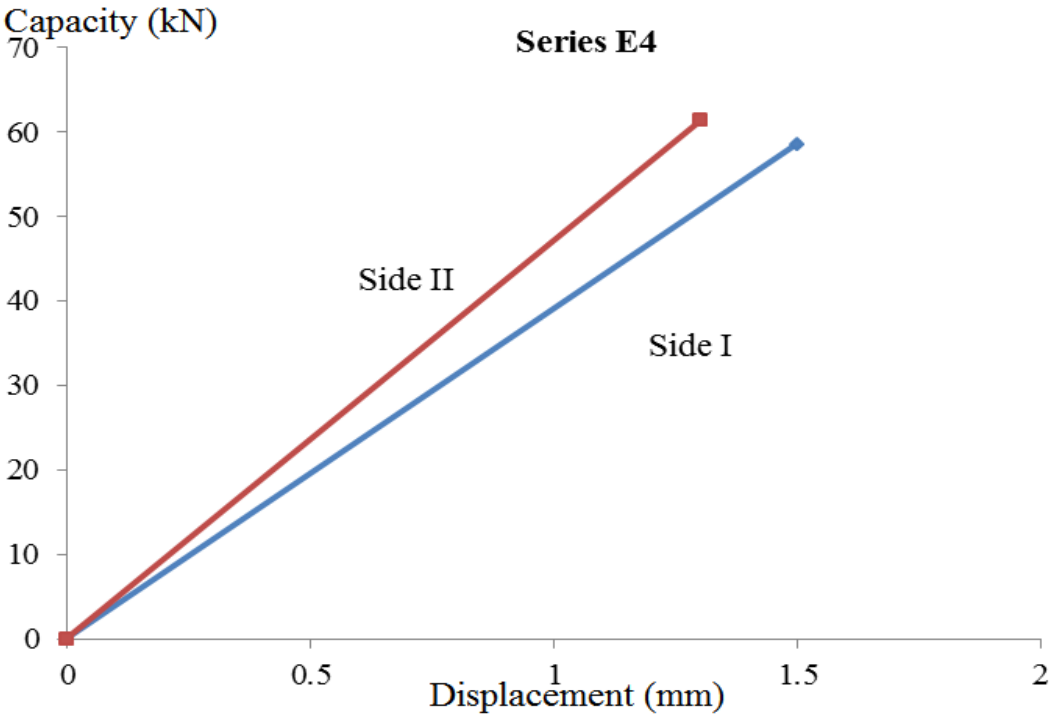

Figure B-24: Displacement vs Capacity of Two Sides (Series E4)

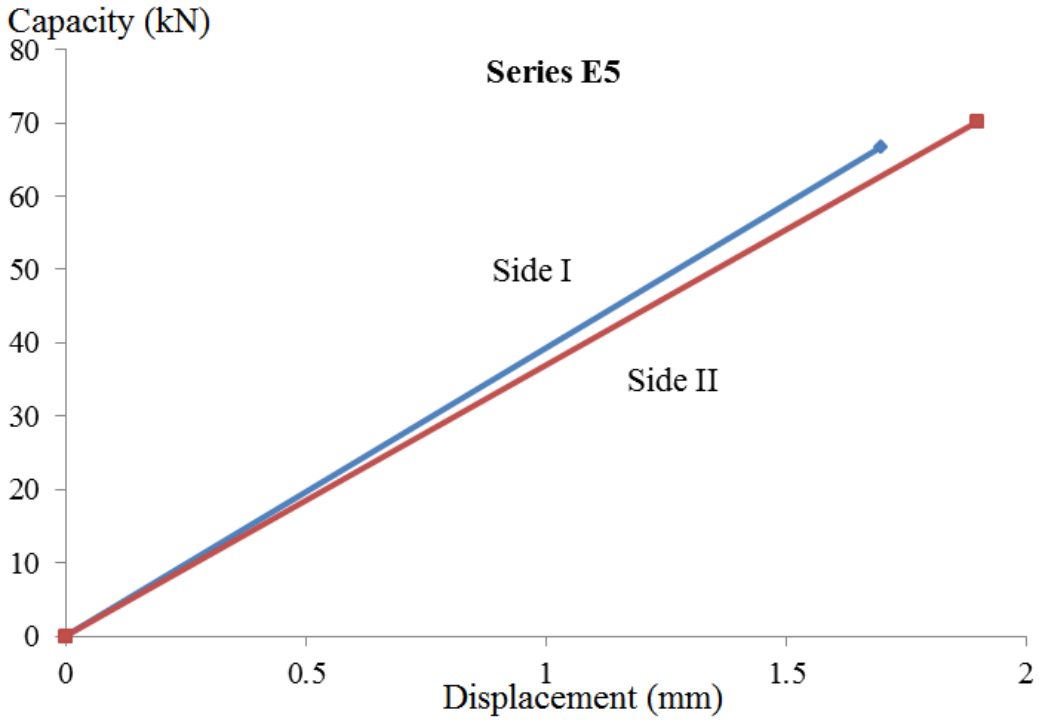

Figure B-25: Displacement vs Capacity of Two Sides (Series E5)

APPENDIX C: LOAD-DISPLACEMENTS IN FATIGUE TESTS

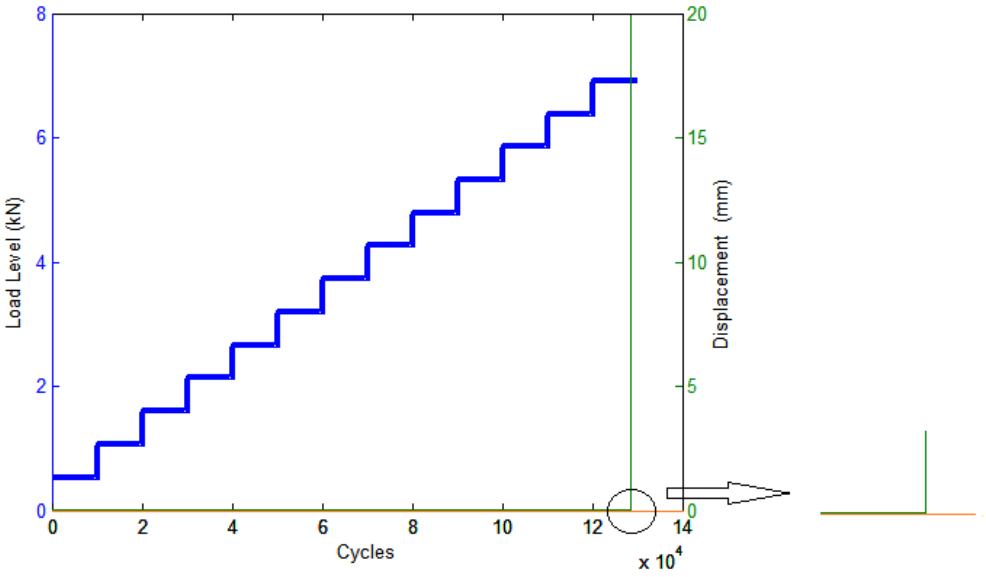

Figure E-1: Load Level and Displacement of F-1-5 Specimen

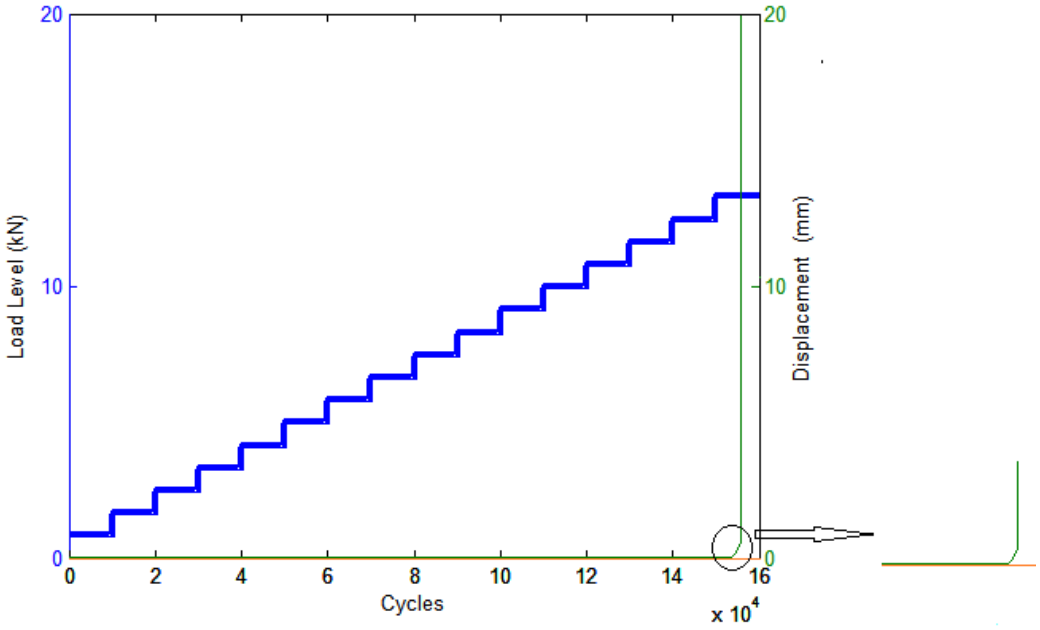

Figure E-2: Load Level and Displacement of F-2-1 Specimen

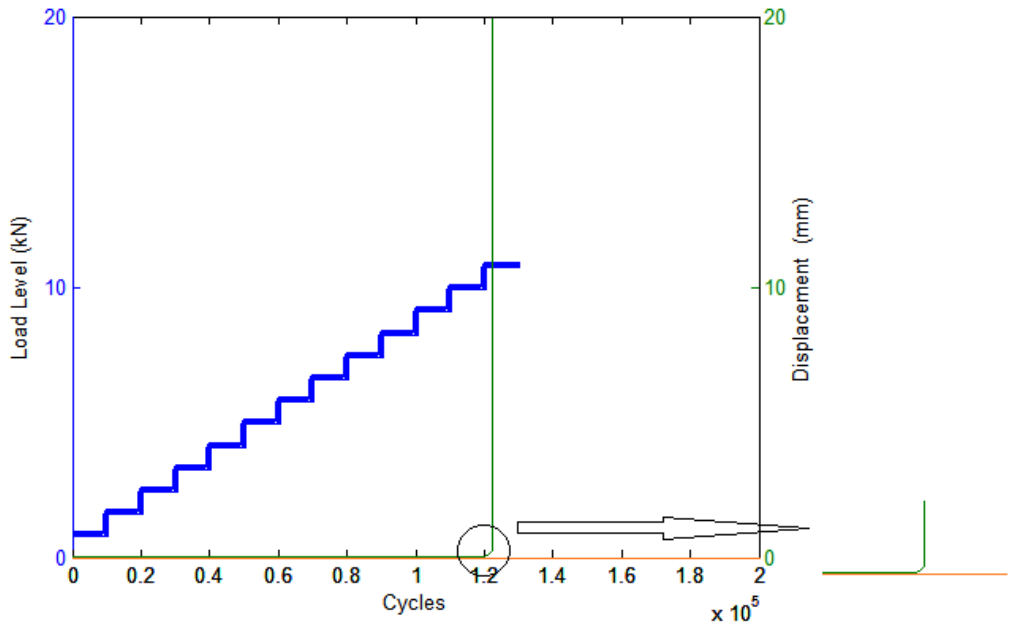

Figure E-3: Load Level and Displacement of F-2-3 Specimen

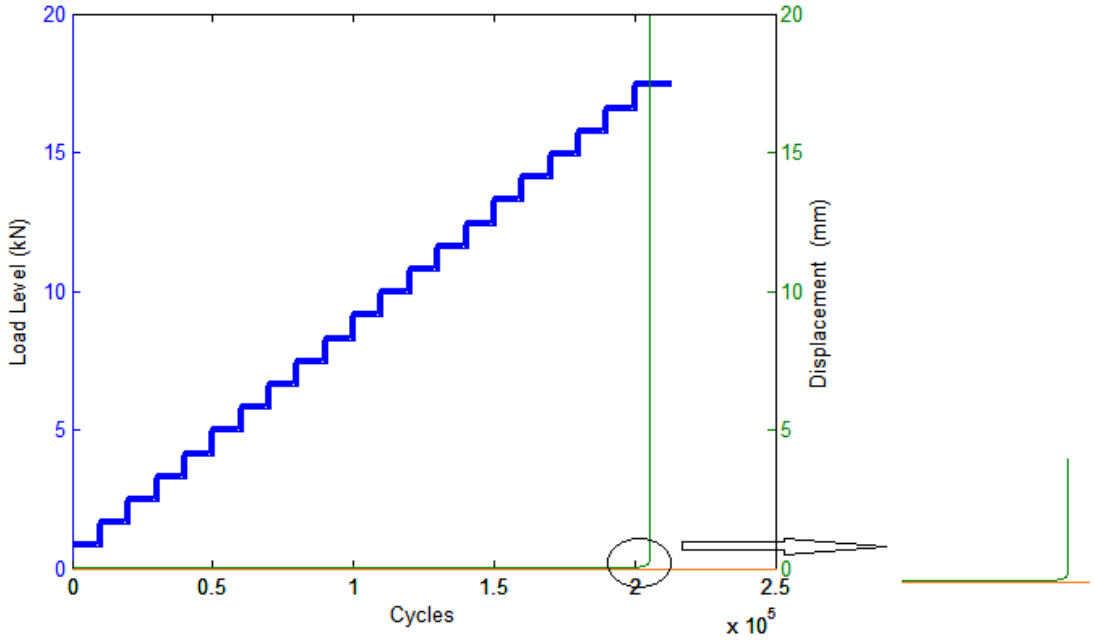

Figure E-4: Load Level and Displacement of F-2-6 Specimen

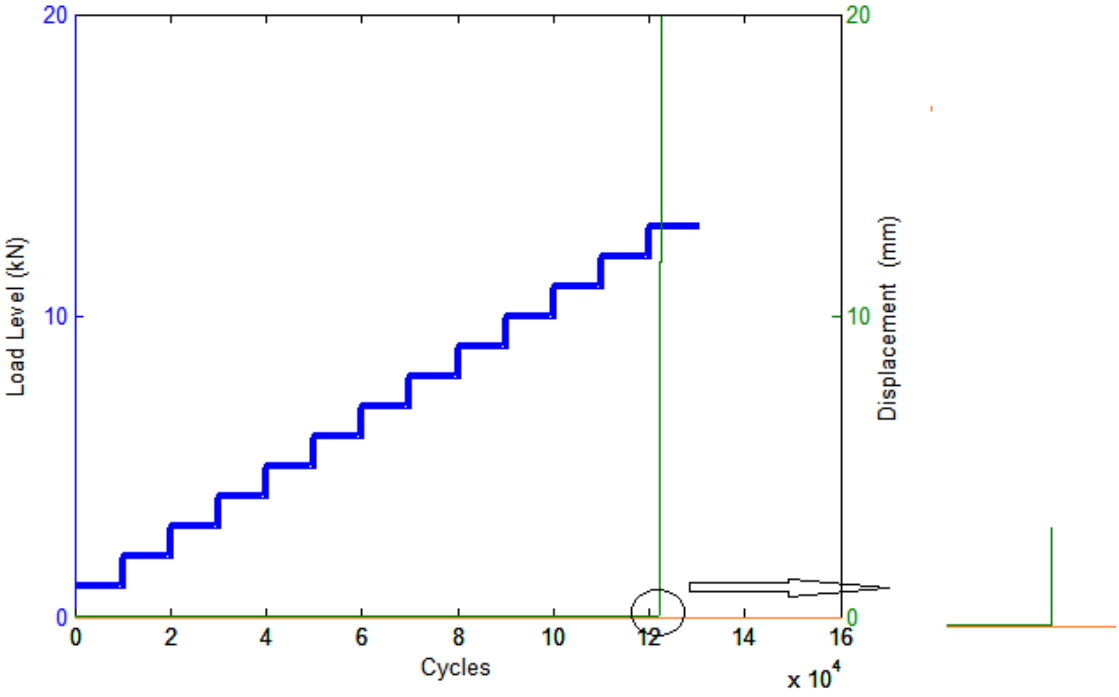

Figure E-5: Load Level and Displacement of F-3-1 Specimen

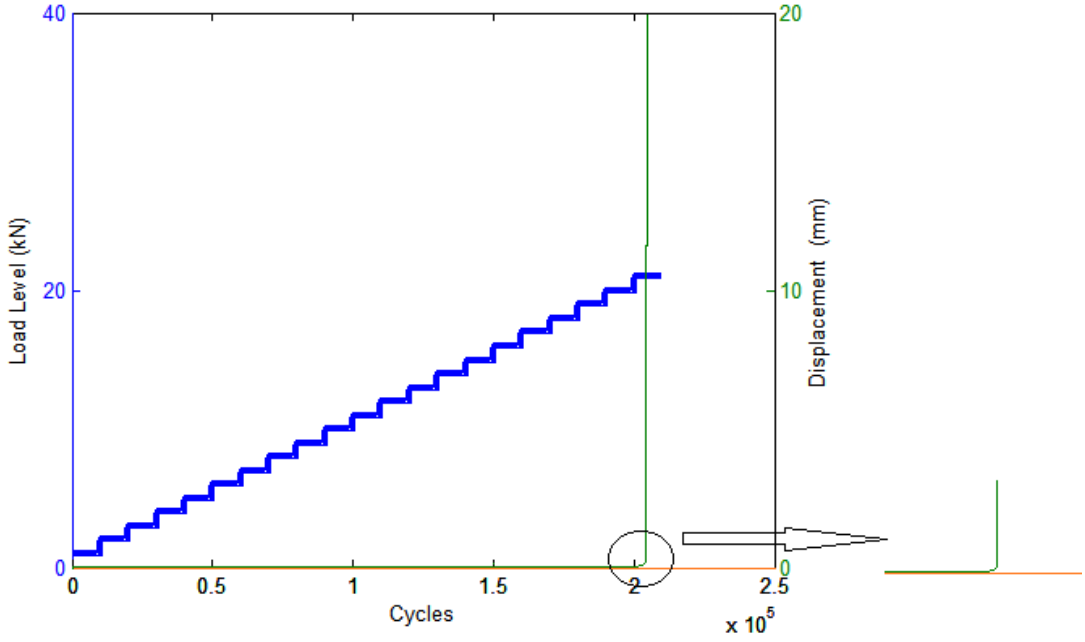

Figure E-6: Load Level and Displacement of F-3-2 Specimen

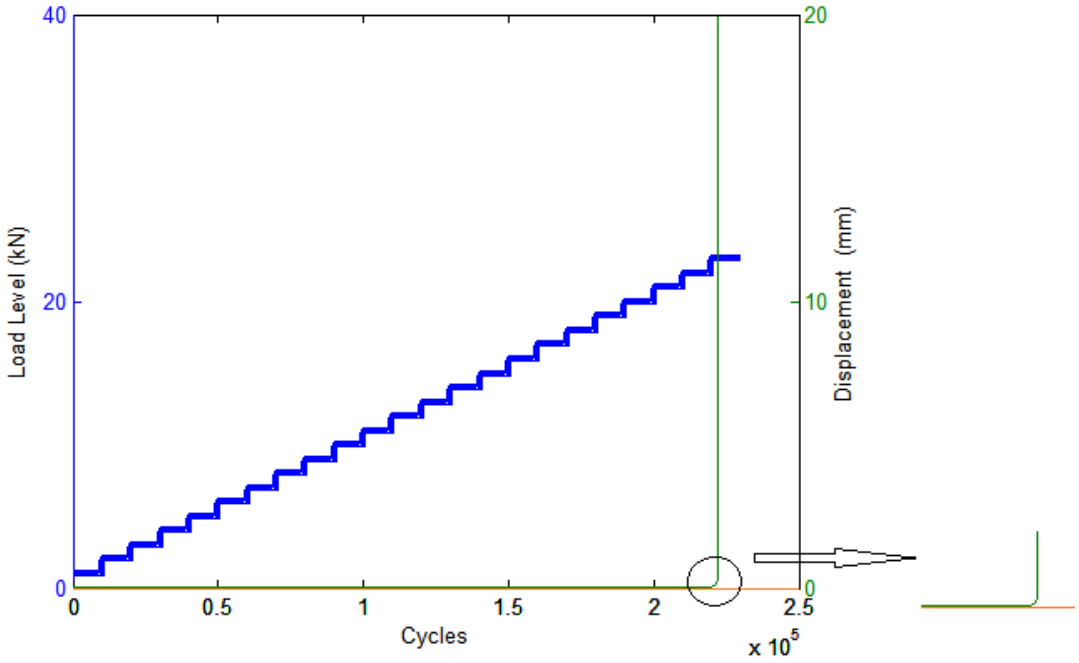

Figure E-10: Load Level and Displacement of F-3-3 Specimen

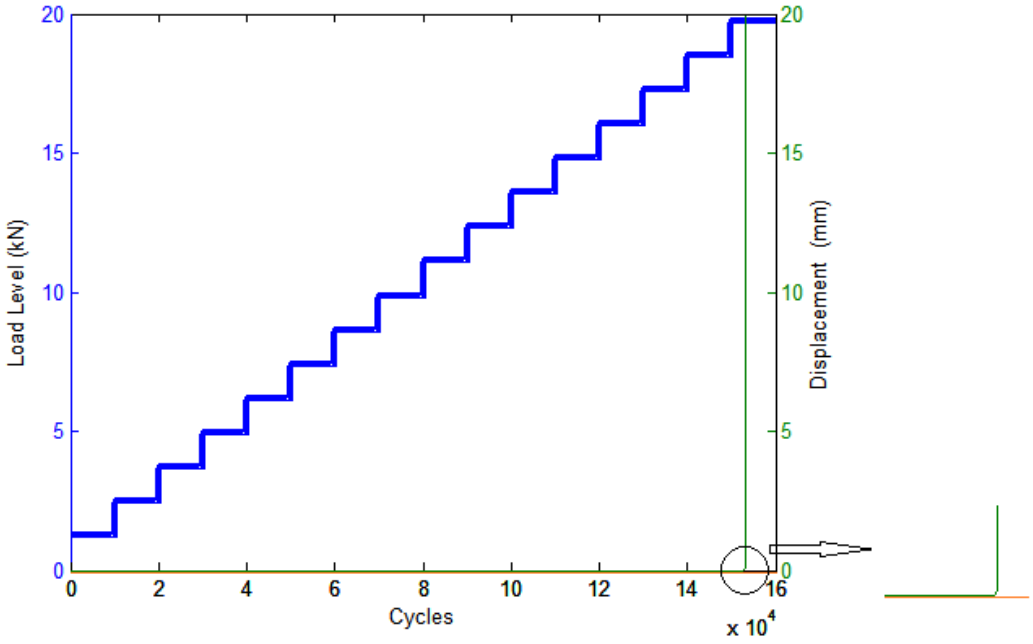

Figure E-11: Load Level and Displacement of F-4-2 Specimen

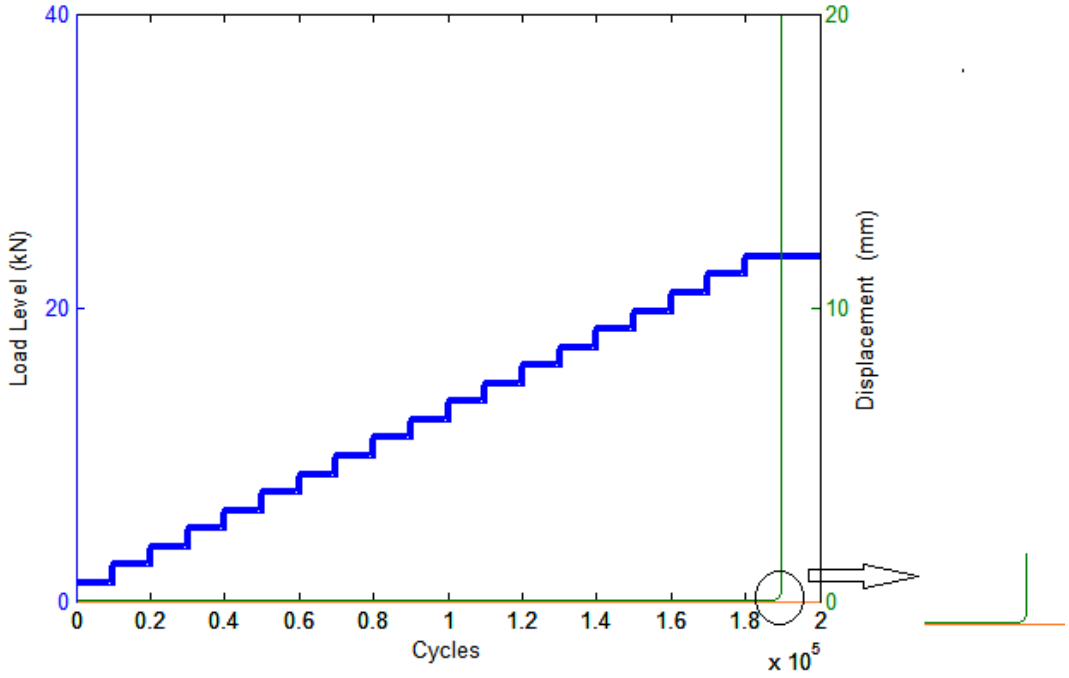

Figure E-12: Load Level and Displacement of F-4-3 Specimen

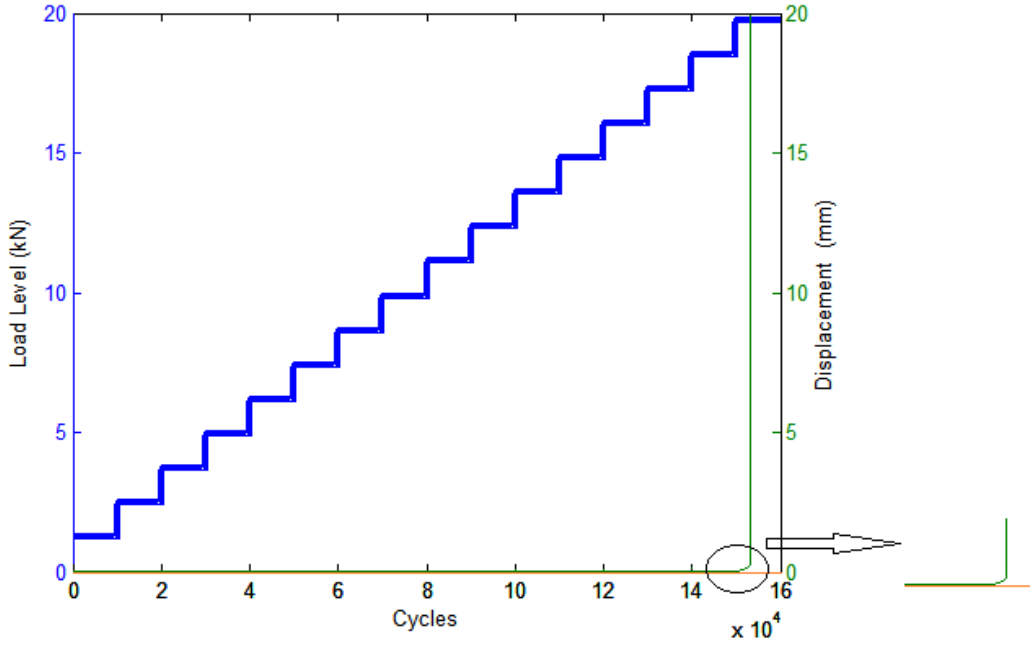

Figure E-13: Load Level and Displacement of F-4-5 Specimen

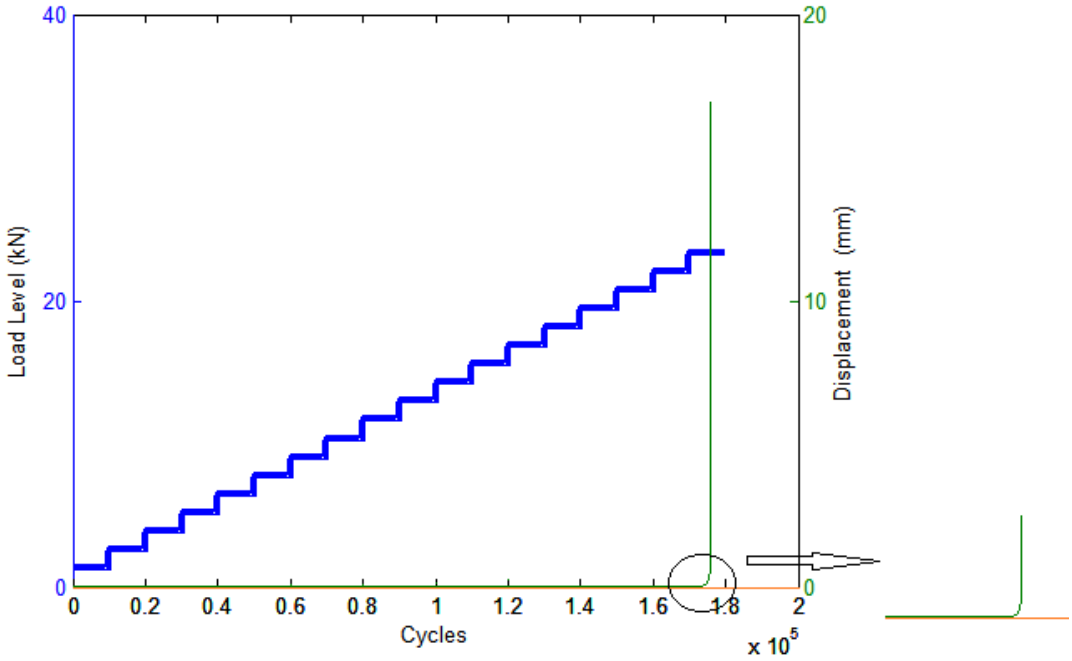

Figure E-14: Load Level and Displacement of F-5-2 Specimen

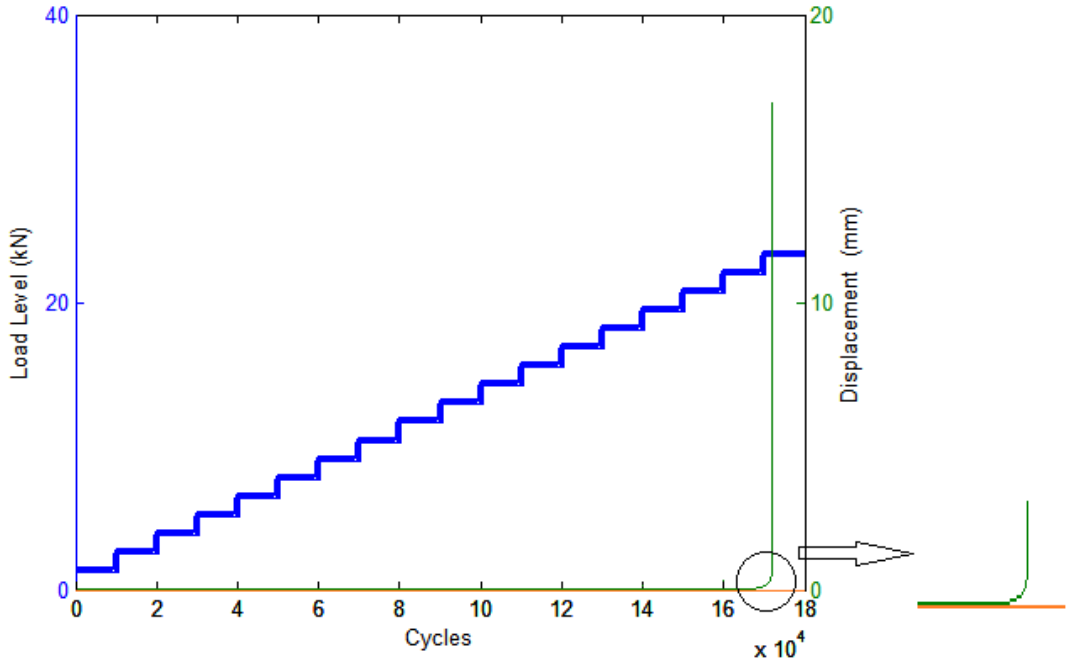

Figure E-15: Load Level and Displacement of F-5-4 Specimen

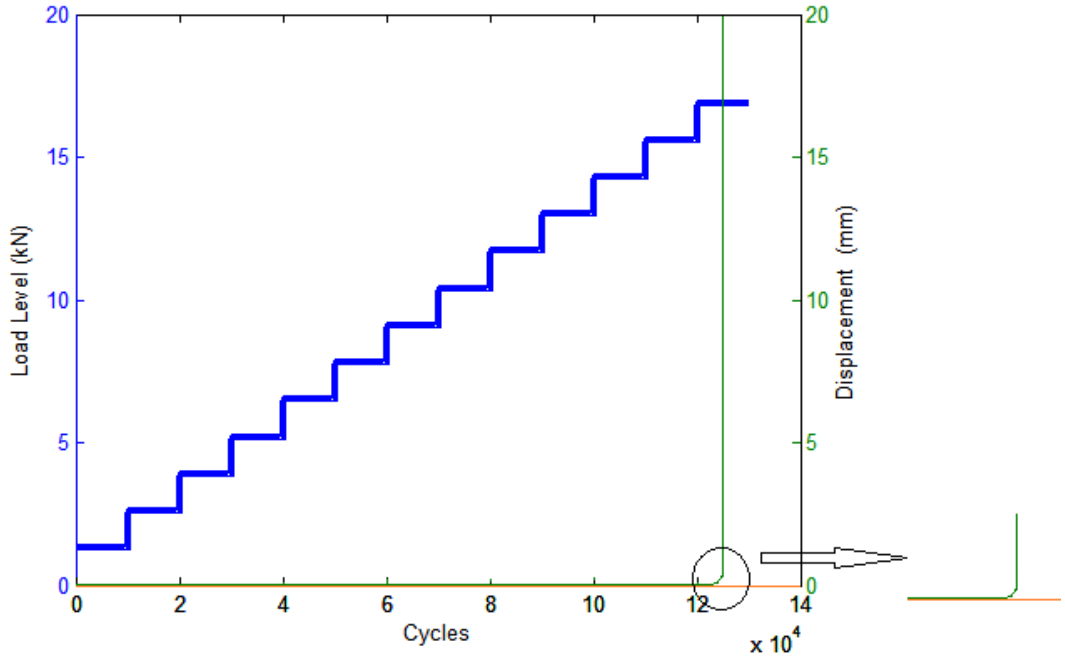

Figure E-16: Load Level and Displacement of F-5-6 Specimen